OIPE IAP29
SEP 29 2005
PATENT & TRADEMARK OFFICE

OIPE IAP29
SEP 29 2005
PATENT & TRADEMARK OFFICE

PATENTS

IN THE UNITED STATES PATENT AND TRADEMARK OFFICE

Applicants:	Colin L. Masters *et al.*	**Examiner:**	Chernyshev, O. N.
Serial No:	10/716,924	**Art Unit:**	1646
Filed:	19 November, 2003	**Docket:**	9287ZYA
For:	A METHOD FOR ASSAYING AND TREATING ALZHEIMER'S DISEASE	**Confirmation No.:**	6426

Commissioner for Patents
Alexandria, VA 22313-1450

DECLARATION PURSUANT TO 37 C.F.R. §1.132

Sir:

I, **ROBERTO CAPPAI**, hereby declare as follows:

1. I am an Australian Citizen residing at 27 Barkers Road Victoria, Commonwealth of Australia.

2. I am a NHMRC Senior Research Fellow within the Department of Pathology at the University of Melbourne, Victoria, Commonwealth of Australia.

3. I have been an author of a number of scientific publications especially in the area of the clinical, pathologic, physiological and molecular aspects of Alzheimer's Disease. My Curriculum Vitae is attached hereto as **Exhibit A**. In particular, I have conducted research to identify agents that interact with amyloid precursor protein (APP) and which affect APP processing, which is discussed further below.

4. I have reviewed U.S. Patent Application Serial No. 10/716,924 ("the '924 application") and am familiar with the contents therein. The '924 application presently claims methods of treating Alzheimer's disease in a patient by subjecting the patient to a therapeutically effective amount of a zinc-binding agent which is capable of crossing the

blood brain barrier and which modulates the interaction within the central nervous system between a divalent/trivalent cation and/or heparin with amyloid precursor protein (APP) in the patient. The '924 application also claims methods of reducing abnormal protease-mediated processing of amyloid precursor protein (APP) in a patient with Alzheimer's disease by administering a zinc-binding agent which is capable of crossing the blood brain barrier and which modulates the interaction within the central nervous system between a divalent/trivalent cation and/or heparin with amyloid precursor protein (APP) in the patient. I have been asked to comment on whether the '924 application has provided adequate teaching for those skilled in the art to practice the claimed methods.

5. At the time when the '924 application was filed, Alzheimer's Disease (AD) was known to be a progressive dementia characterized by the deposition of amyloid protein in the intracellular and extracellular compartments of the cerebral cortex. Amyloid protein is defined as an aggregated protein that forms a regular β-sheet conformation that is able to refract polarised light to a characteristic glow. Prior to the filing of the '924 application, it had been determined that the extracellular deposits consists of a protein, referred to as βA4 at the time, which was believed to result from abnormal cleavage of amyloid precursor protein (APP). Normal cleavage occurs at or near a lysine residue within the βA4 sequence, which would prevent formation of the amyloidogenic βA4 fragment. As APP had been shown to have neurotrophic activities (e.g., activities in promoting the survival or outgrowth of nerve processes), it was believed that abnormal APP processing could account for the loss of certain populations of neurons seen in Alzheimer's disease, and either caused or contributed to the progression of the disease. See the '924 application on page 1, lines 28 through page 2, line 4. It was against this scientific background that the invention of the '924 was developed.

6. Specifically, it is disclosed in the '924 application that a reduction in amyloidogenic protein can be achieved by reducing the interaction of divalent/trivalent metal cations and/or heparin with APP, thereby treating Alzheimer's Disease. As stated in the '924 application, at page 6, lines 18-20, by manipulating the interaction between cations, preferably zinc, and APP, protease mediated digestion of APP (i.e. APPase activity) is altered. More specifically, the '924 application describes on page 7, lines 1-7, that by modulating the levels of divalent

cations or heparin, the range, type and/or extent of APP cleavage can be altered such that incorrect protease-mediated processing of APP can be reduced or inhibited. More particularly, the '924 application on page 8, lines 21-31, teaches that modulation of the levels of divalent or trivalent cations can be achieved by administering to a patient a therapeutically effective amount of a binding agent, e.g., a zinc binding agent or zinc chelator, which reduces the bioavailability of the cations. Further, the '924 application provides on page 9, lines 10-15, a number of examples of zinc-specific chelating agents including heterocyclic pyridones such as 1,2-diethyl-3-hydroxypyridin-4-one (also referred to as "CP94"). Moreover, the '924 application teaches on page 9, lines 2-7, that particularly preferred binding agents are those that are capable of crossing the blood/brain barrier and thus modulate free zinc concentrations within the brain thereby protecting against improper APP processing. The various aspects of the invention are also illustrated by Examples set forth on pages 16-34 of the '924 application.

7. It is my scientific opinion that the '924 application has provided to those skilled in the art sound scientific reasoning of the basis of the claimed methods. Consistent with the disclosure of the '924 application, additional evidence in support of the role of amyloidogenic APP species (e.g., Aβ) in the pathogenesis of Alzheimer's Disease has been documented subsequent to the filing of the '924 application. See review articles by John Hardy (*Trends Neurosci.* 20: 154-159, 1997) and by Price et al. (*Annu. Rev. Genet.* 32: 461-493, 1998), attached hereto as **Exhibit B** and **Exhibit C**.

8. It is my scientific opinion that, based on the teaching in the '924 application and the information available prior to the filing of the '924 application, those skilled in the art would be able to practice the methods claimed in the '924 application. That is, in my opinion, the '924 application provides sufficient guidance for those skilled in the art to practice a method of reducing aberrant APP processing in a patient with Alzheimer's Disease and therefore treating the disease in the patient by subjecting the patient to a therapeutically effective amount of a zinc-binding agent, which agent is capable of crossing the blood brain barrier and which modulates the interaction within the central nervous system between a

divalent/trivalent cation such as zinc and/or heparin with amyloid precursor protein (APP) in the patient.

9. My opinion is based on the observation that, at the time when the priority document of the '924 application was filed, chelators of cations were well-known to those skilled in the art. In addition to those specifically identified in the '924 application, clioquinol (5-chloro-7-iodo-8-hydroxy quinoline, or "CQ"), TPEN (N,N,N'N',-tetrakis (2-pyridylmethyl) ethylenediamine) and Zinquin ([(2-methyl-8-p-toluenesulphonamido-6-quinolyloxy)acetic acid] are other zinc chelators that had been documented in the art. See, for example, Kidani et al. (*Jap. Analyst* 23:1375-1378, 1974), McCabe et al. (*Lab Invest.* 69(1):101-10, 1993), and Zalewski et al. (*Biochem J.* 296 (Pt 2):403-8, 1993), copies of abstracts of which are attached hereto as **Exhibits D**, **E** and **F**.

10. My opinion is further based on the observation that, at the time when the priority document of the '924 application was filed, those skilled in the art could readily determine whether a compound is capable of crossing the blood brain barrier (BBB). The ability of a chemical compound to enter the brain by permeating the BBB is strongly dependent upon its lipid solubility, which has been recognized since the 1930's. Lipid solubility or lipophilicity of a compound, as measured by the octanol (lipid)/ buffer distribution coefficient of the compound (as described in Levin, *J. Med. Chem.* 23: 682-684, 1980, attached hereto as **Exhibit G**, for example), has been recognized to best reflect the BBB permeability of the compound.

11. Therefore, at the time when the priority document of the '924 application was filed, those skilled in the art would be able to readily identify zinc chelators and determine their BBB permeability and thus the suitability of such candidates for use in the methods claimed in the '924 application. For example, those skilled in the art would be able to readily determine that zinc chelators, CP94 and CQ, are able to cross the BBB. In this connection, I observe that the octanol (lipid)/ buffer distribution coefficient for CP94 and other related compounds is the subject of a paper by Dobbin *et al.* (*J. Med. Chem.* 36: 2448-2458, attached hereto as **Exhibit H**). CP94 is identified as compound 49 in this publication. The authors

conclude that CP94 and other related compounds that are lipophilic are highly BBB permeable, as shown in Table IX, page 2455 of the publication.

12. In support of the conclusion that zinc chelators capable of crossing BBB will be effective in modulating APP processing thereby treating Alzheimer's disease, an experiment I conducted demonstrated that CP94 altered APP processing resulting in the reduction of Aβ40 levels in an *in vitro* system. In this experiment, Chinese Hamster ovary (CHO) cells were stably transfected from cDNA encoding APP695. The APP695 corresponds to the full-length APP gene encoding amino acid residues 1 to 695 and was cloned into the mammalian expression vector pIRESpuro (Clontech, USA). The resulting CHO cells, referred to as CHO-APP cells, were plated into 12-well plates and were treated with CP94 at 20 μM for 18 hours. The supernatant was collected and assayed for Aβ40 by ELISA. As a control, CHO-APP cells were separately treated with DMSO (i.e., without CP-94) and 20 μM JLK6, which is a positive β-secretase inhibitor (7-amino-4-chloro-3-methoxyisocoumarin). The results of the assay are shown in Figure 1, attached hereto as **Exhibit I**. It can be seen that CP94 inhibited the formation of Aβ species, whereas DMSO showed no effect. This result provides support for the conclusion that Alzheimer's Disease in a patient can be treated by administering a cation binding agent capable of crossing BBB, such as CP94, which modulates the interaction between a divalent or trivalent cation with APP.

13. As further support that zinc chelators capable of crossing BBB will be effective in modulating APP processing thereby treating Alzheimer's disease, additional experiments I conducted demonstrated that multivalent zinc-binding agents, including clioquinol (CQ) and several other compounds, also altered APP processing resulting in the reduction of Aβ40 levels in the *in vitro* system as described above. In these experiments, CHO-APP cells were plated into 24 well plates and treated with a candidate multivalent cation-binding agent at a concentration of 10 μM for 24 hours. The agents tested were CQ and six compounds referred to as 1076, 1084, 1085, 1089, 1090 and 1091. These compounds were produced by Prana Biotechnology Ltd., the structures of which are shown in **Exhibit J**. The levels of Aβ40 were then detected by ELISA and the cells were assayed for viability with the MTT assay. The MTT test is a quantitative colorimetric method to determine cell proliferation. This is to

ensure changes in Aβ levels were not due to cell loss. The controls in this experiment included the vehicle (DMSO) referred to as VEH, 10 μM DAPT (N-[N-(3,5-Difluorophenacetyl-L-alanyl)]-S-phenylglycine *t*-Butyl Ester) as a positive gamma-secretase inhibitor, and 1% v/v Triton X100 to generate full cell lysis and hence cell death. The data was shown in Figure 2 (attached as **Exhibit K**), with Aβ40 concentrations graphically represented in ng/ml and cell viability as percentage of VEH control. The results show that each of the compounds tested reduced Aβ40 levels from 14% to 42% as shown in the following table:

Agent	**% Reduction in Aβ40 Levels**
CQ	14
1076	32
1084	42
1085	25
1089	37
1090	24
1091	20

These compounds showed no or a negligible change in cell viability and hence I conclude that reduction in Aβ40 levels was due to modification of APP processing.

14. One of the agents shown to be effective in reducing Aβ40 levels in the *in vitro* assay above, clioquinol (CQ), has also been shown to be effective in reducing toxic Aβ levels *in vivo*. Ritchie and his colleagues investigated the clinical effect of CQ on the toxic accumulation of β–amyloid in humans (*Arch Neurol.* 60: 1685-1691 (2003), attached hereto as **Exhibit L**). The results of the investigation show a significant lowering of plasma Aβ42

levels over the placebo controls. Analysis of Aβ40 levels in this paper shows overall trends similar to Aβ42, with significant differences between the placebo and CQ-treated groups at each major stage of the observed timeline. The drug was well tolerated and inhibited cognitive decline in patients who, untreated, otherwise experienced deterioration. See, in particular, page 1685, "Results"; and page 1686, left column, first paragraph. These results provide further support for the conclusion that cation (e.g., zinc) chelators capable of crossing BBB, which modulate the interaction between a cation with APP, will be effective in modulating treating Alzheimer's Disease.

15. It is therefore my opinion that based on the teaching of the '924 application, those skilled in the art would be able to readily identify a zinc-binding agent which crosses the blood brain barrier and which modulates the interaction between zinc and/or heparin and APP, and to administer such an agent in an effective amount to a patient to treat Alzheimer's Disease in the patient.

16. I declare that all statements made herein of my own knowledge are true and that all statements made on information and belief are believed to be true; and that further that these statements were made with knowledge that wilful false statements and the like so made are punishable by fine or imprisonment, or both, under Section 1001 of Title 18 of the United States Code and that wilful false statements may jeopardise the validity of the Application or any patent issuing therefrom.

Dated this 6th day of September 2005.

Roberto CAPPAI

EXHIBIT A

(Curriculum Vitae)

Curriculum Vitae

Name:	Roberto **CAPPAI**
Date of Birth:	15th October 1964
Country of Birth:	Australia
Marital Status:	Married
Address:	27 Barkers Road, Kew, Victoria, 3101 Australia
Phone:	03-8344 5882 (work) 03-9852 7349 (home)
Fax:	03-8344 4004 (work)
E.mail:	r.cappai@unimelb.edu.au

QUALIFICATIONS

1987 B.Sc (Hons)	Monash University, Australia,
Honours Title:	The cloning, manipulation and expression of human interferon α2.
1991 Ph.D	The Walter and Eliza Hall Institute of Medical Research, The University of Melbourne, Australia
Ph.D Title:	Analysis of gene expression in *Plasmodium falciparum*.

PROFESSIONAL EXPERIENCE

Past Appointments:

1987	Research Assistant, Department of Biochemistry, Monash University, Australia
1991-93	Research Officer, The Walter and Eliza Hall Institute of Medical Research, Melbourne, Australia
1993-94	Research Officer, Department of Pathology, The University of Melbourne, Australia
1995-00	Senior Research Officer, Department of Pathology, The University of Melbourne, Australia
2000-03	Senior Research Fellow Department of Pathology, The University of Melbourne, Australia

Current Appointments:

2004-08	NHMRC Senior Research Fellow, Department of Pathology, Department of Pathology, The University of Melbourne, Australia

2004	Deputy Head of Department (until Dec 2004) Department of Pathology, The University of Melbourne, Australia
2002-	Honorary Fellow, Centre for Neuroscience, The University of Melbourne, Australia

AWARDS and SCHOLARSHIPS

1988-89 Commonwealth Postgraduate Research Award
1990 Australian Postgraduate Research Award
1998 Travel Award , 6th International Conference on Alzheimer's Disease and Related Disorders, Amsterdam
1999 Travel Award , International Society for Neurochemistry Conference, Berlin
2000 Travel Award , World Alzheimer Congress 2000, Washington
2004 Colloquium Speaker Award, Asian-Pacific Society for Neurochemistry Meeting, Hong Kong
2005 Young Investigator Award, 20th Biennial Meeting of the International Society for Neurochemistry, Innsbruck

GRANTS

Chief Investigator:

Currently held

2002-06 NHMRC Program Grant. (# 208978)
C.L. Masters, A.I. Bush, R. **Cappai**, G. Evin, A.F. Hill. K.J. Barnham, D.H. Small.
S.J. Collins, E. Storey, I Trounce
Diseases of the aging brain. ($6,525,000 total)

2003-05 Neurosciences Victoria-Schering AG (Industry Grant)
R. **Cappai**
Isolation of amyloid beta binding ligands

2004-08 NHMRC Fellowship (299980) - Senior Research Fellow + SEO ($581,250 total)

Past

1995-97 NHMRC Project Grant. (# 950562)
R. **Cappai** and C.L. Masters
Creutzfeldt-Jakob Disease: Conformation-dependent epitopes of PrP. ($140,166 total)

1995 The Hugh D.T. Williamson Foundation,
R. **Cappai**
Analysis of the neurite promoting activity of the amyloid precursor protein of Alzheimer's disease ($5,000)

1996-98 National Pituitary Hormones Advisory Council Grant.
R.**Cappai** and S.J. Collins
Investigating the normal function of the PrP molecule. ($225,677 total)

1999 NHMRC Equipment Grant.

Masters, C.L., **Cappai**, R., Evin, G., Bush, A.I.
Ultramass-700 Inductivity Couples Plasma Mass Spectrometer. ($25,000)

2000 ARC Small Grant
R. **Cappai**
Investigating how metals modulate the amyloidogenicity and neurotoxicity of the prion peptide PrP106-126 ($6,000)

2000-01 The Ramaciotti Foundation
G. Evin and R. **Cappai**
A novel genetic screening assay for Alzheimer's disease gamma-secretase ($18,000 total)

2000-02 Alzheimer's Association (USA)
R. **Cappai**
Crystallisation of the beta-secretase proteins BACE and BACE2. ($166,000 total)

2000-02 NHMRC Project Grant. (#114212)
S.J. Collins, A.R. White, R. **Cappai** and A.F. Hill
The role of oxidative stress in the patho-aetiology of prion disorders using infected cell culture and animal models. ($169,311 total)
Rolled over into NHMRC Program grant 2002-06

2001-03 NHMRC Project Grant. (#145761)
R. **Cappai**, D.H. Small
Functional studies on a neuroprotective activity of the amyloid precursor protein of Alzheimer's disease ($490,000 total)
Rolled over into NHMRC Program grant 2002-06

2001-03 NHMRC Project Grant. (# 156701)
M.W. Parker, R. **Cappai**, K.J. Barnham
Structural studies of amyloid precursor protein ($405,000 total).

2002 NHMRC Equipment Grant.
Cappai, R., Bush, A.I., Cherny, R.A., Barnham, K.J., Culvenor, J., Evin, G., Li, Q-X.
Luminescence fluorimeter-spectrometer instrument package for analysis of biochemical and cellular pathways of cell death and survival. ($66,000)

2003 NHMRC Equipment Grant.
Cappai, R., Barnham, K.J., Bush, A.I., Cherny, R.A., Culvenor, J., Evin, G., Hill A.F., Lawson V., Li, Q-X., Masters C.L. Digital data recording system comprising a Digital Chemiluminescence/UV and white light detection system and Digital Camera. ($60,000)

2004 NHMRC Equipment Grant.
Cappai, R., Barnham, K.J., Bush, A.I., Cherny, R.A., Culvenor, J., Evin, G., Hill A.F., Lawson V., Li, Q-X., Masters C.L. Brain microdialysis system ($45,500)

SUPERVISION

Post-Doctoral

1996-2001	Dr. Anthony White
2001-2003	Dr Nicholas Williamson
2001-	Dr Giuseppe Ciccotosto
2003-2004	Dr Lisa Fodero
2003-2004	Dr Feda Ali

Research Assistants

1991	Ms. Amelia Osborn
1995-96	Ms. Leanne Stewart
1995-	Ms. Denise Galatis
2001-2004	Ms. Gulcan Kocak
2003-	Ms Michelle Fodero-Tavoletti

Ph.D Students

1994-98 Ph.D. Ms. Anna Henry
Project title: Structure and function studies of the amyloid precursor protein gene family.

1995-02 Ph.D. Ms. Margaret Smith (co-supervisor)
Project title: Screening for familial Alzheimer's disease in the Australian population.

1995-02 Ph.D. Ms. Amanda Tammer (co-supervisor)
Project title: Immunological assays for diagnosing Alzheimer's disease.

1997-01 Ph.D. Ms. Leanne Stewart
Project title: Neurotoxic pathways involved in Alzheimer's disease and Prion disease .

1997-00 Ph.D. Mr. Michael Jobling (co-supervisor)
Project title: Structural analysis of the prion protein.

1997-04 Ph.D. Ms. Christa Maynard (co-supervisor)
Project title: Metals, oxidative stress and Alzheimer's disease.

1997-03 Ph.D. Mr. James Thyer. (co-supervisor)
Project Title: Identifying conformational-dependent ligands of the prion molecule.

1999-04 Ph.D. Ms. B. Elise Needham.

Project title: The role of the amyloid precursor protein family.

2000-03 Ph.D. Ms M. Fleur Sernee (co-supervisor)
Genetic screening assay for gamma secretase.

2002- Ph.D. Ms. Danielle Smith (co-supervisor)
Project title: Identification of amyloid-beta binding peptides.

2002- Ph.D. Mr. Geoffrey Kwai-Wai Kong (co-supervisor)
Project title: Structural studies of Alzheimer's disease amyloid precursor protein.

2003- Ph.D. Ms. Amee George (co-supervisor)
Project title: The effect of dietary cholesterol on aged/young mice models of AD.

2004- Ph.D. Ms. Laura Vella (co-supervisor)
Project title: Characterisation of cellular factors involved in the pathogenesis of prion disease.

2004- Ph.D. Mr. Sen Han (co-supervisor)
Project title: Identification and characterisation of disease associated epitopes of mammalian prion proteins.

Masters Student
1995-99 M.Sc. Mr. Darren Le Brocque (co-supervisor)
Project title: Proteases involved in the secretion of the Alzheimer's βA4 amyloid protein.

Honours Student
1995 B.Sc. (Honours) Mr. David Tucker.
Project title: Expression and characterization of recombinant amyloid precursor protein.

1999 B.Sc. (Honours) Mr. Stephen Luke (co-supervisor)
Project title: The role of astrocytes in neuroprotection against copper toxicity.

Third Year Students:
1995 B.Sc. Mr. David Khan: 12 week laboratory project

1996 B.Sc. Ms. Fiona Spratt: 12 week laboratory project

1997 B.Sc.	Ms. Riki Gibson (co-supervisor): 12 week laboratory project
2000 MBBS	Ms. Zeng Zeng Yap: 12 week laboratory project
2001 B.Sc	Mr. Luke Dow, Mr Elie Khalil, Mr Kenneth Liu, Mr. Tri Tran: Department of Biochemistry and Molecular Biology, Medical Genomics Project
2002 B.Sc	Ms. Carla McDeremott , Carlie Di Camillo, Analise Mutton, Kristen Burn: Department of Biochemistry and Molecular Biology, Medical Genomics Project
2003 B.Sc	Ms. Avantika Banerjee, Shan Shan Law, Naomi Mitchell, Ngoc-Anh Nguyen, Mr. Tony Manila Department of Biochemistry and Molecular Biology, Medical Genomics Project
2004 B.Sc	Ms. Elizabeth Commons, Carolyn de Graaf, Emily Remnant, Leanne Fung Department of Biochemistry and Molecular Biology, Medical Genomics Project

SCIENTIFIC PRESENTATIONS

INVITED SPEAKER

International

1989 Napa Valley	Mac Arthur Foundation -DNA Technologies Workshop
1989 Santa Cruz	Mac Arthur Foundation Consortium on the Biology of Parasitic Diseases Meeting
1999 Berlin	Max-Planck-Institute for Molecular Biology
1999 Boston	Massachusetts General Hospital
2001 Brisbane	International Congress of Toxicology Conference
2001 Buenos Aires	International Society for Neurochemistry Conference
2001 Cambridge	Copper and prion disease Workshop
2001 London	Imperial College School of Medicine, Department of Neurogenetics
2002 Miami	Neurological Aspects of Wilson's Disease Meeting
2003 Berlin	Institute for Chemistry and Biochemistry, Freie University,
2004 Hong Kong	Asian-Pacific Society for Neurochemistry Meeting
2004 Hong Kong	International Society for Neurochemistry Satellite Meeting on Metal-induced Neurodegeneration
2004 Lund	Neurobiology Club, Lund University
2005 Innsbruck	Young Investigator Colloquia, International Society for Neurochemistry

National

2000 Brisbane	University of Queensland, Institute for Molecular Bioscience

	Centre for Drug Design and Development
2001 Brisbane	Australian Neuroscience Society Meeting
2001 Sydney	Red Cross Blood Centre
2002 Wollongong	Protein Conformational Diseases and Therapeutics Meeting
2003 Adelaide	Bio Innovation SA's 3rd Networking Forum

Local

1995 Melbourne	International Workshop on Creutzfeldt-Jakob Disease
1995 Melbourne	Workshop on Yeast *Pichia pastoris* expression system
1996 Melbourne	The University of Melbourne, Neuroscience Society Seminar
1998 Melbourne	The University of Melbourne, Department of Anatomy and Cell Biology
1998 Melbourne	La Trobe University, School of Biochemistry
1998 Melbourne	The University of Melbourne, Department of Biochemistry and Molecular Biology, Protein Expression Workshop
2000 Lorne	Lorne Protein Conference
2000 Melbourne	Monash University, Department of Biochemistry and Molecular Biology
2000 Melbourne	The University of Melbourne, Department of Biochemistry and Molecular Biology. Mini-symposium on metal ions
2002 Melbourne	Neurosciences Victoria Symposium- Neuroprotection in epilepsy and other neurodegenerative disorders
2002 Melbourne	The University of Melbourne, Department of Genetics
2002 Melbourne	Neurosciences Victoria Seminar Series, Monash University
2003 Melbourne	Brain and Mind Symposium
2004 Melbourne	Science Teachers' Association of Victoria VCE Psychology Conference

CONFERENCE PRESENTATIONS

International

1990 Woods Hole	Poster	Molecular Parasitology Meeting
1995 Harlow	Oral	SmithKline Beecham Symposium of the Alzheimer's Amyloid Research Collaboration
1998 Amsterdam	Oral	6th International Conference on Alzheimer's Disease and Related Disorders
1999 Berlin	Poster	International Society for Neurochemistry
1999 Miami	Oral	US Society for Neuroscience
2000 Washington	Poster	World Alzheimer Congress
2002 Stockholm	Poster	World Alzheimer Congress
2004 Philadelphia	Oral	9th International Conference on Alzheimer's Disease and Related Disorders

National

1990 Lorne	Poster	Protein Conference
1991 Lorne	Oral	Australian Society of Parasitology
1993 Lorne	Poster	Protein Conference
1995 Lorne	Poster	Protein Conference
1998 Lorne	Poster	Protein Conference
1999 Lorne	Poster	Protein Conference

2001 Lorne	Poster	Protein Conference
2002 Lorne	Poster	Protein Conference
2003 Lorne	Poster	Protein Conference
2003 Queensland	Poster	Australian Peptide Conference
2005 Perth	Oral	Australian Neuroscience Society

CONFERENCE CHAIRPERSON

2003 Lorne Protein Conference Proposed and chaired session on "Metallobiology of Proteins

2003 ComBio (Melbourne) Invited chairperson for session on "Protein folding and aggregation in disease."

2003 International Peptide Meeting, Daydream Island Australia. Invited co-chairperson for session on "Neuropeptides"

2005 Biomolecular Dynamics and Interactions Symposium (Melbourne), Invited chairperson for session on Protein misfolding and assembly of higher order structures

2005 International Society for Neurochemistry Innsbruck, Proposed and to chair symposium on Neurodegenerative diseases.

COLLABORATIONS

1994-With Dr. Michael Parker (St Vincents Institute of Medical Research, Victoria, Australia) on determining the crystal structure of the amyloid precursor protein (APP) of Alzheimer's disease.

1996-00 With Dr. Colin Barrow (School of Chemistry, The University of Melbourne, Australia) on the physical characterization of the prion protein and its peptides.

1998-With Professor Elsdon Storey (Alfred Hospital, Victoria, Australia) on the expression of the spinocerebellar ataxia (SCA) disease causing proteins.

1998-With Dr. Erich Wanker (Max-Planck-Institut fuer Molekulare Genetik, Berlin, Germany) on the screening of aggregation inhibitors to the amyloid ß (Aß) peptide of Alzheimer's disease.

1998-With Dr. Gerd Multhaup (ZMBH-Center for Molecular Biology, Heidelberg, Germany) on studying how the interaction between copper and the APP-family and Aβ is involved in the genesis of Alzheimer's disease.

1998-Assoc Prof James Camakaris, (Department of Genetics, The University of Melbourne, Australia) on the interaction between copper and the APP-family in the modulation of copper homeostasis.

2000-03 With Dr Perry Bartlett (The Walter and Eliza Hall Institute of Medical Research) on the role of the presenilin proteins in modulating the actions of the notch protein in neuronal differentiation.

2001-With Dr Joseph Kourie (Department of Chemistry, The Australian National University) on the channel forming properties of amyloid proteins.

2002-With Dr John Carver (Department of Chemistry, University of Wollongong) structure-function studies on the chaperone activity of alpha-synuclein.

2002-With Dr Luke Miles (St Vincents Institute of Medical Research, Victoria, Australia) on the application of cell-free protein expression for the structural determination of the α-synuclein protein of Parkinson's disease and the multi-protein γ-secretase enzyme complex.

2003- With Drs Olav Andersen and Thomas Willnow (Max-Delbrück-Center for Molecular Medicine, Berlin, Germany) on the interaction between the amyloid precursor protein and lipoprotein receptor molecules.

2003-With Dr David de Pomerai (School of Life and Environmental Sciences. University of Nottingham, UK) on the development of α-synuclein transgenic *Caenrhabditis elegans* models of Parkinson's disease.

2003-With Dr Lars-Åke Fransson (Department of Cell and Molecular Biology, Lund University, Lund Sweden) on the interaction between the amyloid precursor protein and glypican-1.

Departmental Collaborations

1995-With Dr Genevieve Evin on studying the proteases involved in the processing of APP and the generation of the Aβ peptide.

1996-With Dr. Qiao-Xin Li on the generation and analysis of an APP transgenic mouse and the role of the synuclein protein in Parkinson's disease.

1996-With Dr Robert Cherny on studying the properties of recombinant Aβ peptides.

1998-Assoc Prof Ashley Bush on studying how the interaction between copper and the APP-family and Aβ is involved in Alzheimer's disease pathogenesis.

2000-02 With Dr David Small on studying the neuritogenic and neuroprotective activity of the amyloid
precursor protein.

2000- Dr Kevin Barnham structural studies on molecules implicated in neurodegenerative diseases.

TEACHING EXPERIENCE

1994	Lecture, Molecular Pathology 531-304/305
	Co-coordinator Neoplastic Section of Molecular Pathology 531-304/305
	Exam Assessor, Molecular Pathology 531-304/305

	Assessor, Cellular Pathology Course Projects 531-303 Assessor, Pathology Honours Course 531-400
1995	Lecture, Molecular Pathology 531-304/305 Co-organizer of Pathology Honours Course 531-400 Lecture, Pathology Honours Course 531-400 Assessor, Pathology Honours Course 531-400 Practical Class, Molecular Pathology 531-304/305
1996	Lecture, Pathology Honours Course 531-400 Assessor, Pathology Honours Course 531-400 Lectures (two), Molecular Pathology 531-304/305 Lecture, Cellular Pathology 531-303 Practical Class, Molecular Pathology 531-304/305
1997	Lecture, Pathology Honours Course 531-400 Assessor, Pathology Honours Course 531-400 Lectures (three), Molecular Pathology 531-304/305 Lecture, Cellular Pathology 531-303 Practical Class, Molecular Pathology 531-304/305
1998	Lecture, Pathology Honours Course 531-400 Assessor, Pathology Honours Course 531-400 Lectures (three), Molecular and Genetic Basis of Disease 531-302
1999	Lecture, Pathology Honours Course 531-400 Assessor, Pathology Honours Course 531-400 Lectures (three), Molecular and Genetic Basis of Disease 531-302
2000	Lecture, Pathology Honours Course 531-400 Assessor, Pathology Honours Course 531-400 Lectures (three), Molecular and Genetic Basis of Disease 531-303
2001	Lecture, Pathology Honours Course 531-400 Lectures (three), Molecular and Genetic Basis of Disease 531-303
2001	Medical Genomics course- project supervisor
2002	Medical Genomics course- project supervisor Lecture, Pathology Honours Course 531-400 Assessor, Pathology Honours Course 531-400 Lectures (one), Molecular and Genetic Basis of Disease 531-303
2003	Medical Genomics course- project supervisor Lecture, Pathology Honours Course 531-400 Assessor, Pathology Honours Course 531-400 Lecture, Molecular and Genetic Basis of Disease 531-303

2004 Medical Genomics course- project supervisor
Lecture, AMS Student
Lecture, Pathology Honours Course 531-400
Lecture, Molecular and Genetic Basis of Disease 531-303

COMMITTEES

Current
1998- Member, Environmental Health and Safety Committee, Department of Pathology
1998- Member, Occupational Health and Safety Committee, The University of Melbourne
2001- Co-organiser, Neurosciences Victoria Seminar series (Parkville node)
2003- Member, Environmental Health and Safety Committee Faculty of Medicine, Dentistry and Health Sciences
2003- Chairman, University of Melbourne-PRANA Biotechnology Scientific Management Committee
2003- Member, Neurosciences Victoria Neurogenomics & Neuroproteomics Platform Committee.
2004- Member, Faculty of Medicine, Dentistry and Health Sciences Grant Mentoring Scheme.
2004- Member, Departmental Executive Committee, Department of Pathology

Past
1996-97 Occupational Health and Safety Committee, Department of Pathology and Faculty of Medicine
1995-02 Academic Liason Officer (Department of Pathology)
1998-02 ARC Grants Mentor, Department of Pathology
1998-02 Member, Building Emergency Controllers Committee, Faculty of Medicine, Dentistry and Health Sciences
2002-04 Member, Department of Pathology- IT committee

THESIS EXAMINER

2002 Ph.D Thesis Ms. Filomena Li (La Trobe University)

PROFESSIONAL AFFILIATIONS

Australian Society of Biochemistry and Molecular Biology
Australian Neuroscience Society
Society for Neuroscience , USA
National Association of Research Fellows of NHMRC

GRANTS REVIEWER

2004- Member, Grant Review Panel (Peripheral and Cellular Nervous System), National Health and Medical Research Council of Australia

Ad hoc reviewer for:
National Health and Medical Research Council, Australia

Alzheimer Forschung Initiative, Germany
Australian Research Council, Australia
Neurological Foundation of New Zealand
Alzheimer Association-USA
Medical Research Council, UK

EDITORIAL BOARDS

Journal of Neurochemistry: Reviews Advisory Board

JOURNAL REVIEWER

Ad hoc reviewer for:

- Journal of Neuroscience
- Journal of Neurochemistry
- Biochemistry
- British Journal of Pharmacology.
- The International Journal of Biochemistry and Cell Biology
- Free Radical Biology & Medicine
- European Journal of Neuroscience
- Brain Research
- Chemico-Biological Interactions
- BMC Biochemistry
- Neurobiology of Aging

CONSULTANCIES

Prana Biotechnology LTD

COMMERCIAL ACTIVITIES

1995-1997 Smith Kline Beecham- Project leader studying the structure function relationships of the amyloid precursor protein.

1998-2000 Merck Sharp Dohme- collaborator on project studying gamma-secretase

1999-2000 Red Cross Australia- Project leader on developing monoclonal antibodies to the prion protein

2000- Prana Biotechnology- Project leader on drug screening for Alzheimer drugs

2002- Member, Prana Biotechnology Focus Team

2003- Schering AG-Neurosciences Victoria-Prana Biotechnology- Project leader on Aβ binding proteins

PATENTS

Henry A., **Cappai** R., Beyreuther K., Masters C.L., (1997). SmithKline Beecham. Use of the amyloid precursor protein as an anti-thrombotic agent for human use. UK patent.

Barnham, K.J., **Cappai** R., Parker M.J. (2001) Method of screening for inhibitors of Alzheimer's disease. Australian patent. PCT/AU01/01603

PUBLICATIONS (Total 1989-2004: 90)

Refereed Journal Article

89.1 **Cappai**, R., van Schravendijk, M.R., Anders, R.F., Peterson, M.G., Thomas, L.M., Cowman, A.F. and Kemp, D.J. Expression of the RESA gene in *Plasmodium falciparum* isolate FCR3 is prevented by a subtelomeric deletion. **Molecular and Cellular Biology**. (1989) 9, 3584-3587.

92.1 **Cappai**, R. and Cowman, A.F. The *Plasmodium falciparum* hypoxanthine-guanine phosphoribosyl transferase gene has a 5' upstream intron. **Molecular and Biochemical Parasitology**. (1992) 54, 117-120.

92.2 **Cappai**, R., Kaslow, D.C., Peterson, M.G., Anders, R.F., Cowman, A.F. and Kemp, D.J. Cloning and analysis of the RESA-2 gene: a DNA homologue of the ring-infected erythrocyte surface antigen gene of *Plasmodium falciparum*. **Molecular and Biochemical Parasitology**. (1992) 54, 213-222.

93.1 **Cappai, R**., Osborn, A.H., Gleeson, P.A. and Handman, E. Cloning and characterization of a Golgi-associated GTP-binding protein homologue from *Leishmania major*. **Molecular and Biochemical Parasitology**. (1993) 62, 73-82.

94.1 **Cappai**, R., Morris, L., Aebischer, T., Bacic, A., Curtis, J.M., Kelleher, M., McLeod, K.S., Moody, S.F., Osborn, A.H. and Handman, E. Ricin-resistant mutants of *Leishmania major* cause lesions in BALB/c mice. **Parasitology.** (1994) 108, 397-405.

94.2 **Cappai**, R., Osborn, A.H. and Handman, E. Cloning and sequence of a *Leishmania major* homologue to the fibrillarin gene. **Molecular and Biochemical Parasitology**. (1994) 64, 353-355.

94.3 Symons, F., Murray, P.J., Hong, L., Simpson, R.J., Osborn, A.H., **Cappai**, R. and Handman, E. Characterization of a polymorphic family of integral membrane proteins in promastigotes of different *Leishmania* species. **Molecular and Biochemical Parasitology**. (1994) 67, 103-113.

95.1 Handman, E., Osborn, A.H., Symons, F., van Driel., R. and **Cappai**, R. The *Leishmania* promastigote surface antigen 2 complex is differentially expressed during the parasite life cycle. **Molecular and Biochemical Parasitology.** (1995) 74, 189-200.

95.2 Evin, G., **Cappai**, R., Li, Q-X., Culvenor, J., Small, D.H., Beyreuther, K. and Masters, C.L. Candidate γ-secretases in the generation of the carboxyl-terminus of the Alzheimer's disease ßA4 amyloid: Possible involvement of cathepsin D. **Biochemistry**. (1995) 34, 14185-14192.

96.1 Williamson, T.G., Mok, S.S., Henry, A., **Cappai**, R., Lander, A.D., Nurcombe, V., Beyreuther, K., Masters, C.L. and Small, D.H. Secreted glypican binds to amyloid precursor protein of Alzheimer's disease (APP) and inhibits APP-induced neurite outgrowth. **Journal of Biological Chemistry**. (1996) 271, 31215-31221.

97.1 Clarris, H.J., **Cappai**, R., Heffernan, D., Beyreuther, K., Masters, C.L. and Small, D.H. Identification of heparin-binding domains in the amyloid precursor protein of Alzheimer's disease by deletion mutagenesis and peptide mapping. **Journal of Neurochemistry**. (1997) 68, 1164-1172.

97.2 Henry, A., Masters, C.L., Beyreuther, K. and **Cappai**, R. Expression of the ectodomains of the human amyloid precursor protein in *Pichia pastoris*. **Protein Expression and Purification**. (1997) 10, 283-291.

97.3 Culvenor, J G., Maher, F., Evin, G., Malchiodi-Albedi, F., **Cappai**, R., Underwood, J.R., Davis, J.B., Karran, E.H., Roberts, G.W., Beyreuther, K. and Masters, C.L. Alzheimer's disease-associated presenilin 1 in neuronal cells: evidence for localization to the endoplasmic reticulum-golgi intermediate compartment. **Journal of Neuroscience Research**. (1997) 49, 1-13.

97.4 Bayer, T.A., Weggen. S., Hesse, L., **Cappai**, R., Masters, C.L., Beyreuther, K. and Multhaup, G. Distribution of amyloid precursor-like protein 2 in normal and Alzheimer´s disease hippocampal formation. **Alzheimer's Research**. (1997) 3, 199-203.

97.5 Mok, S.S., Sberna, G., Heffernan, D., **Cappai**, R., Galatis, D., Clarris, H., Sawyer, W. H., Beyreuther, K., Masters, C.L. and Small, D.H. Expression and analysis of heparin-binding regions of the amyloid precursor protein of Alzheimer's disease. **FEBS Letters**. (1997) 415, 303-307.

98.1 Potsuma, R.B., Martins, R.N., **Cappai**, R., Beyreuther, K., Masters, C.L., Strickland, D.K., Mok, S.S. and Small, D.H. Effects of the amyloid protein precursor of Alzheimer's disease and other ligands of the LDL-receptor-related protein on neurite outgrowth from sympathetic neurons in culture. **FEBS Letters**. (1998) 428, 13-16.

98.2 Culvenor, J.G., Henry, A., Hartmann, T., Evin, G., Galatis, D., Friedhuber. A., Jayasena,U.L.H.R., Underwood, J.R., Beyreuther, K., Masters, C.L. and **Cappai**, R. Immunogold labelling of the Alzheimer's disease amyloid precursor protein and derived peptides expressed in a recombinant yeast system. **Amyloid: The International Journal of Experimental and Clinical Investigation.** (1998) 5, 79-89.

98.3 White, A.R., Zheng, H., Galatis, D., Hesse, L., Multhaup, G., Maher, F., Beyreuther, K., Masters, C.L. and **Cappai**, R. Survival of cultured neurons from APP knockout mice against Alzheimer's amyloid Aβ toxicity and oxidative stress. **Journal of Neuroscience.** (1998) 18, 6207-6217.

98.4 Li, Q-X., **Cappai**, R., Evin, G., Tanner, J. E., Gray, C. W., Beyreuther, K and Masters, C.L. Products of the Alzheimer's disease amyloid precursor protein generated by β-secretase are present in human platelets, and secreted upon degranulation. **American Journal of Alzheimer's Disease.** (1998) 13, 236-244.

98.5 Henry, A., Li, Q-X., Galatis, D., Hesse, L., Multhaup, G., Beyreuther, K., Masters, C.L. and **Cappai**, R. Inhibition of platelet activation by the Alzheimer's disease amyloid precursor protein. **British Journal of Haematology.** (1998) 103, 402-415.

98.6 Le Brocque, D., Henry, A., **Cappai**, R., Tanner, J.E., Galatis, D., Li, Q-X., Gray, C., Holmes, S., Underwood, J.R., Beyreuther, K., Masters, C.L. and Evin. G. Processing of the Alzheimer's disease amyloid precursor protein in *Pichia pastoris* : Immunodetection of α-, β- and γ-secretase products. **Biochemistry.** (1998) 37, 14958-14965.

99.1 Jobling, M.F., Barrow, C.J., White, A.R., Masters, C.L., Collins, S.J. and **Cappai**, R. The synthesis and spectroscopic analysis of the neurotoxic prion peptide 106-126: Comparative use of manual Boc and Fmoc chemistry. **Letters in Peptide Science.** (1999) 6, 129-134.

99.2 **Cappai**, R., Mok, S.S., Galatis, D., Tucker, D.F., Henry, A., Beyreuther, K., Small, D.H. and Masters, C.L. Recombinant human amyloid precursor-like protein 2 (APLP2) expressed in the yeast *Pichia pastoris* can stimulate neurite outgrowth. **FEBS Letters.** (1999) 442, 95-98.

99.3 Rossjohn, J., **Cappai**, R., Feil, S.C., Henry, A., McKinstry, W.J., Galatis, D., Hesse, L., Multhaup, G., Beyreuther, K., Masters, C.L. and Parker, M.W. Crystal structure of the N-terminal, growth factor-like domain of Alzheimer amyloid precursor protein. **Nature Structural Biology.** (1999) 6, 327-331.

99.4 **Cappai**, R., Stewart, L.R., Jobling, M. R., Thyer, J.M., White, A.R., Collins, S.J., Beyreuther, K., Masters, C.L. and Barrow, C.J. Familial prion disease mutation alters the secondary structure of recombinant mouse prion protein: Implications for the mechanism of prion formation. **Biochemistry.** (1999) 38, 3280-3284.

99.5 Smith, M.J., Gardner, R.J.M., Knight, M., Forrest, S.J., Beyreuther, K., Storey, E., McLean, C.A., Cotton, R.G.H., **Cappai**, R. and Masters, C.L. Early-onset Alzheimer's disease caused by a novel mutation at codon 219 of the presenilin-1 gene. **Neuroreport.** (1999) 38, 3280-3284.

99.6 White, A.R., Bush, A.I., Beyreuther, K., Masters, C.L. and **Cappai**, R. Exacerbation of copper toxicity in primary neuronal cultures depleted of cellular glutathione. **Journal of Neurochemistry.** (1999) 72, 2092-2098.

99.7 Li, Q-X., Maynard, C., **Cappai**, R., McLean, C.A., Cherny, R.A., Lynch, T., Culvenor, J.G., Trevaskis, J., Tanner, J.E., Bailey, K.A., Czech, C., Bush, A.I., Beyreuther, K. and Masters, C.L. Intracellular accumulation of detergent-soluble amyloidogenic Aβ fragment of Alzheimer's disease precursor protein in the hippocampus of aged transgenic mice. **Journal of Neurochemistry.** (1999) 72, 2479-2487.

99.8 Christie, G., Markwell, R.E., Gray, C.W., Smith, L., Godfrey, F., Mansfield, F., Howlett, D.R., Wadsworth, H., King, R., McLaughlin, M., Cooper, D.G., Ward, R.V., Hartmann, T., Lichentahler, S., Beyreuther, K., Underwood, J., Gribble, S.K., **Cappai**, R., Masters, C.L., Tamaoka, A., Gardner, R.L., Rivett, A.J., Karran, E.H and Allsop, D. Alzheimer's disease: correlation of the suppression of Aβ peptide secretion from cultured cells with inhibition of the chymotrypsin-like activity of the proteasome. **Journal of Neurochemistry.** (1999) 73, 195-204.

99.9 **Cappai, R.** and White, A.R. Molecules is Focus: Amyloid β. **The International Journal of Biochemistry and Cell Biology**. (1999) 31, 885-889.

99.10 Jobling, M.F., Stewart, L.R., White, A.R., McLean, C., Friedhuber, A., Maher, F., Beyreuther, K., Masters, C.L., Barrow, C.J., Collins, S.J. and **Cappai**, R. The hydrophobic core sequence modulates the neurotoxic and secondary structure properties of the prion peptide 106-126. **Journal of Neurochemistry.** (1999) 73, 1557-1565.

99.11 White, A.R., Collins, S.J., Maher, F., Jobling, M.F., Stewart, L.R., Thyer, J.M., Beyreuther, K., Masters, C.L. and **Cappai**, R. PrP deficient neurons reveal lower glutathione reductase activity and increased susceptibility to hydrogen peroxide toxicity. **American Journal of Pathology** (1999) 155, 1723-1730.

99.12 White, A.R., Reyes, R., Mercer, J.F.B., Camakaris, J., Zheng, H., Bush, A.I., Multhaup, G., Beyreuther, K., Masters, C.L. and **Cappai**, R. Copper levels are increased in the cerebral cortex and liver of APP and APLP2 knockout mice. **Brain Research** (1999) 842, 439-444.

99.13 White, A.R., Multhaup, G., Maher, F., Bellingham, S., Camakaris, J., Zheng, H., Bush, A.I., Beyreuther, K., Masters, C.L. and **Cappai**, R. The Alzheimer's disease amyloid precursor protein (APP) modulates copper-induced toxicity and oxidative stress in primary neuronal cultures. **Journal of Neuroscience.** (1999) 19, 9170-9179.

99.14 Borchardt, T., Camakaris, J., **Cappai**, R., Masters, C.L., Beyreuther, K. and Multhaup, G. Copper inhibits β-amyloid production and stimulates the non-amyloidogenic pathway of amyloid precursor protein (APP) secretion. **Biochemical Journal.** (1999) 344, 461-467.

99.15 Caswell, M.D., Mok, S.S., Henry, A., **Cappai**, R., Klug, G., Beyreuther, K., Masters, C.L. and Small, D.H. The amyloid β-protein precursor (APP) of Alzheimer's disease is degraded extracellularly by a Kunitz protease inhibitor domain-sensitive trypsin-like serine protease in cultures of chick sympathetic neurons. **European Journal of Biochemistry.** (1999) 266, 509-516.

00.1 Smith, M.J., Humphrey, K.E., **Cappai**, R., Beyreuther, K., Masters, C.L. and Cotton, R.G.H. Correct heteroduplex formation for mutation analysis. **Molecular Diagnosis.** (2000) 5, 63-69.

00.2 Evin, G., Le Brocque, D., Culvenor, J.G., Galatis, D., Weidemann, A., Beyreuther, K., Masters, C.L. and **Cappai**, R. Presenilin 1 expression in yeast lowers secretion of the amyloid precursor protein. **Neuroreport** (2000) 11, 405-408.

00.3 Campbell, B.C.V., Li, Q-X., Culvenor, J.G., Jäkälä, P., **Cappai**, R., Beyreuther, K., Masters, C.L. and McLean, C.A. Accumulation of insoluble α-synuclein in dementia with Lewy bodies. **Neurobiology of Disease** (2000) 7, 192-200.

00.4 Thompson A., White, A.R., Masters C.L., **Cappai** R. and Barrow C.J. Amyloidogenicity and neurotoxicity of peptides corresponding to the helical regions of PrP^{C}. **Journal of Neuroscience Research** (2000) 62:293–301.

00.5 Borchardt T., Schmidt C., Camakaris J., **Cappai** R., Masters C.L., Beyreuther K. and Multhaup G. Differential effects of zinc on amyloid precursor protein (APP) processing in copper-resistant variants of cultured Chinese hamster ovary cells. **Cellular and Molecular Biology**. (2000) 46: 785-795.

01.1 Smith M., Kwok J.B.J., McLean C.A., Kril J.J., Broe G.A., Nicholson G.A., **Cappai** R., Hallupp M., Cotton R.G.H., Masters C.L., Schofield P.R. and Brooks W.S. Variable phenotype of Alzheimer's disease with spastic paraparesis. **Annals of Neurology** (2001) 49: 125-129.

01.2 Yakubovskaya M.G., Neschastnova A.A., Humphrey K.E., Babon J.J., Popenko V.I., Smith M.J., Lambrinakos A., Lipatova Z.V., Dobrovolskaia M.A., **Cappai** R., Masters C.L., Belitsky G.A., Cotton R.G. Interaction of linear homologous DNA duplexes via Holliday junction formation. **European Journal of Biochemistry** (2001) 268: 7-14

01.3 White, A.R., Huang, X, Jobling, M.F., Barrow, C.J., Beyreuther, K., Masters, C.L., Bush, A.I., and **Cappai**, R. Homocysteine potentiates copper toxicity in primary neuronal cultures: possible risk factors in the Alzheimer's-type neurodegenerative pathways. **Journal of Neurochemistry** (2001) 76: 1509-1520

01.4 White, A.R., Guirguis, R., Brazier M.W., Jobling, M.F., Hill A.F., Beyreuther, K., Barrow, C.J., Masters, C.L., Collins, S.J. and **Cappai**, R. Sub-lethal concentrations of prion peptide PrP106-126 or the amyloid beta peptide of Alzheimer's disease activates expression of pro-apoptotic markers in primary cortical neurons. **Neurobiology of Disease** (2001) 8, 299–316

01.5 Jobling M.F., Huang X., Stewart L.R., Barnham K.J., Curtain C., Volitakis I., Perugini M., White A.R., Cherny R., Masters C.L., Barrow C.J., Collins S.J., Bush A.I., and **Cappai** R. Copper and zinc binding modulates the aggregation and neurotoxic properties of the prion peptide PrP106-126. **Biochemistry** (2001) 40, 8073-8084

01.6 Stewart L.R., Jobling M.F., Needham B.E., Maher F., Thyer J., White A.R., Beyreuther, K., Masters, C.L., Collins S.J., and **Cappai** R. Involvement of the 5-lipoxygenase pathway in the neurotoxicity of the prion peptide PrP106-126. **Journal of Neuroscience Research** (2001) 65, 565–572

01.7 Faux C.H., Turnley, A.M., Epa R., **Cappai** R. and Bartlett P.F. Interactions between fibroblast growth factor and notch regulate neuronal differentiation. **Journal of Neuroscience** (2001) 21, 5587–5596

01.8 Nunan J., Shearman, M.S., Checler F., **Cappai** R., Evin G., Beyreuther K., Masters C.L. and Small D.H. The C-terminal fragment of Alzheimer's disease amyloid protein precursor is degraded by a proteaosome-dependent mechanism distinct from γ-secretase. **European Journal of Biochemistry** (2001) 268, 5329-5336

02.1 White A.R., Multhaup G., Galatis, D., McKinstry W.J., Parker M.W., Pipkorn R., Beyreuther K., Masters C.L. and **Cappai** R. Contrasting, species-dependent modulation of copper-mediated neurotoxicity by the Alzheimer's disease amyloid precursor protein. **Journal of Neuroscience** (2002) 22:365–376

02.2 Tammer A.H., Coia, G., **Cappai** R., Fuller S., Masters C.L., Hudson P., Underwood J.R. Generation of a recombinant Fab antibody reactive with the Alzheimer's disease-related peptide, β-amyloid. **Clinical and Experimental Immunology**. (2002) 129: 453-463

02.3 Evin G, Smith M.J., Tziotis A, McLean C., Canterford L., Sharples R.A., **Cappai** R., Weidemann A., Beyreuther K., Cotton R.G., Masters C.L., Culvenor J.G. Alternative transcripts of presenilin-1 associated with frontotemporal dementia. **Neuroreport** (2002)13:917-921

02.4 Hamilton J.A., Whitty G., White A.R., Jobling M.F., Thompson A., Barrow C.J., **Cappai** R., Beyreuther K., Masters C.L. Alzheimer's disease amyloid beta and prion protein amyloidogenic peptides promote macrophage survival, DNA synthesis and enhanced proliferative response to CSF-1 (M-CSF). **Brain Research** (2002) 940:49-54

02.5 Simons A., Thomas Ruppert T., Schmidt C., Schlicksupp A., Pipkorn R., Reed J., Masters C.L., **Cappai** R., Beyreuther K., Bayer T.A. and Multhaup G. Evidence for a copper-binding superfamily of the amyloid precursor protein. **Biochemistry** (2002) 41: 9310-9320

02.6 Opazo C., Huang X., Cherny R.A:, Moir R.D., Roher A.E., White A.R., **Cappai** R., Masters, C.L., Tanzi R.E., Inestrosa N.C. and Bush A.I. Metalloenzyme-like activity of Alzheimer's disease β-amyloid: Cu-dependent catalytic conversion of dopamine, cholesterol and biological reducing agents to neurotoxic H_2O_2 **Journal of Biological Chemistry** (2002) 277: 40302–40308

02.7 Maynard C.J., **Cappai** R., Volitakis I., Cherny, R.A., White A.R., Beyreuther K., Masters, C.L., Bush A.I., Li Q-X. Overexpression of Alzheimer's disease amyloid-β opposes the age-dependent elevations of brain copper and iron **Journal of Biological Chemistry** (2002) 277: 44670–44676

03.1 White A.R. and **Cappai** R. Neurotoxicity from glutathione depletion is dependent on extracellular trace copper. **Journal of Neuroscience Research** (2003) 71: 889-897

03.2 Sernee M.F., Evin G., Culvenor J.G., Villadangos J.A., Beyreuther K., Masters C.L. and **Cappai** R. Selecting cells with different Alzheimer's disease γ-secretase activity using FACS: differential effect of presenilin exon 9 deletion on γ- and ε-cleavage. **European Journal of Biochemistry** (2003) 270, 495–506

03.3 White, A.R., Maher F., Brazier M.W., Jobling, M.F., Thyer J., Stewart L.R., Thompson A., Gibson R., Masters, C.L., Multhaup G. Beyreuther, K., Barrow, C.J., Collins, S.J. and **Cappai**, R. Diverse fibrillar peptides directly bind the Alzheimer's amyloid precursor protein and amyloid precursor-like protein 2 resulting in cellular accumulation. **Brain Research** (2003) 966, 231-244.

03.4 Kourie J.I., Kenna B.L., Tew D., Jobling M.F., Curtain C.C., Masters C.L., Barnham K.J. and **Cappai** R. Copper modulation of ion channels of PrP[106-126] mutant prion peptide fragments. **Journal of Membrane Biology** (2003) 193, 35-45

03.5 Barnham K.J, McKinstry W.J., Multhaup G., Galatis D., Morton C.J., Curtain C.C., Williamson N.A., White A.R., Hinds M.G., Norton R.S., Beyreuther K., Masters C.L., Parker M.W. and **Cappai** R. Structure of the Alzheimer's disease amyloid precursor protein copper binding domain: a regulator of neuronal copper homeostasis. **Journal of Biological Chemistry** (2003) 278:17401-17407

03.6 Bahadi R., Farrelly P.V., Kenna B.L., Curtain C.C., Masters C.L., **Cappai** R., Barnham K.J.,and Kourie J.I. Cu^{2+}-induced modification of the kinetics of Aβ[1-42] channels. **American Journal of Physiology-Cell Physiology** (2003) 285: C873–C880

03.7 Barnham K.J, Ciccotosto G.D., Tickler A.K., Ali F.E., Smith D.G., Williamson N.A., Lam Y-H., Carrington D., Tew D., Kocak G., Volitakis I., Separovic F., Barrow C.J., Wade J.D., Masters C.L., Cherny R.A., Curtain C.C., Bush A.I.,. and **Cappai** R. Neurotoxic, redox-competent Alzheimer's β-amyloid is released from lipid membrane by methionine oxidation. **Journal of Biological Chemistry** (2003) 278: 42959–42965.

04.1 White, A.R., Barnham K.J., Huang X., Volitakis I., Beyreuther K., Masters, C.L., Cherny R.A., Bush A.I. and **Cappai**, R. Iron inhibits neurotoxicity induced by trace copper and biological reductants. **Journal of Biological Inorganic Chemistry** (2004) 9: 269–280.

04.2 Barnham K.J, Haeffner F., Ciccotosto G.D., Curtain C.C., Tew D., Mavros C., Beyreuther K., Carrington D., Masters C.L., Cherny R.A., **Cappai** R. and Bush A.I. Tyrosine gated electron transfer is key to the toxic mechanism of Alzheimer's disease β-amyloid. **FASEB Journal** (2004) 18: 1427-1429

04.3 Rekas A., Adda C.G., Aquilina J.A., Barnham ,K.J. Sunde M., Galatis D., Williamson ,N.A. Masters C.L., Anders R.F.,. Robinson C.V., **Cappai** R. and Carver J.A. Interaction of the molecular chaperone αβ-crystallin with α-synuclein: effects on amyloid fibril formation and chaperone activity. (2004) **Journal of Molecular Biology** (2004) 340: 1167-1138

04.4 Culvenor J.G., Smith M.J., Sharples R.A., Evin G., McLean C.A. Dean B., Pavey G., Fantino E., Cotton R.G., Imaizumi K., Masters C.L. and **Cappai** R. Expression of Truncated

Presenilin 2 Splice Variant in Alzheimer's Disease, Bipolar Disorder, and Schizophrenia Brain Cortex. **Molecular Brain Research** (2004) 127: 128-135.

04.5 Bellingham S.S., Ciccotosto G.D., Needham B.E., Fodero L.R., White A.R., Masters C.L., **Cappai** R*. and Camakaris* J. Gene knockout of Amyloid Precursor Protein and Amyloid Precursor-like Protein-2 increases cellular copper levels in primary mouse cortical neurons and embryonic fibroblasts. **Journal of Neurochemistry** (2004) 91: 423–428. *joint corresponding authors

04.6 Ciccotosto G.D., Tew D., Curtain C.C., Smith D., Carrington D., Masters C.L., Bush A.I., Cherny R.A., **Cappai** R and Barnham K.J. Enhanced toxicity and cellular binding of a modified Amyloid β Peptide with a methionine to valine substitution. **Journal of Biological Chemistry** (2004) 279 42528–42534

04.7 Treiber C., Simons A., StraussM., Hafner M., **Cappai** R., Bayer T.A. and Multhaup G. Clioquinol mediates copper uptake and counteracts Cu efflux activities of the amyloid precursor protein of Alzheimer's disease. **Journal of Biological Chemistry** 279: 51958–51964

04.8 Kong K-W., Galatis D., Barnham K.J., Polekhina G., Adams J.J., Masters C.L., **Cappai** R., Parker M.J. and M^{c}Kinstry W.J. Crystallisation and preliminary crystallographic studies of the copper binding domain of the amyloid precursor protein of Alzheimer's disease. **Acta Crystallographica D** (accepted 15th November 2004)

04.9 Crouch P.J., Blake R., Duce J.A. , Ciccotosto G.D., Li Q-X., Barnham K.J., Curtain C.C., Cherny R.A., **Cappai** R., Dyrks T., Masters C.L. and Trounce I.A. Copper-dependant inhibition of human cytochrome c oxidase by a dimeric conformer of Aβ1-42. **Journal of Neuroscience** (accepted 25th November 2004)

Total Refereed Journal Articles (1989-2004): 71

Review

R1 Collins, S.J., **Cappai**, R. and Masters, C.L. Recent developments in the transmissible spongiform encephalopathies: implications for clinical practice. **Journal of Clinical Neuroscience.** (1996) 3, 1-5.

R2 Sberna, G., **Cappai**, R., Henry, A. and Small, D.H. Advantages of the methylotrophic yeast *Pichia pastoris* for high level expression and purification of heterologous proteins. **Australian Biotechnology.** (1996) 6, 82-87.

R3 Bayer, T.A., **Cappai**, R., Masters, C.L., Beyreuther, K. and Multhaup, G.
It all sticks together-the APP-related family of proteins and Alzheimer's disease. **Molecular Psychiatry.** (1999) 4, 524-528

R4 Storey, E. and **Cappai**, R. The amyloid precursor protein of Alzheimer's disease and the Aβ peptide. **Journal of Neuropathology and Applied Neurobiology.** (1999) 25, 81-97.

R5 Multhaup, G., Hesse, L., Borchardt, T., Ruppert, T., **Cappai**, R., Masters, C. L., and Beyreuther, K. Autoxidation of amyloid precursor protein and formation of reactive oxygen species. **Advances in Experimental Medicine and Biology.** (1999) 448, 183-92.

R6 Multhaup, G.,Scheuermann, S., Schlicksupp, A., Simons, A., Strauss, M., ,Kemmling, A., Oehler, C., **Cappai**, R., Pipkorn, R. and Bayer, T.A. Possible mechanisms of APP-mediated oxidative stress in Alzheimer‘s disease. **Free Radicals In Biology and Medicine** (2002) 33: 45-51.

R7 Brazier, M.W., **Cappai** R. and Collins S.J. Prions in skeletal muscle. **Australian Veterinary Journal** (2002) 80: 84-485

R8 Ciccotosto G.D., Barnham K.J., Cherny R.A., Masters C.L., Bush A.I., Curtain C.C., **Cappai** R. and Tew D. Methionine oxidation: implications for the mechanism of toxicity of the β-amyloid peptide from Alzheimer's disease. **Letters in Peptide Science** (2003) 10: 413–417

R9 Barnham K.J., Cherny R.A., **Cappai** R., Melov S., Masters C.L. and Bush A.I Metal-Protein Attenuating Compounds (MPACs) for the treatment of Alzheimer's disease. **Drug Design Reviews – Online** (2004) 1: 75-82

R10 Maynard C.J., Bush A.I., Masters C.L. **Cappai** R. and Li Q-X. Metals and Amyloid-β in Alzheimer's disease. **Brain Pathology** (in press)

Book Chapter

B1 **Cappai**, R. and Kemp, D.J. Application of recombinant DNA technology to genetic analysis of sporozoan parasites. In. **Animal Parasite Control Utilising Biotechnology.** (ed W. K Yong) CRC Press Inc., Florida. (1992) pp 9-24.

B2 Kemp, D.J. and **Cappai**, R. Analysis of the genomes of protozoan parasites using PFGE. In. **Pulsed field gel electrophoresis: A practical approach**. (ed A.P Monaco) IRL Books., Oxford. (1995) pp 177-191.

B3 Williamson, T.G., Clarris, H.J., Mok, S.S., Henry, A., **Cappai**, R., Nurcombe, V., Beyreuther, K., Masters, C.L. and Small, D.H. Secreted glypican binds to amyloid precursor protein (APP) of Alzheimer's disease and inhibits APP-induced neurite outgrowth. In, **Alzheimer's Disease: Biology, Diagnosis and Therapeutics.** (ed. K. Iqbal, B. Nishimura, M. Takeda and H. M. Wisniewski) John Wiley and Sons Ltd. London. (1997) pp 413-427.

B4 Multhaup, G., Masters, C L., Beyreuther, K. and **Cappai**, R. The biological activities and function of the amyloid precursor protein of Alzheimer's disease. In: **The Molecular Biology of Alzheimer's disease - Genes and Mechanisms Involved in Amyloid Generation.**
(ed. C. Haass) Harwood Academic Publishers, Amsterdam. (1998) pp 75-94.

B5 **Cappai**, R. Jobling, M.F. Barrow, C.J. and Collins, S.J. Structural Biology of Prions. In: **Contributions To Microbiology, Prions - A Challenge for Science, Medicine and**

Public Health System. (eds. H.F. Rabenau, J. Cinatl, H.W. Doerr) Karger Publishers, Basel. (2001) pp 32-47.

B6 **Cappai** R. Metals modulate the aggregation and neurotoxic properties of the prion peptide PrP106-126 Biology of Prions. In: **Prion Diseases and Copper Metabolism.** (eds. D.R. Brown) Horwood Publishing, Chichester. (2002) pp: 108-118.

B7 Evin G, Sernee M.F., Barnham K.J., Damian Holsinger R. M., Culvenor J.G., Hoke D, Li Q-X., Smith D., Maynard C., Tickler A., Huang X., Opazo C., Carrington D., Kocak G., Volitakis I., Mok S.S., Ciccotosto G., Williamson N.A., Beyreuther K., Wade J., Curtain C.C., Cherny R.A., Bush A.I., Masters C.L. and **Cappai** R. Modulation of Alzheimer's Disease Aβ pathways for rational therapeutic intervention : secretase inhibition and metalloprotein active compounds. In: **Alzheimer's Disease and Related Disorders: Research Advances** (eds. K. Iqbal, and Bengt Winblad,) (2003) pp:513-523

B8 **Cappai** R and Collins, S.J. Structural Biology of Prions. In: **Contributions To Microbiology, Prions. A Challenge for Science, Medicine and the Public Health System.** (eds. H.F. Rabenau, J. Cinatl, H.W. Doerr) Karger Publishers, Basel. (2003) pp:14-32

B9 McKinstry W.J., Feil S.C., Galatis D., **Cappai** R. and Parker M.W. Strategies for crystallizing the N-terminal, growth factor domain of amyloid precursor protein. In: **Amyloid Precursor Protein. A Practical Approach**. (eds. H. Xu and W. Xia) CRC Press (2004) (in press)

B10 Vella L., Hill A.F. and **Cappai** R. Mechainisms of prion toxicity and its relation to prion infectivity. In: **Neurodegeneration and Prion disease.** (eds D.R. Brown) Springer, Massachusetts (in press)

Conference Abstracts (published)

Le Brocque, D.S., Evin, G., Henry, A., **Cappai**, R., Fuller, S. Beyreuther, K. and Masters, C.L. Characterisation of APP secretases in *P.pastoris* transfected with human full length APP695 cDNA. **Neurobiology of Aging.** (1996) 17(4S): 394

Evin, G., Li, Q-X., Culvenor, J., **Cappai**, R., Mok. S.S., Hartmann, T., Beyreuther, K and Masters, C.L. Characterization of APP γ-secretase activities in human brains. **Neurobiology of Aging.** (1996) 17(4S): 401

Williamson,T.G., Mok, S.S., **Cappai**, R., Henry, A., Beyreuther, K., Masters, C.L. and Small, D.H. Glypican purified from PC12 cells binds to APP and inhibits APP-induced neurite outgrowth. **Neurobiology of Aging.** (1996) 17(4S): 325.

Hesse,L., Ruppert, T.H., Pipkorn, R., **Cappai**, R., Masters, C.L., Beyreuther, K. and Multhaup G.
Biochemical characterization of an Amyloid Precursor Protein fragment expressed at high levels in the yeast *Pichia pastoris*. **Neurobiology of Aging.** (1998) 19(4S): 455.

Cappai R., White, A., Zheng, H., Galatis, D., Maher, F., Hesse, L., Multhaup, G., Beyreuther, K., and Masters, C. Survival of cultured neurons from APP knockout mice against Alzheimer's amyloid Aβ toxicity and oxidative stress: a compensatory role for APLP molecules. **Neurobiology of Aging.** (1998) 19(4S): 603.

White, A., Stewart, L., Thyer, J., Collins, S., Masters, C. and **Cappai**, R. Prion protein-deficient neurons reveal lower glutathione reductase activity and increased susceptibility to oxidative stress induced by hydrogen peroxide and glutamate. **Neurobiology of Aging.** (1998) 19(4S): 820.

Li Q., **Cappai**, R., Trevaskis, J., Tanner, J., McLean, C., Maynard, C., Bailey, K., Evin, G., Czech, C., Beyreuther, K. and Masters, C. Mutant APP-C100 expressed in transgenic mice accumulates in the aged brain. **Neurobiology of Aging.** (1998) 19(4S): 1147.

Cappai R., Stewart, L., White, A., Maher, F., Jobling, M., Galatis, D., Beyreuther, K., and Masters, C. Increased sensitivity of primary APLP2 knockout neurons to neurotoxic insults. **Journal of Neurochemistry** (1999) 73 Suppl: S18D.

Cappai R., White A., Multhaup G., K. Barnham K., McKinstry W.J., Needham B.E., Galatis D., Rossjohn J., Parker M.W. and Masters, C. The structure and function of the amyloid precursor protein. **Neurobiology of Aging.** (2000) 21 (1S): S46.

Overexpression of the β-amyloid protein regulates metal levels in transgenic mouse brain Maynard C., **Cappai** R., Volitakis I., Cherny R., White A., Beyreuther K., Masters C., Bush A., Li Q-X. Overexpression of the β-amyloid protein regulates metal levels in transgenic mouse brain **Neurobiology of Aging.** (2002) 23 (1S): S726

Cappai R., Barnham K., McKinstry W., Multhaup G., Williamson N., Galatis D., Curtain C., White A., Hinds M, Norton R., Beyreuther K., Masters C. and Parker M. Structure-function of the amyloid precursor protein copper binding domain. **Neurobiology of Aging.** (2002) 23 (1S): S1863

Semee F., Evinl G., Culvenor J., Beyreuther K., Masters C.and **Cappai** R. A fluorescent assay to monitor gamma-secretase activity on APP and Notch substrates. **Neurobiology of Aging.** (2002) 23 (1S): S686

Amyloid, the presenilins and Alzheimer's disease

John Hardy

Various mutations in the amyloid protein precursor and presenilin genes can lead to early onset, autosomal Alzheimer's disease. A series of mis-sense mutations (with one exception) in each of these genes has been shown to cause disease in a fully penetrant fashion. It has recently been shown, both *in vivo* and in model systems, that tissues expressing these mutations have increased production of amyloid (Aβ) ending at residue 42. It has also recently been shown that this form of Aβ is deposited early and selectively in the disease process and is more fibrillogenic *in vitro*. It is argued that these genetic and molecular biological data provide strong support for the veracity of the 'amyloid cascade hypothesis' for disease pathogenesis, and that this hypothesis offers a coherent framework for drug discovery.

Trends Neurosci. (1997) 20, 154–159

ALZHEIMER'S DISEASE (AD) is the most common form of dementia, accounting for about 50–70% of the typical, late-onset cases of dementia. AD is characterized clinically by a dementia of insidious onset and inexorable progression, and pathologically by the presence of large numbers of neuritic plaques and neurofibrillary tangles. The neuritic plaques, which are largely extracellular lesions, consist of a deposit of a 40–42/43 amino acid peptide called amyloid (Aβ), derived through the processing of the amyloid precursor protein (APP) (see below); the neurofibrillary tangles are intracellular lesions consisting of twisted filaments of the cytoskeletal tau protein.

Although the majority of cases of AD occur at a late age, there are many reported pedigrees in which the disease segregates as an autosomal dominant disease of early onset. There are three genetic loci now known to be important in the etiology of early onset Alzheimer's disease: the *APP* gene on chromosome 21 (Ref. 1), the presenilin 1 (*PS1*) gene on chromosome 14 (Ref. 2) and the presenilin 2 (*PS2*) gene on chromosome 1 (Ref. 3). It is now clear that mutations in all these genes alter APP processing in a precise and interesting way: the mutations all result in a shift in the metabolism of APP such that more of a 42–43 amino acid form of Aβ is produced. This is termed $A\beta_{1-42(43)}$ or, in this review, 'long Aβ' to distinguish it from the more prevalent species of Aβ that has just 40 residues, $A\beta_{1-40}$, or 'short Aβ'. The purpose of this review is to discuss the genetics of early onset AD and the molecular effects of the pathogenic mutations in APP and the presenilins (PS), and to highlight the probable role of long Aβ in disease pathogenesis in general.

APP structure, function and metabolism, and the effects of the pathogenic mutations

John Hardy is at the Mayo Clinic Jacksonville, 4500 San Pablo Rd, Jacksonville, FL 32224, USA.

APP is a single transmembrane (TM) domain protein with multiple alternate transcripts[4], which is expressed ubiquitously. Despite intensive study, the functions of APP have not yet been defined. Mice in which the *APP* gene has been disrupted 'fail to thrive', but do not have a biochemically definable phenotype[5].

APP has a short half-life and is metabolized rapidly down two pathways in all cells. The α pathway involves cleavage between residues 687 and 688 of APP (Ref. 6) [this cleavage is described as the α-secretase process, although the enzyme(s) responsible for it has(ve) not been characterized], followed by cleavage somewhere C-terminus of residue 712 (Ref. 7) [this cleavage is described as the γ-secretase process, although again the enzyme(s) responsible for it has(ve) not been characterized]. The α pathway does not yield Aβ, as the α cut occurs within the Aβ domain. The β pathway involves cleavage between residues 671 and 672 of APP (Ref. 8) [this cleavage is described as the β-secretase process, although the enzyme(s) responsible for it has(ve) not been characterized], followed by cleavage somewhere C-terminus of residue 712 (Ref. 7) (by 'γ-secretase'). This pathway yields Aβ. Of key importance in this pathway is the position of the 'γ-secretase' cleavage (Fig. 1). If the cut is at residue 712–713, short Aβ is the result; if it is cut after residue 714, long Aβ is the result. Thus, the γ-secretase process is central to the production of long Aβ. There are several possibilities to explain this process: either different enzymes are responsible for the different cleavage positions, or there is a single enzyme with sloppy specificity, or there is cleavage distal to residue 714 followed by carboxypeptidase nibbling back. Which of these possibilities is correct is not yet clear[9,10].

A total of five mutations have been described in the *APP* gene that lead purely to AD (Fig. 1; Table 1). In addition, a further mutation, (A692G) has been described that leads to AD in some cases and cerebral hemorrhages and angiopathy in others[11]. The first mutation described in APP (G693Q) leads to cerebral angiopathy through the deposition of Aβ in the cerebral vasculature. The AD-causing APP mutations typically lead to a disease with an onset age from 45–60 years, with the precise onset age typically being influenced by the apolipoprotein E genotype[12].

The biochemical effects of the APP mutations on APP processing have been studied extensively (Table 1).

Copyright © 1997, Elsevier Science Ltd. All rights reserved. 0166 - 2236/97/$17.00 PII: S0166-2236(96)01030-2

Those that cause the 'pure' AD phenotype all have in common the fact that they lead to the production of more long Aβ (see Table 1 and Refs 13,14). The production of long Aβ is of particular importance because long Aβ has been shown to be the earliest and most abundant species of Aβ in neuritic plaques[15], and in biophysical experiments it has been shown to be the species most prone to fibril formation[16].

These data are the intellectual underpinning of the 'amyloid cascade hypothesis' for AD (Refs 14,17,18), a version of which is illustrated in Fig. 2. Transgenic mouse models made using the APP mutations replicate some, but not all of the features of AD (Refs 19,20). A prediction of the general form of this hypothesis is that all causes of AD should have in common the feature that they make amyloid deposition more likely. The identification of the PS as pathogenic loci for AD (Refs 2,3,21,22) made testing of this hypothesis possible.

Presenilin structure, function and metabolism, and the effects of the pathogenic mutations

The PS were identified through positional cloning strategies[2,3]. They are TM proteins with six to nine TM domains[2,3,21–23]. Like APP, they appear to be expressed ubiquitously[2,3,21–23]. The first predictions were of seven TM domains[2,3,17]: however, recent data suggest that there are eight TM domains[24,25], with the N- and C-termini being cytoplasmic[22,24,25] (see Fig. 3). Both proteins show some alternate splicing, particularly of exon 8 (Refs 21,22,26). In addition, there is an alternately spliced phophorylation motif in PS1 (Ref. 22). The PS show a high degree of homology to each other[3,21,22], especially in the putative TM domains.

The functions of the PS are not understood clearly: however, there are a number of clues. Two *Caenorhabditis elegans* isologues of the PS have been identified. The first is *spe-4*, mutations in which disrupt spermatogenesis through disruption of protein trafficking in the Golgi[31]; the second is *sel-12* (Refs 24,32), mutations in which produce an egg-laying defect, probably through disruption of the Notch signaling pathway. A functional relationship between *sel-12* and PS1 is illustrated by the observation that PS1 can rescue *sel-12* mutant *C. elegans*[33,34]. Further support for a role of the PS in Notch signaling comes from the observation that PS1 knockout mice show developmental abnormalities similar to those seen in mice in which other components of the Notch system have been knocked out[35].

Presenilins, like APP, are processed, and in most systems examined the bulk of the proteins have been cleaved in exon 9 yielding a ~25 kDa N-terminus fragment and a ~19 kDa C-terminus fragment[27,36]. It is not at all clear whether the holoprotein or either or both of the protein fragments are physiologically or pathologically important.

A large number of *PS* mutations have been described (Table 2). All but one of these are mis-sense mutations: the single exception is an in-frame deletion of exon 9 (Δ9; Ref. 28) (S290C; see Table 2). This preponderance of mis-sense mutations (as opposed to frame-shift and chain-termination mutations) leads to the suggestion that the mutant proteins have a toxic gain-of-function[39]. This gain-of-function might relate to the normal function of the PS or it might be that the mutant PS inactivate the normal allele of the PS (by forming inactive dimers, for example). It is often difficult to imagine what a 'toxic gain-of-function' might be. As an illustration, if we suppose that the PS were ion channels, then a toxic gain-of-function could be imagined to be one in which the ion permeability were relaxed (allowing Ca^{2+} ions in to a Na^+ channel, for example), or one in which the channel stayed open too long: the important point is that the 'toxic gain-of-function' can easily be imagined as an exaggeration of the normal function (for a discussion of mutation mechanism and type, see Ref. 33).

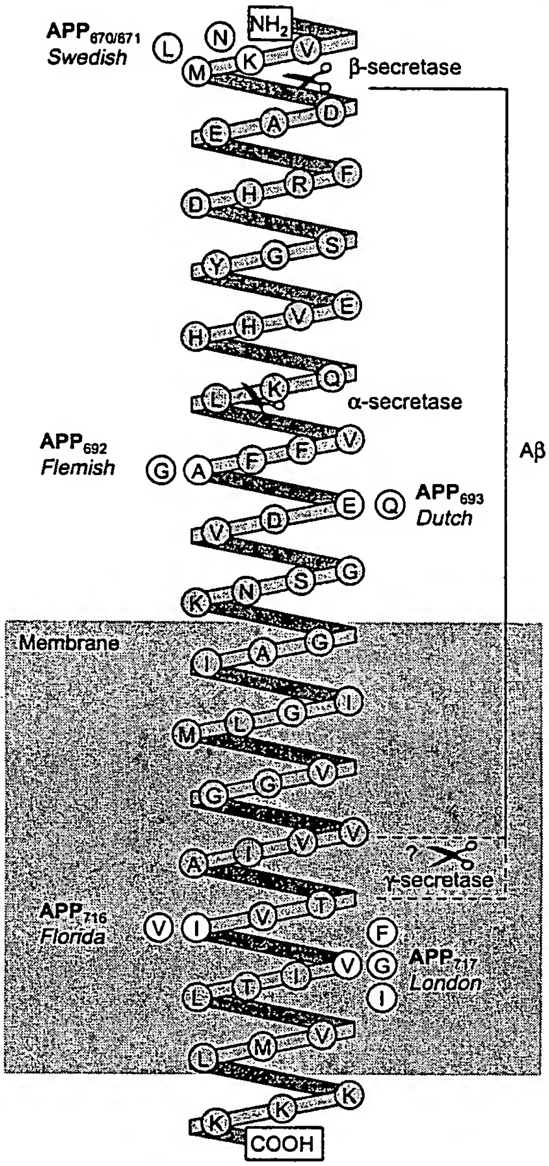

Fig. 1. *Amyloid precursor protein (APP) mutation helix. APP mutations showing the relationship between the sites of the mutations and the sites of cleavage of the perimembrane stub of APP around the Aβ part of the molecule.*

As illustrated (Fig. 3), the PS mutations occur throughout the protein, including both sides of the cleavage. While there have been reports that the mutations alter PS processing[36], this has not been found to be a general phenomenon, although the Δ9

TABLE 1. The known routes to Alzheimer's disease

Mutation	Biochemical cause	Molecular effect
Down's syndrome	More APP production	More $A\beta_{1-42(43)}$ and more $A\beta_{1-40}$
$APP_{670/671}$ (Swedish)	Potentiation of β-secretase	More $A\beta_{1-42(43)}$ and more $A\beta_{1-40}$
APP_{692} (Flemish)	Inhibition of α-secretase	More $A\beta_{1-42(43)}$
APP_{716} (Florida)	Alteration of site of γ-secretase cut	More $A\beta_{1-42(43)}$
APP_{717} (London)	Alteration of site of γ-secretase cut	More $A\beta_{1-42(43)}$
PS1 mutations	Subtle alteration of APP processing	More $A\beta_{1-42(43)}$
PS2 mutations	Subtle alteration of APP processing	More $A\beta_{1-42(43)}$

Abbreviations: Aβ, amyloid; APP, amyloid precursor protein; PS, presenilin.

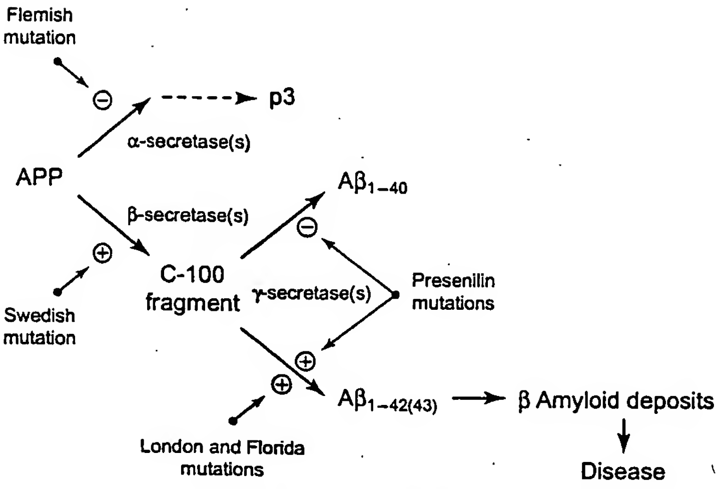

Fig. 2. *The initial steps in the amyloid cascade hypothesis. A redrawing of the initial stages of the amyloid cascade hypothesis showing the positions of the effects of mutations in amyloid precursor protein (APP) and presenilin (PS). It is not clear whether the effects of the PS mutations are direct or indirect. C-100 is the C-terminus fragment, which starts at Met621. p3 is the shorter fragment derived by α-secretase cleavage followed by β-secretase cleavage.*

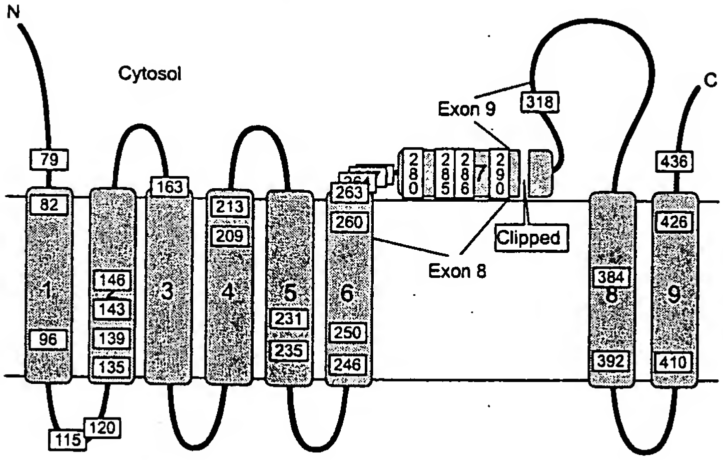

Fig. 3. *A diagram of PS1 (PS2 is similar) showing the sites of the mutations. (For a list of the mutations see Table 2.) The α-helical array of mutations in transmembrane region 2 (TM2) is apparent: however, it is also possible that residues 82 and 96 (TM1), 209 and 213 (TM4), 231 and 235 (TM5), and 246, 250, 260 and 263 (TM6) will also align. Protein segments encoded by exons 8 and 9 are shown: the former because it is alternately spliced in some tissues[22,26]; the latter because it is spliced out in the Δ9 mutation in which PS1 is not processed[27,28]. The site of cleavage of PS1 is shown (see Ref. 29): it is likely that PS2 is cleaved at around the same position[30].* Figure compiled from data in Refs 22,24,25.

mutation clearly and completely inhibits PS processing[27]. Whether inhibition or processing, especially by the Δ9 mutation, relates to the pathogenesis is not clear; however, it would fit with the idea of a gain-of-function if it led to functional overexpression of full-length protein in mutation carriers.

While the mutations are found throughout the PS proteins, their distributions are not random in several ways. First, they generally occur at residues conserved between the PS, and are also conserved in *sel-12*. Second, in relation to this, they occur largely in TM domains. Third, specifically, the cluster of mutations in TM2 line up on one side of the α-helix, suggesting that this helical face is important, probably in interacting with other TM domains or other TM proteins[22,40] (while there have been fewer mutations found in other TM domains, it is possible that this helical alignment is a general phenomenon). Fourth, the major cluster of mutations is in exon 8 (Ref. 37). This mutation cluster is interesting, both because it is close to the cleavage site and because in both PS1 and PS2 there are minor isoforms in which this exon is skipped. This suggests that this exon might be a functional domain (analogous to the Kunitz domain in APP), and that disruption of its function is central to mutation pathogenicity.

The distribution of mutations is thus of interest. It is noteworthy that the pathogenic APP mutations are in three clusters (Fig. 1; see above), and that the mutations in the different clusters have different molecular mechanisms, while leading to the same outcome. This might also be true for the PS mutations.

While the physiological roles of the PS are not clear, their effects on APP metabolism are now well documented. The first clue that the PS might have an involvement in APP trafficking came with the demonstration that plasma from individuals with PS mutations contained more long Aβ (Ref. 13). This seminal observation has now been extended into many other systems: the brains of individuals with PS mutations have particularly abundant deposits of long Aβ (Refs 37,41,42); fibroblasts from these individuals appear to produce more long Aβ (Ref. 13); transgenic animals overexpressing mutant, but not wild-type, PS1 produce more long Aβ (Refs 43–45); and cells transfected with mutant PS produce more long Aβ (Ref. 44). Thus, all the available data show very clearly that the PS can easily be accommodated in the amyloid cascade hypothesis for disease etiology (Fig. 2). Indeed, all the known and molecularly defined causes of the disease can be so accommodated (Table 1). This has two

TABLE 2. List of presenilin mutations

	Mutation	Base-pair change	Exon	Location	Homologous residue in PS1/PS2
PS1	A79V	gCc–gTc	4	N/TM1	A85
	V82L	Gtg–Ttg	4	TM1	V88
	V96F	Gtc–Ttc	4	TM1	V102
	Y115H	Tat–Cat	5	TM1/2	Y121
	Y115C	tAt–tGt	5	TM1/2	Y121
	E120K	Gaa–Aaa	5	TM1/2	E126
	E120D	gaA–gaT	5	TM1/2	E126
	N135D	Aat–Gat	5	TM2	N141
	M139V	Atg–Gtg	5	TM2	M145
	M139T	aTg–aCg	5	TM2	M145
	M139I	atG–at?	5	TM2	M145
	I143F	Att–Ttt	5	TM2	I149
	I143T	aTt–aCt	5	TM2	I149
	M146L	Atg–Ctg	5	TM2	M152
	M146V	Atg–Gtg	5	TM2	M152
	H163Y	Cat–Tat	6	TM2/3	H169
	H163R	cAt–cGt	6	TM2/3	H169
	G209V	gGa–gTa	7	TM4	G215
	I213T	aTt–aCt	7	TM4	I219
	A231T	Gcc–Acc	7	TM5	A237
	A231V	gCc–gTc	7	TM5	A237
	L235P	cTg–cCg	7	TM5	L241
	A246E	gCg–gAg	7	TM6	A252
	L250S	tTg–tCg	7	TM6	L256
	A260V	gCt–gTt	8	TM6	A266
	C263R	Tgt–Cgt	8	TM6/HP7	C269
	P264L	cCg–cTg	8	TM6/HP7	P270
	P267S	Cca–Tca	8	TM6/HP7	P273
	R269G	Cgt–Ggt	8	TM6/HP7	R275
	R269H	cGt–cAt	8	TM6/HP7	R275
	E280A	gAa–gCa	8	HP7	E286
	E280G	gAa–gGa	8	HP7	E286
	A285V	gCt–gTt	8	HP7	A291
	L286V	Ctc–Gtc	8	HP7	L292
	S290C	–	8/9 splice	HP7	S296
	E318G	gAa–gGa	9	HP7/TM8	E322
	G384A	gGa–gCa	11	TM8	G365
	L392V	Ctg–Gtg	11	TM8	L373
	C410Y	tGt–tAt	11	TM9	C391
	A426P	Gcc–Ccc	12	TM9	A407
	P436S	Cca–Tca	12	TM9/C	P417
PS2	N141I	aAc–aTc	5	TM2	N135
	M239V	Atg–Gtg	7	TM5	M233

Updated from Refs 37,38. Abbreviations: C, C terminus; HP, hair-pin loop; N, N terminus; TM, transmembrane region.

important implications. First, it implies that all other causes of AD should involve the deposition of Aβ as a primary event. This does not mean that they should all cause the production of more long Aβ, since some might, for example, involve inhibition of the resolution of deposits. There is, however, already evidence that some other causes do indeed involve excess production of long Aβ (Ref. 13). Second, it implies that treatment strategies that are aimed at targets downstream of the production of long Aβ could have a general efficacy.

These genetic data strongly support the 'amyloid cascade hypothesis'. At present, this hypothesis appears to be the only coherent hypothesis that attempts to explain the disease pathogenesis. There are, however, arguments against this idea, and it is worth discussing them briefly.

Arguments against and alternatives to the 'amyloid cascade hypothesis'

It is clear that the 'amyloid cascade hypothesis' is presently the dominant hypothesis concerning the etiology and pathogenesis of AD, and the major reasons for its dominance are reviewed above. The key question is 'is it correct?', or better 'to what extent is it correct?'.

At present, the major evidence used to dismiss the amyloid cascade hypothesis has come from two related areas: (1) from pathological studies, which show that amyloid deposition does not correlate well with degree of dementia (for example, see Ref. 46), or, perhaps more tellingly, that demonstrable neuropathology precedes frank amyloid deposition[47]; and (2) from transgenic animal work, which seems to show that behavioral deficits precede amyloid deposition in mice that overexpress APP (with a pathogenic mutation)[20].

The charge that there is a poor correlation between amyloid deposition and clinical features is not worrying, since such analyses depend upon the unproven and unlikely premise that amyloid deposits stay around for neuropathologists to count them. However, it is worrying that tangle formation precedes plaque deposition by several years, and while the same charge could be made about such studies (that the amyloid deposits had resolved before analysis), this is not a compelling explanation. Perhaps though, the definition of 'deposit' is what is misleading in these cases. Recent data have suggested that the toxic forms of amyloid are relatively soluble amyloid dimers[48], and these might be imagined to do some of the damage by forming 'flickering' deposits on the neural membranes, with larger deposits and neuritic plaques forming later in the disease process (it is clear, however, that plaques disrupt neuronal circuitry, and this must underlie some of the clinical expression of the disease). This same type of argument can be applied to the analysis of the transgenic animals, in which it is noteworthy that amyloid deposits do form eventually (for further discussion, see Ref. 38).

Another strand of this argument is that long Aβ is a surrogate marker for the disease process. In other words, this argument accepts the data presented in Table 1, showing that all molecularly defined causes of AD lead to increases in long Aβ, and suggests that the disease process causes both AD and the production of long Aβ, but not that the disease process produces more long Aβ which results in the disease process. This is a very difficult argument to counter, except facetiously (if it walks like a duck, and quacks like a duck, it most likely is a duck!), because the argument evades the issue of what the increases in long Aβ are a surrogate for. One possibility is that disruption of APP function is central to disease pathogenesis, and the mutations, especially the APP mutations, act to disrupt this function. One proposed function for APP has been in G-protein coupling, and it has been reported that APP$_{717}$ mutations disrupt this function[49,50]. However, it needs to be stated, in this regard, that for this hypothesis to overtake the amyloid cascade hypothesis, it should explain at least all of the APP mutations, and not just some of them, and this criterion has not been met for all mutations. Furthermore, this hypothesis makes no attempt, as yet, to accommodate the PS data, and there is no evidence that PS interferes with APP function except for the multiply documented increase in long Aβ.

Evidence has been presented that the PS are involved in apoptosis[51,52], and that the mutant PS and APP are more pro-apoptotic than their wild-type counterparts[49–52]. The implication inherent in the reporting of these studies seems to be that apoptosis might be a key component of AD. However, there is no solid evidence that AD is a disease of apoptosis. Furthermore, there is also no evidence that transgenic mice that massively overexpress mutant APP or mutant PS show any evidence of the gross abnormalities one might expect if apoptosis were being provoked[19,20,43–45]. It remains possible that the mutant PS somehow put metabolic stress on neurons, and that this metabolic stress underlies the marginal alteration in APP processing (that is, the effect of the PS mutations on long Aβ is very indirect)[53]. However, this too would seem unlikely: since APP mutations (which have an identical phenotype) have such 'clean' effects, solely on APP processing, it would seem unlikely that the PS effects would be so indirect and have so many other possible outcomes besides Aβ deposition.

In summary, all known AD-causing mutations have effects that relate directly to the increased formation of long Aβ, and this is deposited in the disease process. It is parsimonious to suppose that this is not coincidental. For any other hypothesis to supplant the view that this is central to disease pathogenesis, it should at least explain the pathogenicity of all the known mutations. Until such a testable hypothesis is formulated, it would seem that the amyloid cascade hypothesis should continue to hold sway, and continue to attract an ever-increasing proportion of the funds available, especially from those who are seriously interested in developing a treatment for this devastating and currently untreatable disease. This statement is not intended as an exhortation to be blind to the many gaps in our understanding of AD and the many deficiencies of the cascade hypothesis (some of which are touched upon above and most of which relate to the paucity of data relating amyloid deposition to cell death). However, from the treatment perspective, the amyloid cascade hypothesis offers a large number of potential targets: we now need to know whether attacking these targets can lead to amelioration of this tragic disease.

Acknowledgements

Work in the author and Mike Hutton's laboratory was supported by an NIH program project grant. Peter Hyslop, Dennis Selkoe, Sam Sisodia, Mark Mattson and Rudi Tanzi are thanked for manuscripts before publication, Marc Cruts for information in Table 2 and Richard Crook for the diagrams. Dedicated to George Glenner.

Selected references

1 Goate, A. *et al.* (1991) *Nature* 349, 704–706
2 Sherrington, R. *et al.* (1995) *Nature* 375, 754–760
3 Levy-Lahad, E. *et al.* (1995) *Science* 269, 973–977
4 Kang, J. *et al.* (1987) *Nature* 325, 733–736
5 Zheng, H. *et al.* (1995) *Cell* 81, 525–531
6 Anderson, J.P. *et al.* (1991) *Neurosci. Lett.* 128, 126–128
7 Seubert, P. *et al.* (1992) *Nature* 359, 325–327
8 Haass, C. *et al.* (1992) *Nature* 359, 322–325
9 Tischer, E. and Cordell, B. (1996) *J. Biol. Chem.* 271, 21914–21919
10 Klafki, H.W. *et al.* (1996) *J. Biol. Chem.* 271, 28655–28659
11 Hardy, J. (1996) *Ann. Med.* 28, 255–258
12 Houlden, H. *et al.* (1993) *Lancet* 342, 737–738
13 Scheuner, D. *et al.* (1996) *Nat. Med.* 2, 864–870
14 Younkin, S. (1995) *Ann. Neurol.* 16, 737–745
15 Mann, D.M.A. *et al.* (1996) *Ann. Neurol.* 40, 149–156
16 Jarrett, J.T. *et al.* (1993) *Biochemistry* 32, 4693–4697
17 Hardy, J. and Allsop, D. (1991) *Trends Pharmacol. Sci.* 12, 383–388
18 Selkoe, D. (1994) *Annu. Rev. Cell Biol.* 10, 373–403
19 Games, D. *et al.* (1995) *Nature* 373, 523–527
20 Hsiao, K. *et al.* (1996) *Science* 274, 99–102
21 Rogaev, E. *et al.* (1996) *Nature* 376, 775–778
22 Clark, R.F. *et al.* (1996) *Nat. Genet.* 11, 219–222
23 Slunt, H.H. *et al.* (1996) *Amyloid* 2, 188–190
24 Li, X. and Greenwald, I. (1996) *Neuron* 17, 1015–1021
25 Doan, A. *et al.* (1996) *Neuron* 17, 1023–1030
26 Prihar, G. *et al.* (1996) *NeuroReport* 7, 1680–1684
27 Thinakaran, G. *et al.* (1996) *Neuron* 17, 181–190
28 Perez-Tur, J. *et al.* (1995) *NeuroReport* 7, 297–301
29 Podlisny, M.B. *et al. Neurobiol. Dis.* (in press)
30 Kim, T.W. *et al.* (1997) in *Alzheimer's Disease: Biology, Diagnosis and Treatment* (Iqbal, K. *et al.*, eds), John Wiley & Sons
31 L'Hernault, S.W. and Arduengo, P.M. (1992) *J. Cell Biol.* 119, 55–68
32 Levitan, D. and Greenwald, I. (1996) *Nature* 377, 351–354
33 Levitan, D. *et al.* (1996) *Proc. Natl. Acad. Sci. U. S. A.* 93, 14940–14944
34 Haass, C. (1994) *Soc. Neurosci. Abstr.* 20, 1413

35 Wong, P.C. *et al.* (1994) *Soc. Neurosci. Abstr.* 20, 1968
36 Mercken, M. *et al.* (1996) *FEBS Lett.* 389, 297–303
37 Cruts, M. *et al.* (1996) *Hum. Mol. Genet.* 5, 1449–1455
38 Tanzi, R.E. *et al.* (1996) *Neurobiol. Dis.* 3, 159–168
39 Van Broeckhoven, C. (1995) *Nat. Genet.* 11, 230–233
40 Crook, R. *et al. Ann. Neurol.* (in press)
41 Gomez-Isla, T. *et al. Ann. Neurol.* (in press)
42 Lemere, C.A. *et al.* (1996) *Nat. Med.* 2, 1146–1150
43 Duff, K. *et al.* (1996) *Nature* 710–713
44 Borchelt, D. *et al.* (1996) *Neuron* 17, 1005–1013
45 Citron, M. *et al.* (1996) *Nat. Med.* 3, 67–72
46 Roses, A.D. (1994) *J. Neuropathol. Exp. Neurol.* 53, 429–437
47 Braak, H. and Braak, E. (1994) *Neurobiol. Aging* 15, 353–356 (and following articles in that journal)
48 Roher, A.E. *et al.* (1996) *J. Biol. Chem.* 271, 20631–20635
49 Yamatsuji, T. *et al.* (1996) *Science* 272, 1349–1352
50 Yamatsuji, T. *et al.* (1996) *EMBO J.* 15, 498–509
51 Vito, P. *et al.* (1996) *Science* 271, 623–626
52 Wolozin, B. *et al.* (1996) *Science* 274, 1710–1713
53 Guo, Q. *et al.* (1996) *NeuroReport* 8, 379–383

The role of neurotrophic factors in regulating the development of inner ear innervation

B. Fritzsch, I. Silos-Santiago, L.M. Bianchi and I. Fariñas

Several neurotrophins and their receptors regulate the survival of vestibular and cochlear neurons and probably also the efferent and autonomic neurons that innervate the inner ear. Mice lacking either brain-derived neurotrophic factor (BDNF) or its associated receptor, TrkB, lose all innervation to the semicircular canals and have reduced innervation of the outer hair cells in the apical and middle turns of the cochlea. Mice lacking neurotrophin-3 (NT-3) or its receptor, TrkC, lose many spiral ganglion cells predominantly in the basal turn of the cochlea. Nerve fibers from spiral ganglion cells in the middle turn extend to inner hair cells of the base. In mice lacking both BDNF and NT-3, or both TrkB and TrkC, there is a complete loss of innervation to the inner ear. Thus, these two neurotrophins and their associated receptors have been shown to be absolutely necessary for the normal development of afferent innervation of the inner ear. Current research efforts are testing the therapeutic potential for neurotrophins to treat hearing loss.

Trends Neurosci. (1997) 20, 159–164

THE INNER EAR forms from an invaginating placodal thickening (otocyst) whose polarity becomes fixed through tissue interactions between the periotic mesenchyme and the hindbrain[1–3]. The statoacoustic ganglion cells form from the antero-ventral aspect of the developing ear[4,5], migrate rapidly away and subsequently extend processes towards their peripheral and central targets (the inner ear and brain, respectively). Although Ramón y Cajal[6] speculated about the presence of two different substances that guide statoacoustic nerve fibers and maintain innervation of the inner ear, only in recent years has molecular evidence for this early suggestion been found.

The inner ear, composed of the vestibular (balance) and cochlear (hearing) regions, not only receives innervation from the afferent vestibular and cochlear (spiral) ganglion cells, but also from the centrally located efferent neurons[7] and the autonomic nerve fibers arising from the superior cervical ganglia[8,9]. Otic efferent neurons are derived from facial motoneurons, migrate to their specific positions and project through the vestibular root of the eighth nerve to innervate cochlear and vestibular sensory epithelia, respectively[10]. Thus, the inner ear receives nerve fibers derived from three different sources: (1) the otic placode, which gives rise to the otic afferent neurons (vestibular and cochlear ganglion cells) as well as the sensory epithelia of the inner ear; (2) the brainstem basal plate, which gives rise to the otic efferent neurons; and (3) the neural crest, which gives rise to the superior cervical ganglion (and thus the otic autonomic innervation). It is conceivable that different molecules might be responsible for guiding or maintaining these various nerve fibers.

Molecules likely to be involved in guiding or maintaining otic innervation

Some of the best characterized survival- and neurite-promoting factors are members of the neurotrophin gene family. These molecules include NGF, brain-derived neurotrophic factor (BDNF), neurotrophin-3 (NT-3) and neurotrophin-4/5 (NT-4/5). Each of the neurotrophins binds to high-affinity, signal-transducing receptor tyrosine kinases designated as TrkA (NGF), TrkB (BDNF, NT-4/5) and TrkC (NT-3; Fig. 1). Additional neuronal growth factors include ciliary neurotrophic factor (CNTF), glial cell line-derived neurotrophic factor (GDNF), and members of the fibroblast growth factor (FGF) family. BDNF, NT-3, GDNF and several FGFs are expressed in the inner ear[11,12,16,17].

In this review, we will outline the current level of our understanding of the neurotropic and neurotrophic requirements of these nerve fibers as revealed

B. Fritzsch is at the Creighton University, Dept of Biomedical Sciences, Omaha, NE 68178, USA.
I. Silos-Santiago is at Bristol-Meyers Squibb, Dept of Molecular Oncology, Princeton, NJ 08543, USA.
L.M. Bianchi is at the Medical University of South Carolina, Dept of Otolaryngology, Charleston, SC 29425, USA.
I. Fariñas is at the Howard Hughes Medical Institute, UCLA, San Francisco, CA 94143, USA.

Copyright © 1997, Elsevier Science Ltd. All rights reserved. 0166 - 2236/97/$17.00 PII: S0166-2236(96)01007-7

Annu. Rev. Genet. 1998. 32:461–93
Copyright © 1998 by Annual Reviews. All rights reserved

ALZHEIMER'S DISEASE: Genetic Studies and Transgenic Models

Donald L. Price,[1,2,3,4] *Rudolph E. Tanzi,*[5] *David R. Borchelt*[1,4], *and Sangram S. Sisodia*[1,3,4]
[1]Departments of Pathology, [2]Neurology, and [3]Neuroscience, and [4]The Division of Neuropathology, The Johns Hopkins University School of Medicine, Baltimore, Maryland 21205-2196, and [5]The Laboratory of Genetics & Aging, Massachusetts General Hospital, Boston, Massachusetts 02115;
e-mail: dlprice@welchlink.welch.jhu.edu; tanzi@helix.mgh.harvard.edu; drbor@welchlink.welch.jhu.edu; ssisodia@drugs.bsd.uchicago.edu

KEY WORDS: β-amyloid precursor protein, Tg mice, senile dementia, presenilin 1 and 2, dystrophic neurites

ABSTRACT

Recent advances in a variety of areas of research, particularly in genetics and in transgenic (Tg)/gene targeting approaches, have had a substantial impact on our understanding of Alzheimer's disease (AD) and related disorders. After briefly reviewing the progress that has been made in diagnostic assessments of patients with senile dementia and in investigations of the neuropathology of AD, we discuss some of the genes/proteins that are causative or risk factors for this disease, including those encoding amyloid precursor protein, presenilin 1 and 2, and apolipoprotein E. In addition, we comment on several potential new candidate loci/genes. Subsequently, we review selected recent reports of analyses of a variety of lines of Tg mice that show several neuropathological features of AD, including Aβ-amyloid deposits and dystrophic neurites. Finally, we discuss the several important issues in future investigations of Tg mice, with particular emphasis on the influences of genetic strains on phenotype, especially behavior, and strategies for making new models of neurodegenerative disorders. We believe that investigations of these Tg models will (*a*) enhance understanding of the relationships between impaired performance on memory tasks and the pathological/biochemical abnormalities in brain, (*b*) help to clarify pathogenic mechanisms in vivo, (*c*) lead to identification of new therapeutic targets, and (*d*) allow testing of new treatment strategies first in mice and then, if successful, in humans with AD.

0066-4197/98/1215-0461$08.00

CONTENTS

INTRODUCTION 462
ALZHEIMER'S DISEASE 463
Clinical Syndrome 463
Neuropathology 464
Genes Influencing Alzheimer's Disease 465
TRANSGENIC MODELS OF Aβ AMYLOIDOGENESIS 475
Amyloid Precursor Protein Transgenic Mice Generated by Yeast Artificial Chromosomes/Embryonic Stem Cell Methods 475
Transgenic Mice Generated by Microinjection of cDNA Constructs of Amyloid Precursor Proteins or Presenilin 1 476
Amyloid Precursor Protein and Presenilin 1 Gene-Targeted Mice 478
FUTURE DIRECTIONS IN TRANSGENIC MODELING OF ALZHEIMER'S DISEASE 480
CONCLUSIONS 482

INTRODUCTION

With the changing demographics of society worldwide (141), disorders that affect the elderly are increasingly prevalent. In this age group, impairments in cognition and memory processes are common (114, 174), with the most frequent cause of senile dementia being Alzheimer's disease (AD) (41, 128). Because of the prevalence and the magnitude of the morbidity/mortality associated with AD, it is imperative that we understand the etiologies/risk factors and pathogenic mechanisms involved in AD and related disorders in order to develop effective treatments that ameliorate/prevent these illnesses. Since the early 1990s, it has been known that some forms of AD are associated with the inheritance of mutant genes, including genes encoding amyloid precursor protein (APP) and presenilin 1 and 2 (PS1 and PS2), or with the presence of specific allele types of apolipoprotein E (apoE) (28, 51, 106, 158, 166, 167, 177). Thus, mutant APP, PS1, and PS2 are linked to relatively early onset cases of autosomal-dominant familial AD (FAD) (166), and apoE acts as a modifier, with apoE4 showing a dose-dependent influence in cases of late-onset AD. More recently, it has become evident that other loci/genes must play roles in the disease. With the identification of several genes directly linked to disease, it has been possible to establish in vitro and in vivo model systems to investigate the various abnormalities caused by the presence of these genes/proteins. Moreover, recent studies of transgenic (Tg) mice expressing these genes have begun to define the character and spatial/temporal evolution of cellular/biochemical abnormalities in brain, to delineate the mechanisms that cause these lesions, to identify a variety of new therapeutic targets, and to test novel treatments (151, 152). In this review, after a brief discussion of the clinical syndrome and neuropathology (including vulnerable neuronal systems, cytoskeletal alterations, and amyloidogenesis) of AD, we detail the biology of the genes/proteins implicated in the disease as well as recent advances that have been made in studies of Tg models.

ALZHEIMER'S DISEASE

Clinical Syndrome

Many older persons experience decline in cognitive performance, including difficulties with memory, learning, speed of performance, recall accuracy, and problem solving; a significant proportion of these individuals eventually develop progressively severe impairments in memory and executive functions (4, 14). The majority of these persons subsequently have difficulties in other domains of cognition, including language, calculation, visuospatial perceptions, judgment, and behavior (128, 174). Some patients show evidence of psychoses. Activities of daily living become progressively more impaired, and in the late stage of AD, patients are profoundly demented and often mute, incontinent, and bedridden; they usually die of intercurrent illnesses. Establishment of the diagnosis, which is most challenging early in the course of the illness, is based on clinical histories, physical examinations, neuropsychological testing, and a variety of assessments designed to exclude other causes of dementia; on the basis of criteria formulated by the NINCDS-ADRDA joint task force (11, 128), patients are usually classified as possible, probable, or definite AD. Neuroimaging studies, including computed tomography and magnetic resonance imaging, can identify potentially treatable diseases and disclose abnormalities (particularly in the medial temporal lobe) that may have high predictive value for establishing a diagnosis of AD (4, 75). Positron emission tomography and single photon emission computed tomography techniques show decreased regional glucose metabolism and blood flow in the parietal and temporal lobes, with involvement of other cortical areas at later stages (75). The clinical phenotype of senile dementia can also be caused by a variety of other diseases, including dementia with Lewy bodies (102, 127), frontotemporal dementia with parkinsonism [now linked to chromosome 17 (44, 214) and, in some cases, to mutations in tau (150, 203)], Pick's disease (33), vascular dementia (115), etc. For research purposes, investigators have begun to assess the diagnostic value of determining the levels of β-amyloid protein (Aβ) peptides (soluble monomeric species decreased, multimeric species possibly increased) species and of tau (increased) in the cerebrospinal fluid and of establishing apolipoprotein E (apoE) genotypes (148, 196). Currently, however, these assessments are not appropriate for routine diagnostic evaluations (42, 123). With the exception of brain biopsy, there are no tests that definitively establish the diagnosis of AD in living subjects.

Neuropathology

INVOLVEMENT OF BRAIN REGIONS/NEURAL CIRCUITS The disease process selectively damages brain regions and neural circuits critical for cognition and memory, including neurons in the neocortex, hippocampus, amygdala, basal forebrain cholinergic system, and brainstem monoaminergic nuclei (7, 19, 133, 212, 213). Dysfunction/death of the nerve cell in these circuits leads to reduced levels of generic synaptic markers (i.e. synaptophysin) in target fields (117–119, 189). For example, the severity of memory impairments and densities of senile plaques correlates with levels of synaptophysin (a presynaptic vesicle protein) in the hippocampus of individuals with AD (189). Transmitter-specific markers (i.e. levels of choline acetyltransferase activity, monoaminergic markers, etc) are also reduced in affected regions (45, 49, 221). For example, basal forebrain cholinergic neurons, which innervate the hippocampus and neocortex, are vulnerable in AD (213), and presynaptic markers (i.e. levels of acetylcholine, M2 receptors, and choline acetyltransferase and acetylcholinesterase activities) are reduced in target fields (49). The cellular abnormalities involving these neural circuits, which compromise synaptic interactions in affected regions of the brain, have profound clinical consequences. Abnormalities that interrupt hippocampal and medial temporal cortical circuits are presumed to be critical in memory impairments, whereas higher cognitive deficits (e.g. disturbances in language, calculation, praxis, and judgment) are related to neocortical pathology. Alterations in the basal forebrain cholinergic system are believed to contribute to memory difficulties and to deficits in arousal/attention. Some of the cognitive/psychiatric disturbances that occur in some patients may reflect involvement of the limbic circuits, amygdala, and monoaminergic systems.

PATHOLOGY INVOLVING THE NEURONAL CYTOSKELETON Many neurons exhibit fibrillary accumulations in the cytoplasm, including neurofibrillary tangles (NFT) (neurofibrillary pathology in cell bodies and proximal dendrites), neuropil threads (filamentous accumulations in dendrites), and dystrophic neurites (filament-containing neuronal processes, particularly distal axons/terminals). Ultrastructurally, fibrillary inclusions represent intracellular accumulations of straight filaments and paired helical filaments, both of which are composed principally of hyperphosphorylated isoforms of tau, a low-molecular-weight, microtubule-associated protein (33, 34, 43, 52, 53, 57, 96). Because hyperphosphorylated tau species bind poorly to microtubules and alter microtubule stability, this biochemical modification could affect other cytoskeletal constituents, intracellular transport, cellular geometry, and/or neuronal viability. Recent in vitro studies (52) have shown that exposure of nonphosphorylated three- and four-repeat recombinant tau to high concentrations of sulphated glycosaminoglycans can lead to the formation of paired and straight helical filaments, respectively. These observations raise the question of whether phosphorylation is necessary or sufficient for the formation of these filaments. In addition to tau immunoreactivity, these lesions are associated with immunoreactivities for ubiquitin, another microtubule-associated protein (MAP-2), and neurofilament proteins (6, 57, 121, 147). Oxidative damage and protein glycation, involving cytoskeletal components, may also play roles in filamentous cell pathology (183, 184). Because NFT, neurites, and neuropil threads contain similar filamentous constituents, it is likely that the genesis of these inclusions is the result of common mechanisms. Eventually, NFT-bearing cells die, by mechanisms that may involve apoptotic pathways (197).

Senile plaques are made up of dystrophic neurites displayed around extracellular deposits of thioflavin S/Congo red–positive Aβ amyloid (74, 100, 161, 165). Aβ species, ~4-kDa peptides (50, 121), are derived from APP, a type-I single transmembrane glycoprotein encoded by a gene on chromosome 21 (54, 82, 156, 191). Deposited in the neural parenchyma and around blood vessels, Aβ peptides are up to 40 (Aβ40) and 42 (Aβ42) (43) amino acids in length, with the longer forms deposited early and representing the principal component in diffuse or compact plaques (74, 100, 161). Aβ peptides can be modified at the N terminus; for example, A$\beta_{\mathrm{N3(pE)}}$ is N-terminally truncated at the third residue (glutamate) and is converted to pyroglutamate, and these species have been detected in AD brain (165). Changes in charge may increase hydrophobicity, affect stability, and promote the aggregation and toxicity of Aβ species. In addition, these Aβ fibrillar aggregates can act as a nidus for recruitment of astrocytes and microglia and for the deposition of other proteins, including α_1-antichymotrypsin, components of the complement cascade, apoE and J, cholinesterases, etc (2, 3, 77, 110, 125, 126, 129, 159, 160, 172, 185, 186, 209, 215). Moreover, glial cells can produce a variety of constituents, including cytokines and chemokines, that, by binding to receptors (65, 162, 218) can participate in pathogenic processes occurring in the neural parenchyma (56, 109, 112, 125, 160, 176). Finally, studies using monoclonal antibodies recognizing a ~100-kDa protein (AMY117) have disclosed abundant AMY117-positive Aβ-negative plaques in the gray matter of people with AD (173); the identity of this ~100-kd protein and role of these lesions remain to be elucidated.

Genes Influencing Alzheimer's Disease

Age, genes, and environmental factors influence the development of AD, with the two best-defined risk factors for AD being increased age (36) and a positive family history. In this review, we focus on the roles of genes in the pathogenic process. Approximately 95% of cases of AD occur in individuals >60 years of age. In individuals <60 years of age whose illness has become manifest, there tends to be familial clustering, and of these the majority are inherited in an autosomal-dominant manner. Caused by mutations in at least three different genes (i.e. APP, PS1, and PS2), cases of early-onset AD appear to be similar to each other in terms of clinical and neuropathological features. Although familial clustering is also found in individuals with late-onset AD, "censoring" caused by limited family history and the death of certain family members because of other age-related illnesses makes it difficult to assess the prevalence of late-onset FAD. Thus, in late-onset AD, autosomal-dominant, fully penetrant, causative gene defects are relatively rare. Instead, late-onset AD is characterized largely by the inheritance of modifying genes that predispose the carrier to an increased risk for AD. The best example of a late-onset AD genetic risk factor is a polymorphic variant of the apoE gene on chromosome 19 (123). The genes/proteins implicated in AD are reviewed below.

AMYLOID PRECURSOR PROTEIN The initial clue that led to the first identification of a genetic mutation in FAD was the identification of Aβ as a principal component of amyloid extracted from the blood vessels of individuals with AD and individuals with Down's syndrome (trisomy 21) (50); the latter, trisomic for chromosome 21, show, at an early age, amyloid deposits and other lesions virtually identical to those that occur in AD (99). The publication of the amino acid sequence of the first 28 amino acids of Aβ by Glenner & Wong (50) allowed several groups to clone and map the gene encoding APP (54, 82, 156, 190). The APP gene encompasses ~400 kb of DNA (90), contains 19 exons, and encodes several alternatively spliced APP mRNA. APP are typical type-I integral membrane glycoproteins showing the following features: an N-terminal signal peptide; a large ectodomain with sites for N-glycosylation; an alternatively spliced Kunitz-type serine protease inhibitor (KPI) domain; an Aβ region (comprised of 28 amino acids of the ectodomain and 11–14 amino acids of the adjacent transmembrane domain); a single membrane-spanning helix; and a short cytoplasmic domain with signals for trafficking in the endocytic and secretory pathways (60, 152). Some APP molecules are cleaved endoproteolytically within the Aβ sequence by APP α-secretase, an activity with unusual properties (178), to release the ectodomain of APP (APP$^{s\alpha}$) (39, 178, 179), including residues 1–16 of Aβ, into the culture medium or into the cerebrospinal fluid (179, 210). The cleavage of APP within the Aβ domain precludes the formation of Aβ. In contrast, Aβ is generated by pathways involving the endoproteolytic cleavage of APP by hitherto not fully characterized activities, termed β- and γ-secretase cleavages, which generate the N and C termini of the Aβ peptide, respectively (59). Aβ appears to be produced in endosomes or late Golgi; the endoplasmic reticulum is a site for production of Aβ42 (27, 61). Considerable evidence supports a model in which APP, internalized from the plasma membrane, is subject to β-secretase cleavage within the late Golgi or endocytic compartments. Subsequently, γ-secretase cleavage of the residual ~100–amino acid, membrane-bound fragment within the transmembrane domain leads to the formation and release of Aβ into the extracellular space (85). Approximately 90% of secreted Aβ peptides are Aβ40, a soluble form of the peptide, whereas ~10% of secreted Aβ peptides are Aβ42 and Aβ43—β sheet species that are highly fibrillogenic, readily aggregated, and deposited early and selectively in amyloid plaques (74, 93, 111, 113). In addition, Aβ42 fibrils can apparently recruit Aβ40 into a structured assembly that makes up the deposits in the parenchyma (76, 93). The state of Aβ has been reported to be a crucial factor in Aβ neurotoxic activity in vitro and, possibly, in vivo (93, 122, 220).

APP isoforms are present in many types of cells, including neurons and, at lower abundance, astrocytes (84, 180). In neurons, APP is transported within axons by the fast anterograde system (84), and in peripheral sensory neurons of rodents, APP-695 is the predominant isoform: Full-length APP-695 and, to a lesser extent, APP-751/770 are rapidly transported anterogradely in axons (84, 180). In neurons of the entorhinal cortex, newly synthesized APP (principally APP-695) is transported via the perforant pathway and accumulates at presynaptic terminals in the hippocampal formation. In the terminal fields of the perforant pathway, soluble $COOH^-$ terminally truncated APP and amyloidogenic C-terminal fragments have been identified, which is consistent with the idea that neurons and their processes are one source of the APP that gives rise to Aβ species. This finding is also in accord with studies of APP Tg mice, aged monkeys, and humans with AD showing that Aβ deposits are often located in proximity to APP immunoreactive neurites (16, 116).

After the APP gene was mapped to chromosome 21, genetic linkage studies of four multigenerational, early onset FAD pedigrees were interpreted to indicate that a FAD gene was present on chromosome 21 (168); however, it was later learned that the initial linkage result was spurious (192, 193). In 1991, a pathogenic mutation was reported in the APP gene; a missense substitution (Glu-Gln in codon 693 of APP-770) residing in exon 17 of APP was documented in cases of Dutch-type hereditary cerebral hemorrhage with amyloidosis, a disorder that involves Aβ deposition in cerebral blood vessels, leading to cerebrovascular disease and death, usually by the fifth decade of life (105). Subsequent screening of the same exon led to the identification of a FAD gene mutation (i.e. APPV717I) (51). In fewer than 20 early onset pedigrees of early onset FAD (51), missense mutations have been demonstrated that lead to amino acid substitutions at residue 717 (of APP-770) within the transmembrane domain of APP (51). Cells that express APP harboring the "717" substitutions (near the γ-secretase site) do not appear to secrete higher levels of Aβ but, rather, secrete a higher fraction of longer Aβ peptides (i.e. extending to Aβ42) relative to cells that express wild-type (wt) APP (188). Additional AD-linked

APP mutations have been reported (22, 60, 62, 134, 135). In two large, related families from Sweden, early onset AD has been linked to a double mutation at codons 670 and 671 that resulted in the substitution of Lys-Met to Asn-Leu. Cultured cells that express APPswe secrete six- to eightfold higher levels of ~4-kDa Aβ peptides compared with cells that express wt constructs, with levels of Aβ42 peptides increasing accordingly (24). The elevated secretion of Aβ from cells that express APPswe is likely caused by the initial endoproteolytic cleavage of APP at the β-secretase site during transit of the precursor through the medial and *trans* Golgi compartments and nascent post-TGN vesicles (58), followed by γ-secretase cleavage of the remaining C-terminal ~100 amino acids that contain the entire Aβ peptide. Finally, in one family with a Gly Ala substitution mutation at codon 692 of APP, affected individuals develop presenile dementia, cerebral hemorrhages, diffuse deposits of Aβ, congophilic angiopathy, and scattered senile plaques; tangles are not conspicuous (62, 202).

Thus, the clinical and neuropathological characteristics of patients with FAD-related APP mutations share several features, including onset before 60 years of age (mean family onset between 43–55 years), autosomal-dominant inheritance fully penetrant by the early 60s, and clinical and pathological phenotypes indistinguishable from individuals with sporadic AD. Although APP mutations are virtually 100% penetrant, mutations in this gene are responsible for only a small proportion of all published cases of early-onset FAD (193).

PRESENILIN 1 AND 2 In 1992, a FAD-linked gene was reported on the long arm of chromosome 14 (137, 167, 200), and in 1995, the PS1 gene was identified by a positional cloning strategy (177). It is of interest that in the original four families, which were previously reported to be linked to chromosome 21 (168, 192, 193), the disease has now been demonstrated to be linked to mutations in PS1 (168, 192, 193). Subsequently, a homologous gene, PS2, was isolated and mapped to chromosome 1, a locus shown to be involved in FAD in the Volga German FAD kindreds (106).

PS1 and PS2 are highly homologous polytopic proteins 463 and 448 amino acids in size, respectively (35, 83, 98, 106, 107, 177). In addition to the TM transmembrane helices, PS are predicted to contain a hydrophilic acidic loop region encompassing amino acids 262–407; the N terminus, loop, and C terminus of PS1 are oriented toward the cytoplasm (35). Although PS1 is synthesized as an ~42- to 43-kDa polypeptide, the preponderant PS1-related species that accumulates in cultured mammalian cells and in the brains and other tissues of many species are ~27- to 28-kDa N-terminal and ~16- to 17-kDa C-terminal derivatives (95, 149, 194). The N- and C-terminal fragments accumulate at 1:1 stochiometry, and the absolute levels of these fragments are tightly regulated and saturable. In situ chemical cross-linking and immunoprecipitation analyses have shown that PS fragments are stably associated; although there is some controversy concerning the direct interaction of APP and PS (212, 219), recent evidence suggests that neither PS1 nor PS2 form stable complexes with APP (195). To date, only one FAD-linked mutation, the PS1 ΔE9 variant, which lacks amino acids 290–319, fails to be cleaved.

Although the biological functions of PS are not fully understood, the functions of PS were clarified with the discovery of a homologous gene in *Caenorhabditis elegans*, termed sel-12; mutant alleles of sel-12 were uncovered as suppressors of a hypomorphic multivulval phenotype in *C. elegans* linked to hyperactivity of the *C. elegans* Notch homologs lin12 and glp1 (104). Notch and lin12/glp1 are TM receptors required for the specification of cell fate and lateral inhibition during development (8). The extremely high amino acid homology between PS and sel-12 led to the prediction that related proteins would be functionally interchangeable. Consistent with this hypothesis, an egg-laying (egl) defect associated with loss of sel-12 function in *C. elegans* is rescued efficiently by the expression of human (Hu) PS1 and PS2; the rescue efficiency of HuPS is essentially indistinguishable in Tg worms that express sel-12 (10, 103). The egl defect was only weakly rescued in Tg worms that express several human FAD-linked PS1 variants (10, 103), which suggests that during development, PS1 missense variants exhibit reduced functions. Interestingly, the PS1 ΔE9 variant showed considerable rescue activity relative to other PS1 missense variants. These results indicated that PS1 endoproteolysis cleavage is not obligatory for function (3, 50) and fully supported the earlier biochemical studies documenting that the PS1 ΔE9 variant exhibits biochemical properties not unlike the constitutively generated PS1 derivatives.

Although the *C. elegans* experiments provided valuable insights into PS functions, the biological functions of PS1 and PS2 in mammals during development are not fully understood. Several strategies have been employed to address these issues. Initial in situ hybridization studies and reverse transcriptase–polymerase chain reaction approaches in mouse embryos revealed that PSs are expressed ubiquitously during mouse embryonic development, and as early as embryonic day 8.5 (94). However, the general spatial and temporal expression patterns of *PS* mRNA do not directly coincide with the expression patterns of any specific member of the known mammalian *notch* homologs, results that suggest that during mammalian development, PS1 function is not limited to notch signaling alone (94). The cytosolic domains of PS1 and PS2 are highly divergent (<10% identity in the N-terminal 70 amino acids and between amino acids 305–375 in the loop domain), which suggests that these regions mediate cell- or PS-specific functions via differential interactions with proteins in the cytoplasm. A number of investigations have utilized yeast two-hybrid approaches to identify proteins that interact with the N-terminal and loop domains of PS1 and PS2; one isolate from a two-hybrid screen was a fragment of δ-catenin (223); δ-catenin, expressed predominantly in the nervous system, is a member of a larger family of catenins related to a *Drosophila* protein, termed armadillo, involved in inductive signaling events during development and regulation of cell proliferation. The results of PS1 gene-targeting studies, which demonstrate a critical role for PS in mammalian development, are discussed below.

In adults, PS1 and PS2 mRNA and protein are expressed in a variety of peripheral tissues and in virtually all brain regions (95, 158, 177). In cells, full-length PS1 and PS2 are localized to similar intracellular membranous compartments, including the endoplasmic reticulum and, to varying extents, the Golgi complex (35). In the nervous system, the PS is not abundant but is readily demonstrable in neurons and in the neuropil, including axons and dendrites.

Since 1995, the PS1 gene has been reported to harbor 48 different FAD mutations in fewer than 80 families of various ethnic origins, whereas PS2 has been found to contain only two different FAD mutations and one apparently sporadic AD mutation (30, 60). With two exceptions, all the genetic abnormalities are missense mutations that result in single amino acid substitutions; a mutation that deletes exon 9 from PS1 has been identified in three different FAD families (29, 60, 73, 87, 145), and a splice-donor deletion has been identified in intron 4 of PS1 that leads to truncation of the protein (198). The missense mutations in PS1 account for up to 25–30% of early onset cases of FAD (177) and, with one exception, are fully penetrant. Of the 48 reported FAD mutations in PS1, 36 occur in single-kindreds families, thus characterizing them as "private" mutations. Many of these mutations occur within TM II or immediately adjacent to the predicted loop domain (177). These two major clusters of mutations, which account for >50% of the known PS1 mutations, occur in exons 5 (13 mutations) and 8 (13 mutations). For the mutations in these clusters, the average age of onset is earlier than that of the other mutations in PS1. For the FAD mutations in exon 5, the mean age of onset is roughly 40 years, and one of the youngest ages of onset (28 years) is associated with the P117L mutation in this exon. For exon 8, the average age of onset is ~43 years, compared with a mean age of onset of 48 years for all other mutations in PS1. Interestingly, exon 5 encodes the second predicted TM domain (TM-2) as well as part of the first and largest of the luminal loops [hydrophilic loop (HL)-1] of PS1, whereas exon 8 encodes a portion of predicted TM domain 6 (TM-6) and the largest cytoplasmic loop (HL-6) of PS1. Nine additional mutations reside in exon 7, which also encodes a portion of TM-6, and two other mutations are situated in exon 9 (including one that results in the deletion of this exon), which also encodes a portion of HL-6. These mutation "hot spots" appear to be located in critical functional or conformational domains in PS1, perhaps affecting interactions with other proteins.

Two PS2 mutations have been reported to cause autosomal-dominant AD in Volga German kindreds and in an Italian pedigree (106, 158). The average age of onset in the Volga German families with the N141I PS2 mutation is 52 years, with a highly variable and wide range of onset (40–85 years). The reasons for the differences in the number of FAD mutations in PS1 versus PS2 are unknown, and it may be necessary to look for PS2 mutations in FAD kindreds with later onset than those that have been traditionally used to search for mutations in early onset FAD genes.

Several lines of evidence, including studies of cases of chromosome 1- and 14-linked AD and of Tg mice expressing APP and PS1 mutation, indicate that mutations in PS1 increase levels of Aβ species and deposits of Aβ42(43) (17, 64, 111, 113, 152). In the conditioned medium from fibroblasts or the plasma from affected members of pedigrees with PS1- or PS2-linked mutations, the ratios of Aβ42(43)/Aβ40 in affected individuals are elevated relative to unaffected family members (171). Moreover, in transfected mammalian cells and in the brains of Tg mice (see below), ELISA analyses of the conditioned medium of cells that coexpress HuAPP (25) have clearly documented that a variety of mutant PS1 variants, including ΔE9, influence APP processing in a manner that elevates levels of Aβ42(43) relative to cells expressing wt PS (25, 38). Thus, FAD-linked PS1 and PS2 variants influence processing at the γ-secretase site and increase the extracellular concentration of highly amyloidogenic Aβ42(43) species, thus fostering Aβ deposition in the brain. Consistent with this idea are studies showing that media from cultures of neurons taken from PS1$^{-/-}$ embryos contain low levels of Aβ D42(43) (31, 33a). The mechanisms whereby mutant PS influences amyloidogenesis, whether by direct interactions (212, 219) or by indirect mechanisms (195), are not clarified. Recent evidence suggests that PS do not form stable complexes with APP (195).

APOLIPOPROTEIN E ApoE, a 34-kDa glycoprotein, is the major serum protein involved with cholesterol storage, transport, and metabolism (169, 211). There are three alleles at the single apoE locus on chromosome 19: apoE3 has a cysteine at position 112 and an arginine at position 158; apoE4 has arginine at both positions; and apoE2 has cysteine at both positions. The apoE3 allele is most common in the general population (frequency 0.78); the allelic frequency of apoE4 is 0.14. The association of the e4 allele (apoE4) with AD is based on the fact that the prevalence of the allele in individuals with AD having either one or two copies (45–60%), significantly exceeding that observed in the control populations (23, 28, 46, 55, 124, 155, 169, 186).

Although apoE4 has been claimed to "account for" up to 50% of the genetic risk for AD (28), it must be emphasized that the apoE4 allele is a common or "public" polymorphism present in at least one copy in ~25–33% of the general population. Approximately 1 in 20 individuals >60 years of age is affected with AD or a related dementia, and this rate roughly doubles with every subsequent decade. Thus, it is often difficult to exclude the concurrence of AD and the apoE4 allele as random coincidence, given the increased prevalence of AD with age. The relative risk for AD conferred by apoE4 is dose dependent (28) in that two copies of apoE4 confer significantly greater risk and earlier age of onset than does one copy.

In a prospective longitudinal study, Gómez-Isla and colleagues (55) compared the age of onset and rate of progression of disease in patients with different apoE genotypes. The E4 allele was associated with earlier onset of AD, but had no effect on the rate of progression of dementia. In a recent population-based study of ~2000 individuals >65 years of age, apoE2 and apoE4 genotype affected performance of a delayed recall task carried out over a 4- to 7-year period (71); in this study, the odds ratio for developing impairment was 1.37 for apoE4 and 0.53 for apoE2. Approximately 85% of elderly homozygotes for apoE4 (average 81 years of age) were unimpaired on the test of mental status, indicating that they can reach very old age without cognitive impairments. In another study, apoE4-positive individuals, >65 years of age, had a 2.27-fold increased risk for AD compared with persons with the most common apoE3/apoE3 genotype (40). This study also concluded that if apoE4 were removed as a risk factor for AD, the incidence of AD would decrease by 13.7%. In a third study, the impact of apoE4 on age of onset of AD was investigated in 310 small, AD families and affected sib-pairs (12); the risk for AD conferred by apoE4 was greatest in the group with onset that occurred between 61 and 65 years of age, followed by the group with onset between 65 and 70 years of age. However, after age 70, the influence of apoE4 as a risk factor for AD progressively declined at a sharper rate. After the age of 75, the apoE4 allele frequency did not significantly differ among affected and unaffected siblings. It is also interesting to note that some individuals in this study were apoE4 homozygotes and >85 years of age, but they did not suffer from cognitive impairments. Together, these findings suggest additional genetic risk factors remain to be identified, especially for the development of AD after 70 years of age.

The presence of apoE4 can influence the brain pathology, particularly by enhancing the Aβ burden in a dose-dependent fashion (42, 55, 155, 172). Although NFT are associated with clinical measures of dementia, their presence does not correlate with apoE genotype. The impact of apoE genotype seems to be greatest on Aβ deposition; it is not clear whether apoE isoforms differentially influence production, aggregation, fibrillogenesis, or clearance of Aβ.

With regard to the influence of apoE genotype on FAD, studies of families with the APPswe mutation show that the apoE genotype influences age of onset.

Subjects with an E2/E3 genotype had onset at 57–60 years of age, individuals with E3/E3 genotypes had onset at 51–54 years of age, and a single patient with an E4/E4 genotype had onset at 44 years of age. In an APP-717 family, the mean age of onset was 47.6 ± 3 years (all E3/E4), although one mutation carrier who was E2/E3 was unaffected at 59 years of age (170). In contrast, studies to date suggest that apoE genotype has no effect on the age of onset or phenotype of FAD in patients with PS1 mutations (201).

Recently, polymorphisms in the apoE gene promoter have been found to be associated with increased expression of apoE4 and an increased risk for AD (91, 92). Thus, it is conceivable that the apoE4 genotype is actually in linkage disequilibrium with a genetic alteration in the apoE promoter. Studies will be needed to determine whether these or other polymorphisms in the apoE promoter, which exhibit linkage disequilibrium with apoE4 and with the increased risk for AD, also alter the transcription/expression of the apoE gene in brain. Indeed, allelic distortion of expression of apoE4 in brains of apoE3/apoE4 affected individuals has previously been reported to be 1.5-fold higher than in apoE3/apoE4 aged controls (92).

Currently, apoE4 genotyping is not employed as a predictive test for AD. A recent analysis of the clinical diagnosis and neuropathology of ~2000 cases of AD indicates that apoE genotyping does not provide the degree of sensitivity and specificity that would encourage independent utilization of genotyping as a diagnostic test; however, in concert with clinical criteria, the apoE genotyping improves specificity of the diagnosis (123). Thus, apoE4 genotyping is not recommended for routine diagnostic assessments of patients with senile dementia (42, 71, 123).

OTHER ALZHEIMER'S DISEASE–RELATED GENES With regard to prevalence rates, mutations in the APP and PS genes clearly do not account for all cases of early-onset FAD (30). A subset of early-onset FAD is still genetically unaccounted for by known defects in these genes. In a recent study, Cruts et al (30) suggested that PS1 and PS2 mutation frequencies in presenile AD are 6% and 1%, respectively, and that the prevalence of PS1 mutations in autosomal-dominant FAD is 18%, based on a study of 101 unrelated patients with FAD and sporadic AD. Clearly, many more large population–based studies will be necessary to derive dependable figures for the proportion of early onset FAD that is accounted for by mutations in APP, PS1, and PS2. However, the emerging genetic picture for AD suggests that mutations in the APP and PS genes are associated with 20–50% of cases of AD that occur in individuals under the age of 60 years; the vast majority of these FAD cases occur in those individuals with onset <50 years of age. Meanwhile, the apoE gene and other genetic factors contribute either independently or in combination (epistatically) to influence risk for AD in individuals whose disease onset occurs after >60 years of age. It has recently been suggested that apoE does not appear to predict which subjects are predisposed to develop AD, but rather that it influences the onset in individuals vulnerable for other reasons (130). In considering the charge for priorities in future genetic studies of AD, current findings and data generated thus far indicate that for early onset FAD, the major gene(s) linked to AD with onset in individuals between 50 and 60 years of age largely remain to be determined. Meanwhile, with regard to late-onset AD, genetic factors that work epistatically, or in conjunction, with apoE4, as well as novel late-onset AD genes and especially those associated with risk for AD at >75 years of age, represent the major targets of future genetic studies of AD (130). Several recent genetic studies are reviewed below.

Genetic linkage analyses resulting from a complete genomic screen led to the report of a novel late-onset AD gene in the centromeric region of chromosome 12 in AD families with affected individuals who show a minimal or no association with apoE4 (146). Although this report excluded linkage to the low-density-lipoprotein receptor–related protein (LRP) gene, which encodes the neuronal receptor for apoE (86, 155) and resides on the long arm of chromosome 12, Kang et al (81) reported a genetic association between LRP and late-onset AD, an observation confirmed by Wavrant-DeVrieze et al (208) and Lendon et al (101). In addition to LRP, the gene encoding another apoE receptor, VLDL-R, was also reported to be associated with late onset AD (140).

Most intriguing is the family-based study that has revealed an association between late-onset AD and the presence of an exon 2 splice acceptor deletion in the alpha-2-macroglobulin (A2M) gene on the short arm of chromosome 12 (13). In this study, using several statistical tools, the risk for AD conferred by the A2M deletion was comparable to that associated with apoE4 homozygotic status. A2M-2 appears to predispose to disease, but in contrast to ApoE allele type, it does not influence age of onset. The previous linkage of AD to chromosome 12 (146) was not explained in the A2M association. Significantly, A2M binds to a variety of proteins, including proteases (18, 154); interestingly, A2M, up-regulated following injury (108), is present in senile plaques, binds Aβ (37, 70), and can attenuate Aβ fibrillogenesis and neurotoxicity (70). Moreover, A2M may, via LRP-mediated endocytosis, allow the internalization and subsequent lysosomal degradation of Aβ (48, 138). Thus, currently available evidence suggests that A2M-2 confers vulnerability to late life illnesses.

Two other candidate AD genes, alpha-1-antichymotrypsin (79) and bleomycin hydrolase (131), have been reported to predispose to increased risk for AD perhaps by operating interactively with apoE4. The candidacy of both these genes as AD loci awaits further testing and confirmatory studies in greater numbers of AD samples and using alternative analytical strategies [e.g. family-based association; sibship disequilibrium test (13)].

Other genetic linkage data suggest the existence of a novel late-onset AD gene on chromosome 3q25-26 (RE Tanzi, unpublished results) that appears to be interactive with the apoE4 allele. A candidate gene in this region of chromosome 3 is the butylcholinesterase (BchE) gene; its polymorphism, the K-variant, has been reported to be associated with late-onset AD and to be synergistic with apoE4 as a risk factor for AD (97). However, neither the association between AD and BchE nor the synergy with apoE4 as a risk factor for AD could be confirmed in a study of over 350 AD sib-pairs and small families (RE Tanzi, unpublished findings). The transferrin gene, which also maps to this portion of chromosome 3, has also been reported to be associated with late-onset AD, particularly in apoE4-positive AD patients (137). Additional investigations are clearly necessary to assess this result.

Finally, Davis et al (32), using an unusual method to isolate DNA from enriched pellets of frozen platelet, suggested that patients with AD are heteroplasmic for several missense mutations in mitochondrial DNA genes encoding cytochrome c oxidase subunits CO1 and CO2. More recent studies (63a, 205) indicate that these gene variants are mitochondrial DNA pseudogenes integrated into nuclear DNA.

TRANSGENIC MODELS OF Aβ AMYLOIDOGENESIS

To generate animal models of amyloidogenesis and Aβ-associated abnormalities, many groups have created Tg mice that express wt APP, APP fragments, Aβ, and FAD-linked mutant APP and PS1 transgenes (16, 20, 47, 63, 67, 69, 72, 80, 88–90, 120, 132, 136, 139). Although early efforts were disappointing because Tg mice did not exhibit the cellular abnormalities characteristic of AD, more recent work has shown that multiple lines of Tg mice now exist that show Aβ deposits and neuritic plaques. Selected models are reviewed below.

Amyloid Precursor Protein Transgenic Mice Generated by Yeast Artificial Chromosomes/Embryonic Stem Cell Methods

Tg mice containing a yeast artificial chromosome (YAC) within which resides the entire 400-kDa HuAPP gene with APPswe and/or APPV717I (89), showed increased levels of all Aβ peptides in the brain and diminished levels of α-secretase–generated soluble APP derivatives. In the YAC Tg mice expressing the APPV717I mutation, levels of the longer Aβ peptides (i.e. Aβ42/43) were elevated (89).

Transgenic Mice Generated by Microinjection of cDNA Constructs of Amyloid Precursor Proteins or Presenilin 1

APP V717F TRANSGENIC MICE The platelet-derived growth factor β-promoter was used to drive the expression of a HuAPP minigene that encodes the FAD-linked APP-V717F in an outbred strain of mice; the construct contained portions of APP introns 6–8 that allow alternative splicing of exons 7 and 8. Levels of Hu-APP mRNA and protein significantly exceeded levels of endogenous APP. The transcripts encoded the three major splicing variants, including the KPI-coding forms. There was a high ratio of mutant transgene mRNA to endogenous mRNA. Hu and KPI transcripts were expressed at high levels compared with Hu-APP-695 (157); levels of transgene product were approximately four to five times higher than were endogenous APP (47, 157). The brains showed diffuse Aβ deposits and mature plaques (dystrophic neurites displayed around Aβ cores) associated with astrocytes (47). Dystrophic neurites contained dense lamellar bodies and neurofilaments and some fibrils in neuronal processes were interpreted as containing intracellular amyloid fibrils (120). Extracellular 9- to 11-nm fibrils were abundant in regions of Aβ deposits. There were increased numbers of microglia, often enlarged, clustered in and around plaques in hippocampus and neocortex; NFTs were not evident. To date, the performance of these mice on behavioral tasks has not been published, perhaps because of the difficulties related to establishing control groups for outbred strains of mice (78).

APPSWE TRANSGENIC MICE When the hamster prion protein (PrP) promoter was used to overexpress Hu-APP695swe, the brains of one of these lines of Tg mice (line Tg2576) showed elevated levels of Aβ40 and Aβ42, dystrophic neurites, and Aβ deposits in amygdala, hippocampus, and cortex (67). Recent studies suggest that the brains of these mice exhibit evidence of oxidative stress, including enhanced expression of superoxide dismutase 1 (SOD1) and hemoxygenase-1 and increased amounts of 4-hydroxynonenal (143, 182). There was no evidence of neuronal loss in CA1, decrements in synaptophysin immunoreactivity in the dentate gyrus, or reductions in mRNA for several proteins, including synaptophysin, microtubule-associated protein 2, and cyclooxygenase 2 (72). The Tg2576 mice, which are not congenic, have shown impairments on several memory tests (e.g. Morris water maze, a spatial reference task, and Y-maze alternation tasks). Tg2576 and non-Tg mice were tested at the ages of 3 and 10 months in the Y-maze and at 2, 6, and 10 months in the Morris water maze (67). In the Y-maze, at 3 months of age, Tg2576 mice were not significantly different from non-Tg mice. However, Tg2576 mice had a tendency to alternate less than did non-Tg mice at 10 months of age, a difference that reached statistical significance ($P < 0.03$). Interestingly, Holcolmb and colleagues (64) reported reduced performance in the Y-maze in 3-month-old Tg2576 mice. The basis for the discrepancy between the first (67) and second (64) studies remains unclear. Significantly, the coexpression of mutant PS1 transgenes with the PrP/Hu-APPswe transgene did not further influence spontaneous alternation in the Y-maze, even though the coexpression of mutant PS1 markedly accelerated the rate of amyloid deposition (64). The interpretations of some of the behavioral observations on these mice have been challenged (164) and defended (68).

Using a recently engineered PrP vector (15), two lines of mice were produced that express the APP transgene product at levels two- to threefold higher than the level of endogenous mouse Mo-APP. Levels of Aβ40 and Aβ42 in brain were increased, and at >20 months of age, these Mo/HuAPPswe Tg mice developed diffuse and compact Aβ42 immunoreactive deposits in brain and Aβ40-immunoreactive deposits in blood vessels. Many of the amyloid deposits are surrounded by enlarged dystrophic neurites and glial cells. Preliminary behavioral studies on lines made congenic by backcrossing to C57BL/6J mice suggest that the mice with APPswe mutations develop a memory deficit by 12 months of age (i.e. before overt Aβ deposition) (A Markowska, DR Borchelt, personal observations).

APP-751SWE/V717I TRANSGENIC MICE When the Thy-1 expression cassette was used to drive HuAPP-751 with either the Swedish mutation or the Swedish mutation and the V717I mutation (187), two lines of Tg mice showed pathology that was influenced by the level of transgene expression and the specific mutation. At 18 months of age, a line of mice with twofold overexpression of APPswe V717I showed Aβ deposition in the neocortex. At 6 months old, Tg mice that overexpressed APPswe at a level sevenfold over endogenous showed Congo red–positive Aβ plaques and neurites associated with hyperphosphorylated tau immunoreactivity. The number of plaques and the degree of tau phosphorylation increased with age. Behavioral abnormalities have not been described.

PRESENILIN 1 (WILD-TYPE OR MUTANT) TRANSGENIC MICE In lines of mice expressing wt PS1 under the influence of the prp promotor (15) and in mice expressing either HuPS1 M146L or HuPS1 M146V (38), the HuPS1 mRNA was expressed, spliced correctly, and translated into full-length PS1 46- and 27-kDa PS1 derivatives. The brains of mice expressing mutant PS1, but not wt PS1, showed increased levels of murine Aβ42/43. There was no evidence of Aβ deposition (38); some increased ratios of Aβ42:40.

APPSWE/PRESENILIN 1 (WILD-TYPE OR MUTANT) TRANSGENIC MICE Tg mice that coexpress mutant A246E HuPS1 and Mo/Hu-APPswe were produced

(16, 17), and at 12 months of age, these animals showed numerous amyloid deposits in hippocampus and cortex (16). Many of the Aβ deposits were associated with dystrophic neurites and reactive astrocytes. Parallel analyses of brains from age-matched animals that express APP695swe alone, or mice that express HuPS1 A246E alone, were free of amyloid deposits (16). Thus, the presence of the PS1 mutation accelerates the deposition of Aβ. In another study, APPswe Tg mice were mated with PS1 M146L Tg mice, and double Tg progeny showed an increase in Aβ42/43 in brain and Aβ deposits in cortex and hippocampus (64).

APP V717F/TGFβ1 TRANSGENIC MICE In Tg mice expressing transforming growth factor (TGF) β1 under the influence of the glial fibrillary acid protein promoter, TGFβ1 was produced by brain astrocytes (217), and the expression of the transgene product was most conspicuous in perivascular locations. These animals showed no overt phenotype but did exhibit enhanced susceptibility to experimental autoimmune encephalomyelitis. In progeny of the mating of TGFβ1 Tg mice and APP V717F Tg mice, there was an acceleration of Aβ deposition, with amyloid most prominent around blood vessels. No behavioral studies are described.

APPSWE/APOE$^{-/-}$ TRANSGENIC MICE Recently, the effects of apoE on amyloid deposition have been tested by mating apoE$^{-/-}$ mice with APP V717F Tg mice (9). At 6 months of age, APP V717F:apoE$^{+/+}$ mice showed robust amyloid deposition, whereas APP V717F:apoE$^{-/-}$ mice exhibited only sparse, diffuse Aβ deposits that were not positive with thioflavin S or Congo red. In Tg mice lacking apoE, the average area occupied by Aβ-immunoreactive deposits and the total areas of Aβ immunoreactivity were reduced compared with animals expressing the APP mutants above. There was no obvious influence of the apoE$^{-/-}$ state on APP mRNA or protein or on levels of Aβ; Aβ42 levels were not reduced in APP V717F:apoE$^{-/-}$ mice. These lines of evidence suggest that neither reduced expression of the transgene nor the processing of APP to Aβ accounts for the absence of Aβ deposits in these mice. It was hypothesized that apoE isoforms may differentially promote the aggregation, fibril formation, or influence the clearance of Aβ. No behavioral studies have been reported.

Amyloid Precursor Protein and Presenilin 1 Gene-Targeted Mice

APP$^{-/-}$ MICE When compared with hemizygous APP or wt littermates, homozygous APP knockout mice were fertile and viable but exhibited subtle decreases in locomotor activity and forelimb grip strength as well as reactive astrogliosis (222). The absence of substantial phenotypes in APP knockout mice may be related to functional redundancy provided by homologous amyloid precursor-like proteins (APLP1 and APLP2), molecules expressed with developmental and cellular distributions similar to APP (181, 206, 207). Consistent with this idea is the observation that mice with both APP- and APLP2-targeted alleles show a high incidence of postnatal lethality (204).

PS1$^{-/-}$ MICE Although the *C. elegans* rescue experiments provided compelling evidence that HuPS1 and -PS2 could substitute for sel-12, the role of PS in mammalian development was uncertain. In situ hybridization studies and reverse transcriptase–polymerase chain reaction approaches with mouse embryos revealed that PS are expressed in an ubiquitous manner during embryonic development (i.e. as early as embryonic day 8.5) (95), but the general spatial and temporal expression patterns of PS mRNA do not directly coincide with the expression patterns of any specific member of the known mammalian notch homologs (95). To examine the role of PS1 in development, two groups produced PS1$^{-/-}$ mice. Homozygous mutant mice failed to survive beyond the early postnatal period (175, 216). The most striking phenotype observed in PS1$^{-/-}$ embryos was a severe perturbation in the development of the axial skeleton and ribs. The failed development of the axial skeleton in PS1$^{-/-}$ animals was traced to defects in somitogenesis; in embryos 8.5 and 9.5 days old, elements of the vertebral column were irregularly shaped and misaligned along the entire length of the neural tube and largely absent at the caudalmost regions. The abnormal somite patterns in PS1$^{-/-}$ embryos are highly reminiscent of somite segmentation defects described in mice with functionally inactivated notch1 and Dll1 (encoding a notch ligand) alleles (26, 66). Remarkably, the expression of mRNA that encodes notch1 and Dll1 is reduced considerably in the presomitic mesoderm of PS1$^{-/-}$ mice (216). In addition, all PS1$^{-/-}$ embryos exhibited intraparenchymal hemorrhages after day 11 of gestation. It has also been reported that in the brains of PS1$^{-/-}$ mice, the ventricular zone is thinner by day 14.5 and that massive neuronal loss in specific subregions is apparent after day 16.5. Shen and colleagues (175) interpreted these observations to indicate that PS1 is required for normal neurogenesis and neuronal survival. In the presence of the confounding cerebral hemorrhage, however, the neuronal phenotypes remain unsettled. A more satisfying model, in which the PS1 gene is ablated in a conditional manner, is necessary in order to fully clarify this issue.

In view of the evidence in *C. elegans* that documented that FAD-linked mutant PS failed to completely rescue an egg-laying defect in worms lacking *sel-12*, we tested the ability of an FAD-linked PS1 variant to complement the embryonic lethality and axial skeletal defects in mice lacking PS1. Breeding experiments were performed in which mice, heterozygous for *PS1*, were mated with Tg mice expressing either wt or the A246E PS1 variant driven by the MoPrP or the HuThy1 promoter. Resulting Tg mice on a *PS1*$^{+/-}$ background were intercrossed to generate Tg mice on a *PS1*$^{-/-}$ background. Both wt and mutant HuPS1 transgenes rescued *notch 1* mRNA expression in the presomitic mesoderm in early embryos (31) and the entire spectrum of developmental deficits in PS1$^{-/-}$ mice (31, 153). Thus, the FAD-linked A246E PS1 variant, and presumably other mutants, retain sufficient normal function to allow normal mammalian embryonic development.

FUTURE DIRECTIONS IN TRANSGENIC MODELING OF ALZHEIMER'S DISEASE

Multiple lines of Tg mice now exist that show Aβ deposits and neuritic plaques. However, there is no consensus about whether these mice show several other significant features of AD, including reductions in numbers of synapses/levels of transmitter markers, perturbations of the neuronal cytoskeleton, aberrant processing of APP by subsets of neurons that are affected in AD, death/loss of specific populations of neurons, or progressive impairments in performance on memory tasks. Thus, the presently available lines of Tg mice have not yet been shown to reproduce all of the features of AD. In future studies, investigators will have to deal with a variety of issues, several of which are outlined below.

The effects of genetic strains can have significant effects on behavioral and pathological phenotypes. In a series of collaborative studies, multiple lines of Tg mice were engineered to express a variety of Mo and HuAPP transgenes (wt and mutant) under the transcriptional control of the hamster PrP promoter (69). FVB/N mice were chosen for these initial studies because these mice are an inbred strain, have an easily injectable prominent pronucleus, are highly fertile, and have been used successfully to model a neurodegenerative disorder (i.e. prion diseases). The expression of transgene-encoded APP was largely copy-number dependent (69). Mice with >30 copies produced APP at levels three to five times that of non-Tg mice. Tg mice expressing high levels of several APP transgenes showed a variety of transgene dose-related abnormalities, including inactivity, agitation, neophobia, seizures, diminished glucose utilization and gliosis in corticolimbic areas, and premature death. No extracellular amyloid was detected. Moreover, a similar neurological disorder develops naturally in older non-Tg FVB mice, and our results were consistent with the interpretation that this age- and strain-related phenotype is exacerbated by the presence of APP transgenes. Recently, these APP Tg mice were mated to our wt SOD1 Tg mice; the presence of SOD1 acted to protect mice from premature death associated with the expression of the APP transgene in FVB mice (21). However, it is now clear that these phenotypes are FVB strain specific and the FVB strain is not useful for efforts designed to produce mutant APP Tg mice with AD-type behavioral deficits and pathology. As indicated above, investigators have been much more successful in reproducing AD-like pathology in other strains of mice.

Because AD is characterized by progressive memory deficits, the demonstration of memory impairments in Tg mice will be critical for studying the biological substrates of behavior-brain dysfunction related to AD-linked genes. In the past, many laboratories have produced Tg mice by injecting transgene DNA into fertilized embryos derived from matings of hybrids (mixed strains of mice), an approach used because hybrid mixtures of different strains generally produce larger litters and more robust embryos. Unfortunately, criteria based on fertility, etc, do not screen for some undesirable traits that occur in many inbred strains of mice. Among the traits that are most problematic for studies that seek to model age-associated cognitive/memory disorders are reduced lifespan, a tendency for spontaneous seizures, susceptibility to tumors, and visual impairments. Thus, mice harboring some of these traits may die at relatively young ages, show brain abnormalities related to seizures, and develop tumors before the appearance of age-associated phenotypes. Moreover, many inbred strains of mice carry a recessive mutation, termed *rd*, that causes retinal degeneration at early ages. Many of the paradigms used to assess learning and memory in small rodents, such as the water maze or the radial arm maze, are based on the abilities of the animal to process visual cues, and relative to animals with normal acuity, mice with poor vision perform poorly in these paradigms. If hybrid strains are used as transgene recipients and if one of the strains that is used carries the *rd* mutation, then the reassortment of the *rd* gene within breeding populations of hybrid mice could generate Tg mice that are also blind. Thus, any study that uses hybrid strains of Tg mice and then uses these hybrids in spatial memory paradigms must include an assessment of visual perception. In addition to vision, behavioral paradigms can be influenced by many other factors, including sensorimotor functions, motivation, and emotional responses. Different inbred strains vary in these characteristics, and the reassortment of genes that govern these behaviors can profoundly influence outcomes in learning/memory tasks.

Until recently, there has been no consensus on the use of different inbred strains of mice or hybrids between strains in the production of Tg mouse models of human disease. Because the genetic background of transgene hosts can confound the interpretation of behavioral testing of Tg and gene-targeted mice, a panel of scientists has recommended that behavioral studies be conducted only with mice that are congenic for a specific background. Of the many strains of inbred mice, the panel chose C57BL/6J to be one of the recommended strains because these animals represent a commonly used strain that has been found previously to be suitable for testing in spatial memory tasks. These mice perform well in tests of memory/cognition, including the Morris water maze (142, 199), the eight-arm radial maze (5, 163), and conditional spatial alternation (144).

Therefore, future approaches will probably necessitate back breeding transgenes into C57BL/6J until the mice are congenic.

Finally, the various lines of Tg mice expressing APP and PS1 mutant transgenes have not developed NFT. Significantly, to date, mice do not develop Aβ deposits unless they express Hu-APP or mouse APP with a "humanized" Aβ region. A similar situation may pertain with regard to tau, and perhaps it will be necessary to express a human tau transgene to generate NFT in mice.

CONCLUSIONS

Over the past decade, significant progress has been made in clinical assessments of patients with senile dementia, in the accuracy of making a diagnosis of AD, in understanding the character, evolution, and mechanisms of the biochemical/cellular abnormalities in affected brain tissues, and in identifying some of the genes implicated in AD. *APP*, *PS1*, and *PS2* account for 30–40% of early-onset familial AD. In contrast, late-onset AD has been associated with apoE4 and LRP, which encodes a neuronal receptor for both apoE and APP. More recently, A2M, a major LRP ligand and serum pan-protease inhibitor, has been shown to confer risk for AD.

The discovery that mutations in genes encoding APP, PS1, and PS2 are linked to FAD has ushered in a new and exciting era of research aimed at clarifying the relationships of these genetic abnormalities to the pathogenesis of AD. Moreover, as exemplified by studies of the roles of apoE allele types, LRP, and A2M in late-onset AD, genetic factors undoubtedly play significant roles in influencing the predisposition for or timing of late-onset disease. We believe that investigations of presently available Tg models (and superior variants created in the future) will help define the relationships between impaired behavioral performance and pathological/biochemical abnormalities in brain, help to clarify pathogenic mechanisms in vivo, lead to identification of new therapeutic targets, and allow testing of new treatment strategies first in mice and then, if successful, in humans with AD.

ACKNOWLEDGMENTS

We gratefully acknowledge the contributions of and helpful discussions with our colleagues Drs. Alicja Markowska, Gopal Thinakaran, Michael K Lee, Philip C Wong, Nancy Jenkins, Neal Copeland, Juan C Troncoso, Vassilis E Koliatsos, Peter R Mouton, and Lee J Martin. This work was supported by grants from the US Public Health Service (AG 05146, NS 20471, AG 08325, AG 14248) as well as from the Adler Foundation, the Alzheimer's Association, the Develbiss fund, the American Health Assistance Foundation, and Merck, Sharp & Dohme. Drs. Price and Borchelt are the recipients of a Leadership and

Excellence in Alzheimer's Disease (LEAD) Award (AG 07914). Dr. Price is the recipient of a Javits Neuroscience Investigator Award (NS 10580) and a TLL Temple Foundation Discovery Award for Alzheimer's Disease Research from the Alzheimer's Association. Dr. Sisodia is the recipient of a Zenith Award from the Alzheimer's Association. Dr. Tanzi is the recipient of grants from the NIA, NIMH, and NINDS.

Visit the *Annual Reviews home page* at
http://www.AnnualReviews.org

Literature Cited

1. Deleted in proof
2. Abraham CR, Selkoe DJ, Potter H. 1988. Immunocytochemical identification of the serine protease inhibitor α_1-antichymotrypsin, in the brain amyloid deposits of Alzheimer's disease. *Cell* 52: 487–501
3. Abraham CR, Selkoe DJ, Poter H, Price DL, Cork LC. 1989. α_1-Antichymotrypsin is present together with the β-protein in monkey brain amyloid deposits. *Neuroscience* 32:715–20
4. Albert MS. 1996. Cognitive and neurobiologic markers of early Alzheimer disease. *Proc. Natl. Acad. Sci. USA* 93: 13547–51
5. Ammassari-Teule M, Hoffman H-J, Rossi-Arnaud C. 1993. Learning in inbred mice: strain-specific abilities across three radial maze problems. *Behav. Genet.* 23:405–12
6. Anderton BH, Breinburg D, Downes MJ, Green PJ, Tomlinson BE, et al. 1982. Monoclonal antibodies show that neurofibrillary tangles and neurofilaments share antigenic determinants. *Nature* 298:84–86
7. Arnold SE, Hyman BT, Flory J, Damasio AR, Van Hoesen GW. 1991. The topographical and neuroanatomical distribution of neurofibrillary tangles and neuritic plaques in the cerebral cortex of patients with Alzheimer's disease. *Cereb. Cortex* 1:103–16
8. Artavanis-Tsakonas S, Matsuno K, Fortini ME. 1995. Notch signaling. *Science* 268:225–32
9. Bales KR, Verina T, Dodel RC, Du Y, Altstiel L, et al. 1997. Lack of apolipoprotein E dramatically reduces amyloid B-peptide deposition. *Nat. Genet.* 17:263–64
10. Baumeister R, Leimer U, Zweckbronner I, Jakubek C, Grünberg J, et al. 1997. Human presenilin-1, but not familial Alzheimer's disease (FAD) mutants, facilitate *Caenorhabditis elegans* Notch signalling independently of proteolytic processing. *Genes Funct.* 1:149–59
11. Berg L, Morris JC. 1994. Diagnosis. See Ref. 193a, pp. 9–25
12. Blacker D, Haines JL, Rodes L, Terwedow H, Go RCP, et al. 1997. ApoE-4 and age at onset of Alzheimer's disease: the NIMH genetics initiative. *Neurology* 48:139–47
13. Blacker D, Wilcox MA, Laird NM, Rodes L, Horvath SM, et al. 1998. Alpha-2-macroglobulin is associated with Alzheimer's disease. *Nat. Genet.* In press
14. Blessed G, Tomlinson BE, Roth M. 1968. The association between quantitative measures of dementia and of senile change in the cerebral grey matter of elderly subjects. *Br. J. Psychiatry* 114:797–811
15. Borchelt DR, Davis J, Fischer M, Lee MK, Slunt HH, et al. 1996. A vector for expressing foreign genes in the brains and hearts of transgenic mice. *Genet. Anal. Biomed. Eng.* 13:159–63
16. Borchelt DR, Ratovitski T, Van Lare J, Lee MK, Gonzales VB, et al. 1997. Accelerated amyloid deposition in the brains of transgenic mice co-expressing mutant presenilin 1 and amyloid precursor proteins. *Neuron* 19:939–45
17. Borchelt DR, Thinakaran G, Eckman CB, Lee MK, Davenport F, et al. 1996. Familial Alzheimer's disease-linked presenilin 1 variants elevate Aβ1-42/1-40 ratio in vitro and in vivo. *Neuron* 17:1005–13
18. Borth W. 1992. Alpha 2-macroglobulin,

a multifunctional binding protein with targeting characteristics. *FASEB J.* 6:3345–53

19. Braak H, Braak E. 1994. Pathology of Alzheimer's disease. In *Neurodegenerative Diseases*, ed. DB Calne, 35:585–613. Philadelphia, PA: Saunders
20. Buxbaum JD, Christensen JL, Ruefli AA, Greengard P, Loring JF. 1993. Expression of APP in brains of transgenic mice containing the entire human *APP* gene. *Biochem. Biophys. Res. Commun.* 197:639–45
21. Carlson GA, Borchelt DR, Dake A, Turner S, Danielson V, et al. 1997. Genetic modification of the phenotypes produced by amyloid precursor protein overexpression in transgenic mice. *Hum. Mol. Genet.* 6:1951–59
22. Chartier-Harlin M-C, Crawford F, Houlden H, Warren A, Hughes D, et al. 1991. Early-onset Alzheimer's disease caused by mutations at codon 717 of the β-amyloid precursor protein gene. *Nature* 353:844–46
23. Chartier-Harlin M-C, Parfitt M, Legrain S, et al. 1994. Apolipoprotein E, $\varepsilon 4$ allele as a major risk factor for sporadic early- and late-onset forms of Alzheimer's disease: analysis of the 19q13.2 chromosomal region. *Hum. Mol. Genet.* 3:569–74
24. Citron M, Oltersdorf T, Haass C, McConlogue L, Hung AY, et al. 1992. Mutation of the β-amyloid precursor protein in familial Alzheimer's disease increases β-protein production. *Nature* 360:672–74
25. Citron M, Westaway D, Xia W, Carlson G, Diehl T, et al. 1997. Mutant presenilins of Alzheimer's disease increase production of 42-residue amyloid β-protein in both transfected cells and transgenic mice. *Nat. Med.* 3:67–72
26. Conlon RA, Reaume AG, Rossant J. 1995. *Notch 1* is required for the coordinate segmentation of somites. *Development* 121:1533–45
27. Cook DG, Forman MS, Sung JC, Leight S, Kolson DL, et al. 1997. Alzheimer's Aβ(1–42) is generated in the endoplasmic reticulum/intermediate compartment of NT2N cells. *Nat. Med.* 3:1021–23
28. Corder EH, Saunders AM, Strittmatter WJ, Schmechel DE, Gaskell PC, et al. 1993. Gene dose of apolipoprotein-E type 4 allele and the risk of Alzheimer's disease in late onset families. *Science* 261:921–23
29. Crook R, Chen LS, Bende SM, LaFerla FM. 1998. A variant of Alzheimer's disease wtih spastic paraphrasis and unusual plaques due to deletion of exon 9 of presenilin 1. *Nat. Med.* 4:1–4
30. Cruts M, van Duijn CM, Backhovens H, van den Broeck M, Wehnert A, et al. 1998. Estimation of the genetic contribution of presenilin-1 and -2 mutations in a population-based study of presenile Alzheimer disease. *Hum. Mol. Genet.* 71:43–51
31. Davis JA, Naruse S, Chen H, Eckman C, Younkin S, et al. 1998. An Alzheimer's disease-linked PS1 variant rescues the developmental abnormalities of *PS1*-deficient embryos. *Neuron* 20: 603–9
32. Davis RE, Miller S, Herrnstadt C, Ghosh SS, Fahy E, et al. 1997. Mutations in mitochondrial cytochrome *c* oxidase genes segregate with late-onset Alzheimer disease. *Proc. Natl. Acad. Sci. USA* 94:4526–31
33. Delacourte A, Sereant N, Wattez A, Gauvreau D, Robitaille Y. 1998. Vulnerable neuronal subsets in Alzheimer's and Pick's disease are distinguished by their τ isoform distribution and phosphorylation. *Ann. Neurol.* 43:193–204

33a. De Strooper B, Saftig P, Craessaorts K, et al. 1998. Deficiency of presenilin-1 inhibits the normal cleavage of amyloid precursor protein. *Nature* 391:387–90

34. Dickson DW. 1997. Neurodegenerative diseases with cytoskeletal pathology: a biochemical classification. *Ann. Neurol.* 42:541–44
35. Doan A, Thinakaran G, Borchelt DR, Slunt HH, Ratovitsky T, et al. 1996. Protein topology of presenilin 1. *Neuron* 17: 1023–30
36. Drachman DA. 1997. Aging and the brain: a new frontier. *Ann. Neurol.* 42: 819–28
37. Du Y. 1997. Alpha-2-macroglobulin as a beta-amyloid peptide-binding plasma protease. *J. Neurochem.* 69:299–305
38. Duff K, Eckman C, Zehr C, Yu X, Prada C-M, et al. 1996. Increased amyloid-β42(43) in brains of mice expressing mutant presenilin 1. *Nature* 383:710–13
39. Esch FS, Keim PS, Beattie EC, Blacher RW, Culwell AR, et al. 1990. Cleavage of amyloid β peptide during constitutive processing of its precursor. *Science* 248: 1122–24
40. Evans DA, Beckett LA, Field TS, Feng L, Albert MS, et al. 1997. Apolipoprotein E $\varepsilon 4$ and incidence of Alzheimer disease in a community population of older persons. *JAMA* 277:822–24
41. Evans DA, Funkenstein HH, Albert MS, Scherr PA, Cook NR, et al. 1989.

Prevalence of Alzheimer's disease in a community population of older persons. Higher than previously reported. *JAMA* 262:2551–56

42. Farlow MR. 1997. Alzheimer's disease: clinical implications of the apolipoprotein E genotype. *Neurology* 48:S30–34
43. Feany MB, Dickson DW. 1996. Neurodegenerative disorders with extensive tau pathology: a comparative study and review. *Ann. Neurol.* 40:139–48
44. Foster NL, Wilhelmsen K, Sima AAF, Jones MZ, D'Amato CJ, et al. 1997. Frontotemporal dementia and Parkinsonism linked to chromosome 17: a consensus conference. *Ann. Neurol.* 41: 706–15
45. Francis PT, Cross AJ, Bowen DM. 1994. Neurotransmitters and neuropeptides. See Ref. 193a, pp. 247–61
46. Galasko D, Saitoh T, Xia Y, Thal LJ, Katzman R, et al. 1994. The apolipoprotein E allele $\varepsilon 4$ is overrepresented in patients with the Lewy body variant of Alzheimer's disease. *Neurology* 44:1950–51
47. Games D, Adams D, Alessandrini R, Barbour R, Berthelette P, et al. 1995. Alzheimer-type neuropathology in transgenic mice overexpressing V717F β-amyloid precursor protein. *Nature* 373:523–27
48. Gerlai R. 1996. Gene-targeting studies of mammalian behavior: Is it the mutation or the background phenotype? *Trends Neurosci.* 19:177–81
49. Geula C, Mesulam M-M. 1994. Cholinergic systems and related neuropathological predilection patterns in Alzheimer disease. See Ref. 193a, pp. 263–91
50. Glenner GG, Wong CW. 1984. Alzheimer's disease: initial report of the purification and characterization of a novel cerebrovascular amyloid protein. *Biochem. Biophys. Res. Commun.* 120: 885–90
51. Goate A, Chartier-Harlin M-C, Mullan M, Brown J, Crawford F, et al. 1991. Segregation of a missense mutation in the amyloid precursor protein gene with familial Alzheimer's disease. *Nature* 349:704–6
52. Goedert M, Jakes R, Spillantini MG, Hasegawa M, Smith MJ, et al. 1996. Assembly of microtubule-associated protein tau into Alzheimer-like filaments induced by sulphated glycosaminoglycans. *Nature* 383:550–53
53. Goedert M, Spillantini MG, Cairns NJ, Crowther RA. 1992. Tau proteins of Alzheimer paired helical filaments: abnormal phosphorylation of all six brain isoforms. *Neuron* 8:159–68
54. Goldgaber D, Lerman MI, McBride OW, Saffiotti U, Gajdusek DC. 1987. Characterization and chromosomal localization of a cDNA encoding brain amyloid of Alzheimer's disease. *Science* 235:877–80
55. Gómez-Isla T, West HL, Rebeck GW, Harr SD, Growdon JH, et al. 1996. Clinical and pathological correlates of apolipoprotein E $\varepsilon 4$ in Alzheimer disease. *Ann. Neurol.* 39:62–70
56. Griffin WST, Sheng JG, Roberts GW, Mrak RE. 1995. Interleukin-1 expression in different plaque types in Alzheimer's disease: significance in plaque evolution. *J. Neuropathol. Exp. Neurol.* 54:276–81
57. Grundke-Iqbal I, Iqbal K, Quinlan M, Tung Y-C, Zaidi MS, et al. 1986. Microtubule-associated protein tau. A component of Alzheimer paired helical filaments. *J. Biol. Chem.* 261:6084–89
58. Haass C, Lemere CA, Capell A, Citron M, Seubert P, et al. 1995. The Swedish mutation causes early-onset Alzheimer's disease by β-secretase cleavage within the secretory pathway. *Nat. Med.* 1:1291–96
59. Haass C, Selkoe DJ. 1993. Cellular processing of β-amyloid precursor and the genesis of amyloid β-peptide. *Cell* 75:1039–42
60. Hardy J. 1997. Amyloid, the presenilins and Alzheimer's disease. *Trends Neurosci.* 20:154–59
61. Hartmann T, Bieger SC, Brühl B, Tienari PJ, Ida N, et al. 1997. Distinct sites of intracellular production for Alzheimer's disease $A\beta 40/42$ amyloid peptides. *Nat. Med.* 3:1016–20
62. Hendricks L, van Duijn CM, Cras P, Cruts M, Van Hul W, et al. 1992. Presenile dementia and cerebral haemorrhage linked to a mutation at codon 692 of the β-amyloid precursor protein gene. *Nat. Genet.* 1:218–21
63. Higgins LS, Holtzman DM, Rabin J, Mobley WC, Cordell B. 1994. Transgenic mouse brain histopathology resembles early Alzheimer's disease. *Ann. Neurol.* 35:598–607

63a. Hirano M, Shtilbans A, Mayeux R, et al. 1997. Apparent mtDNA heteroplasmy in Alzheimer's disease patients and in normals due to PCR amplification of nucleus-embedded mtDNA pseudogenes. *Proc. Natl. Acad. Sci. USA* 94: 14894–99

64. Holcomb L, Gordon MN, McGowan E, Yu X, Benkovic S, et al. 1998. Accelerated Alzheimer-type phenotype in transgenic mice carrying both mutant *amyloid precursor protein* and *presenilin* 1 transgenes. *Nat. Med.* 4:97–100
65. Hopkins SJ, Rothwell NJ. 1995. Cytokines and the nervous system. I: Expression and recognition. *Trends Neurosci.* 18:83–88
66. Hrabe de Angelis M, McIntyre J, Gossler A. 1997. Maintenance of somite borders in mice requires the *Delta* homologue *Dll1*. *Nature* 386:717–21
67. Hsiao K, Chapman P, Nilsen S, Eckman C, Harigaya Y, et al. 1996. Correlative memory deficits, Aβ elevation and amyloid plaques in transgenic mice. *Science* 274:99–102
68. Hsiao K, Chapman P, Nilsen S, Eckman C, Harigaya Y, et al. 1997. Measuring memory in a mouse model of Alzheimer's disease. *Science* 277:840–41
69. Hsiao KK, Borchelt DR, Olson K, Johannsdottir R, Kitt C, et al. 1995. Age-related CNS disorder and early death in transgenic FVB/N mice overexpressing Alzheimer amyloid precursor proteins. *Neuron* 15:1203–18
70. Hughes SR. 1997. Alpha-2-macroglobulin associates with β-amyloid peptide and prevents fibril formation. *J. Neurochem.* 69:299–305
71. Hyman BT, Gomez-Isla T, Briggs M, Chung H, Nichols S, et al. 1996. Apolipoprotein E and cognitive change in an elderly population. *Ann. Neurol.* 40:55–66
72. Irizarry MC, McNamara M, Fedorchak K, Hsiao K, Hyman BT. 1997. App$_{Sw}$ transgenic mice develop age-related Aβ deposits and neuropil abnormalities, but no neuronal loss in CA1. *J. Neuropathol. Exp. Neurol.* 56:965–73
73. Ishii K, Ii K, Hasegawa T, Shoji S, Doi A, et al. 1997. Increased Aβ 42(43)-plaque depostion in early-onset familial Alzheimer's disease brains with the deletion of exon 9 and the missense point mutation (H163R) in the PS-1 gene. *Neurosci. Lett.* 228:17–20
74. Iwatsubo T, Odaka A, Suzuki N, Mizusawa H, Nukina N, et al. 1994. Visualization of Aβ42(43)-positive and Aβ40-positive senile plaques with end-specific A β-monoclonal antibodies: evidence that an initially deposited Aβ species is Aβ1-42(43). *Neuron* 13:45–53
75. Jagust WJ. 1998. Neuroimaging of dementing disorders. See Ref. 113a, 2:25–55
76. Jarrett JT, Lansbury PT Jr. 1993. Seeding "one-dimensional crystallization" of amyloid: a pathogenic mechanism in Alzheimer's disease and scrapie? *Cell* 73: 1055–58
77. Johnson SA, Lampert-Etchells M, Pasinetti GM, Rozovsky I, Finch CE. 1992. Complement mRNA in the mammalian brain: responses to Alzheimer's disease and experimental brain lesioning. *Neurobiol. Aging* 13:641–48
78. Jucker M, Ingram DK. 1997. Murine models of brain aging and age-related neurodegenerative diseases. *Behav. Brain Res.* 85:1–25
79. Kamboh MI, Sanghera DK, Ferrell RE, DeKosky ST. 1995. APOE4-associated Alzheimer's disease risk is modified by alpha 1-antichymotripsin polymorphism. *Nat. Genet.* 10:486–88
80. Kammesheidt A, Boyce FM, Spanoyannis AF, Cummings BJ, Ortegón M, et al. 1992. Deposition of β/A4 immunoreactivity and neuronal pathology in transgenic mice expressing the carboxyterminal fragment of the Alzheimer amyloid precursor in the brain. *Proc. Natl. Acad. Sci. USA* 89:10857–61
81. Kang DE, Saitoh T, Chen X, Xia Y, Masliah E, et al. 1997. Genetic association of the low-density lipoprotein receptor-related protein gene (LRP), an apolipoprotein E receptor, with late-onset Alzheimer's disease. *Neurology* 49:56–61
82. Kang J, Lemaire H-G, Unterbeck A, Salbaum JM, Masters CL, et al. 1987. The precursor of Alzheimer's disease amyloid A4 protein resembles a cell-surface receptor. *Nature* 325:733–36
83. Kim T-W, Tanzi RE. 1997. Presenilins and Alzheimer's disease. *Curr. Opin. Neurobiol.* 7:683–88
84. Koo EH, Sisodia SS, Archer DR, Martin LJ, Weidemann A, et al. 1990. Precursor of amyloid protein in Alzheimer disease undergoes fast anterograde axonal transport. *Proc. Natl. Acad. Sci. USA* 87:1561–65
85. Koo EH, Squazzo SL, Selkoe DJ, Koo CH. 1996. Trafficking of cell-surface amyloid β-protein precursor. 1. Secretion, endocytosis and recycling as detected by labeled monoclonal antibody. *J. Cell Sci.* 109:991–98
86. Kounnas MZ, Moir RD, Rebeck GW, Bush AI, Argraves WS, et al. 1995. LDL receptor-related protein, a multifunctional ApoE receptor, binds secreted β-amyloid precursor protein and mediates its degradation. *Cell* 82:331–40

87. Kwok J, Taddei K, Hallupp M, Fisher C, Brooks W, et al. 1997. Two novel (M233T and R278T) presenilin-1 mutations in early-onset Alzheimer's disease pedigrees and preliminary evidence for association of presenilin-1 mutations with a novel phenotype. *Neuroreport* 8:1537–42
88. LaFerla FM, Tinkle BT, Bieberich CJ, Haudenschild CC, Jay G. 1995. The Alzheimer's Aβ peptide induces neurodegeneration and apoptotic cell death in transgenic mice. *Nat. Genet.* 9:21–30
89. Lamb BT, Call LM, Slunt HH, Bardel KA, Lawler AM, et al. 1997. Altered metabolism of familial Alzheimer's disease-linked amyloid precursor protein variants in yeast artificial chromosome transgenic mice. *Hum. Mol. Genet.* 6:1535–41
90. Lamb BT, Sisodia SS, Lawler AM, Slunt HH, Kitt CA, et al. 1993. Introduction and expression of the 400 kilobase *precursor amyloid protein* gene in transgenic mice. *Nat. Genet.* 5:22–30
91. Lambert JC, Pasquier F, Cottel D, Frigard B, Amouyel P, et al. 1998. A new polymorphism in the APOE promoter associated with risk of developing Alzheimer's disease. *Hum. Mol. Genet.* 7:533–40
92. Lambert JC, Perez-Tur J, Dupire MJ, Galasko D, Amouyel P, et al. 1997. Distortion of allelic expression of apolipoprotein E in Alzheimer's disease. *Hum. Mol. Genet.* 6:2151–54
93. Lansbury PT Jr. 1997. Structural neurology: Are seeds at the root of neuronal degeneration? *Neuron* 19:1151–54
94. Lee MK, Borchelt DR, Kim G, Thinakaran G, Slunt HH, et al. 1997. Hyperaccumulation of FAD-linked presenilin 1 variants *in vivo*. *Nat. Med.* 3:756–60
95. Lee MK, Slunt HH, Martin LJ, Thinakaran G, Kim G, et al. 1996. Expression of presenilin 1 and 2 (PS1 and PS2) in human and murine tissues. *J. Neurosci.* 16:7513–25
96. Lee VMY, Balin BJ, Otvos L Jr, Trojanowski JQ. 1991. A68: a major subunit of paired helical filaments and derivatized forms of normal tau. *Science* 251:675–78
97. Lehmann DJ, Johnston C, Smith AD. 1997. Synergy between the genes for butyrylcholinesterase K variant and apolipoprotein E4 in late-onset confirmed Alzheimer's disease. *Hum. Mol. Genet.* 6:1933–36
98. Lehmann S, Chiesa R, Harris DA. 1997. Evidence for a six-transmembrane domain structure of presenilin 1. *J. Biol. Chem.* 272:12047–51
99. Lemere CA, Blusztajn JK, Yamaguchi H, Wisniewski T, Saido TC, et al. 1996. Sequence of deposition of heterogeneous amyloid β-peptides and APO E in Down syndrome: implications for initial events in amyloid plaque formation. *Neurobiol. Dis.* 3:16–32
100. Lemere CA, Lopera F, Kosik KS, Lendon CL, Ossa J, et al. 1996. The E280A presenilin 1 Alzheimer mutation produces increased Aβ42 deposition and severe cerebellar pathology. *Nat. Med.* 2:1146–50
101. Lendon CL, Talbot CJ, Craddock NJ, Han SW, Wragg M, et al. 1997. Genetic association studies between dementia of the Alzheimer's type and three receptors for apolipoprotein E in a Caucasian population. *Neurosci. Lett.* 222:187–90
102. Lennox GG, Lowe JS. 1998. Dementia with Lewy bodies. See Ref. 113a, 10:181–92
103. Levitan D, Doyle TG, Brousseau D, Lee MK, Thinakaran G, et al. 1996. Assessment of normal and mutant human presenilin function in *Caenorhabditis elegans*. *Proc. Natl. Acad. Sci. USA* 93:14940–44
104. Levitan D, Greenwald I. 1995. Facilitation of *lin-12*-mediated signalling by *sel-12*, a *Caenorhabditis elegans* S182 Alzheimer's disease gene. *Nature* 377:351–54
105. Levy E, Carman MD, Fernandez-Madrid IJ, Power MD, Lieberburg I, et al. 1990. Mutation of the Alzheimer's disease amyloid gene in hereditary cerebral hemorrage, Dutch type. *Science* 248:1124–26
106. Levy-Lahad E, Wasco W, Poorkaj P, Romano DM, Oshima J, et al. 1995. Candidate gene for the chromosome 1 familial Alzheimer's disease locus. *Science* 269:973–77
107. Li X, Greenwald I. 1996. Membrane topology of the *C. elegans* SEL-12 presenilin. *Neuron* 17:1015–21
108. Lopes MB, Bogaev CA, Gonias SL, Vandenberg SR. 1993. Expression of alpha-2-macroglobulin receptor/low density lipoprotein receptor-related protein is increased in reactive and neoplastic glial cells. *FEBS Lett.*
109. Lue L-F, Brachova L, Civin WH, Rogers J. 1996. Inflammation, Aβ deposition, and neurofibrillary tangle formation as correlates of Alzheimer's disease neurodegeneration. *J. Neuropathol. Exp. Neurol.* 55:1083–88

110. Mackenzie IRA, Hao C, Munoz DG. 1995. Role of microglia in senile plaques formation. *Neurobiol. Aging* 16:797–804
111. Mann DMA, Iwatsubo T, Cairns NJ, Lantos PL, Nochlin D, et al. 1996. Amyloid β protein (Aβ) deposition in chromosome 14-linked Alzheimer's disease: predominance of A$\beta_{42(43)}$. *Ann. Neurol.* 40:149–56
112. Mann DMA, Iwatsubo T, Fukomoto H, Ihara Y, Odaka A, et al. 1995. Microglial cells and amyloid β protein (Aβ) deposition: association with Aβ_{40}-containing plaques. *Acta Neuropathol.* 90:472–77
113. Mann DMA, Iwatsubo T, Nochlin D, Sumi SM, Levy-Lahad E, et al. 1997. Amyloid (Aβ) deposition in chromosome 1-linked Alzheimer's disease: the Volga German families. *Ann. Neurol.* 41:52–57
113a. Markesbery WR, ed. 1998. *Neuropathology of Dementing Disorders*. London: Arnold
114. Markesbery WR. 1998. Pick's disease. See Ref. 113a, 7:142–57
115. Markesbery WR. 1998. Vascular dementia. See Ref. 113a, 15:293–311
116. Martin LJ, Sisodia SS, Koo EH, Cork LC, Dellovade TL, et al. 1991. Amyloid precursor protein in aged nonhuman primates. *Proc. Natl. Acad. Sci. USA* 88:1461–65
117. Masliah E. 1998. The role of synaptic proteins in neurodegenerative disorders. *Neurosci. News* 1:14–20
118. Masliah E, Ellisman M, Carragher B, Mallory M, Young S, et al. 1992. Three-dimensional analysis of the relationship between synaptic pathology and neuropil threads in Alzheimer disease. *J. Neuropathol. Exp. Neurol.* 51:404–14
119. Masliah E, Hansen L, Albright T, Mallory M, Terry RD. 1991. Immunoelectron microscopic study of synaptic pathology in Alzheimer's disease. *Acta Neuropathol.* 81:428–33
120. Masliah E, Sisk A, Mallory M, Mucke L, Schenk D, et al. 1996. Comparison of neurodegenerative pathology in transgenic mice overexpressing V717F β-amyloid precursor protein and Alzheimer's disease. *J. Neurosci.* 16:5795–811
121. Masters CL, Multhaup G, Simms G, Pottgiesser J, Martins RN, et al. 1985. Neuronal origin of a cerebral amyloid: neurofibrillary tangles of Alzheimer's disease contain the same protein as the amyloid of plaque cores and blood vessels. *EMBO J.* 4:2757–63
122. Mattson MP. 1997. Cellular actions of β-amyloid precursor protein and its soluble and fibrillogenic derivatives. *Physiol. Rev.* 77:1081–132
123. Mayeux R, Saunders AM, Shea S, Mirra S, Evans D, et al. 1998. Utility of the apolipoprotein-E genotype in the diagnosis of Alzheimer's disease. *N. Engl. J. Med.* 338:506–11
124. Mayeux R, Stern Y, Ottman R, Tatemichi TK, Tang M-X, et al. 1993. The apolipoprotein ε4 allele in patients with Alzheimer's disease. *Ann. Neurol.* 34:752–54
125. McGeer PL, Itagaki S, Tago H, McGeer EG. 1987. Reactive microglia in patients with senile dementia of the Alzheimer type are positive for the histocompatibility glycoprotein HLA-DR. *Neurosci. Lett.* 79:195–200
126. McGeer PL, McGeer EG. 1995. The inflammatory response system of brain: implications for therapy of Alzheimer and other neurodegenerative diseases. *Brain Res. Rev.* 21:195–218
127. McKeith IG, Galasko D, Kosaka K, Perry EK, Dickson DW, et al. 1996. Consensus guidelines for the clinical and pathologic diagnosis of dementia with Lewy bodies (DLB): report of the consortium on DLB international workshop. *Neurology* 47:1113–24
128. McKhann G, Drachman D, Folstein M, Katzman R, Price D, et al. 1984. Clinical diagnosis of Alzheimer's disease: report of the NINCDS-ADRDA Work Group under the auspices of the Department of Health and Human Services Task Force on Alzheimer's Disease. *Neurology* 34:939–44
129. Mesulam M-M, Geula C. 1994. Butyrylcholinesterase reactivity differentiates the amyloid plaques of aging from those of dementia. *Ann. Neurol.* 36:722–27
130. Meyer MR, Tschanz JT, Norton MC, et al. 1998. *ApoE* polymorphism predicts when—not whether—individuals are predisposed to develop Alzheimer's disease. *Nat. Genet.* In press
131. Montoya SE, Aston CE, DeKosky ST, Kamboh MI, Lazo JS, et al. 1998. Bleomycin hydrolase is associated with risk of sporadic Alzheimer's disease. *Nat. Genet.* 18:211–12
132. Moran PM, Higgins LS, Cordell B, Moser PC. 1995. Age-related learning deficits in transgenic mice expressing the 751-amino acid isoform of human

β-amyloid precursor protein. *Proc. Natl. Acad. Sci. USA* 92:5341–45

133. Morrison JH, Hof PR. 1997. Life and death of neurons in the aging brain. *Science* 278:412–19
134. Mullan M, Crawford F, Axelman K, Houlden H, Lillius L, et al. 1992. A pathogenic mutation for probable Alzheimer's disease in the APP gene at the N-terminus of β-amyloid. *Nat. Genet.* 1:345–47
135. Murrell J, Farlow M, Ghetti B, Benson MD. 1991. A mutation in the amyloid precursor protein associated with hereditary Alzheimer's disease. *Science* 254:97–99
136. Nalbantoglu J, Tirado-Santiago G, Lahsaini A, Poirier J, Goncalves O, et al. 1997. Impaired learning and LTP in mice expressing the carboxy terminus of the Alzheimer amyloid precursor protein. *Nature* 387:500–5
137. Namekata K, Imagawa M, Terashi A, Ohta S, Oyama F, et al. 1997. Association of transferrin C2 allele with late-onset Alzheimer's disease. *Hum. Genet.* 101:126–29
138. Narita M, Holtzman DM, Schwartz AL, Bu G. 1997. Alpha-2-macroglobulin complexes with and mediates the endocytosis of beta-amyloid peptide via cell surface low-density lipoprotein receptor-related protein. *J. Neurochem.* 69:1904–11
139. Neve RL, Kammesheidt A, Hohmann CF. 1992. Brain transplants of cells expressing the carboxyl-terminal fragment of the Alzheimer amyloid protein precursor cause specific neuropathology in vivo. *Proc. Natl. Acad. Sci. USA* 89:3448–52
140. Okuizumi K, Onodera O, Namba Y, Ikeda K, Yamamoto T, et al. 1995. Genetic association of the very low density lipoprotein (VLDL) receptor gene with sporadic Alzheimer's disease. *Nat. Genet.* 11:207–9
141. Olshansky SJ, Carnes BA, Cassel CK. 1993. The aging of the human species. *Sci. Am.* 268:46–52
142. Owen EH, Logue SF, Rasmussen DL, Wehner JM. 1997. Assessment of learning by the Morris water task and fear conditioning in inbred mouse strains and F1 hybrids: implications of genetic background for single gene mutations and quantitative trait loci analyses. *Neuroscience* 80:1087–99
143. Pappolla MA, Chyan Y-J, Omar RA, Hsiao K, Perry G, et al. 1998. Evidence of oxidative stress and *in vivo* neurotoxicity of β-amyloid in a transgenic mouse model of Alzheimer's disease. A chronic oxidative paradigm for testing antioxidant therapies in vivo. *Am. J. Pathol.* 152:871–77
144. Paylor R, Baskall L, Wehner JM. 1993. Behavioral dissociations between C57BL/6 and DBA/2 mice on learning and memory tasks: a hippocampal-dysfunction hypothesis. *Psychobiology* 21:11–26
145. Perez-Tur J, Froelich S, Prihar G, Crook R, Baker M, et al. 1995. A mutation in Alzheimer's disease destroying a splice acceptor site in the presenilin-1 gene. *Neuroreport* 7:297–301
146. Pericak-Vance MA, Bass MP, Yamaoka LH, Gaskell PC, Scott WK, et al. 1997. Complete genomic screen in late-onset familial Alzheimer disease. *JAMA* 278:1237–41
147. Perry G, Friedman R, Shaw G, Chau V. 1987. Ubiquitin is detected in neurofibrillary tangles and senile plaque neurites of Alzheimer disease brains. *Proc. Natl. Acad. Sci. USA* 84:3033–36
148. Pitschke M, Prior R, Haupt M, Riesner D. 1998. Detection of single amyloid β-protein aggregates in the cerebrospinal fluid of Alzheimer's patients by fluorescence correlation spectroscopy. *Nat. Med.* 4:832–34
149. Podlisny MB, Citron M, Amarante P, Sherrington R, Xia W, et al. 1997. Presenilin proteins undergo heterogeneous endoproteolysis between Thr_{291} and Ala_{299} and occur as stable N- and C-terminal fragments in normal and Alzheimer brain tissue. *Neurobiol. Dis.* 3:325–37
150. Poorkaj P, Bird TD, Wijsman E, Nemens E, Garruto RM, et al. 1998. Tau is a candidate gene for chromosome 17 frontotemporal dementia. *Ann. Neurol.* 43:815–25
151. Price DL, Kawas CH, Sisodia SS. 1998. Aging of the brain and dementia of the Alzheimer's type. In *Principles of Neural Science*, ed. ER Kandel, JH Schwartz, TM Jessell. New York: Elsevier. In press
152. Price DL, Sisodia SS. 1998. Mutant genes in familial Alzheimer's disease and transgenic models. *Annu. Rev. Neurosci.* 21:479–505
153. Qian S, Jiang P, Guan X, Singh G, Trumbauer M, et al. 1998. Mutant human presenilin 1 protects presenilin 1 null mouse against embryonic lethality and elevates Aß1-42/43 expression. *Neuron* 20:611–17

154. Rebeck GW, Harr SD, Strickland DK, Hyman BT. 1995. Multiple, diverse senile plaque-associated proteins are ligands of an apolipoprotein E receptor, the α_2-macroglobulin receptor/low-density-lipoprotein receptor-related protein. *Ann. Neurol.* 37:211–17
155. Rebeck GW, Reiter JS, Strickland DK, Hyman BT. 1993. Apolipoprotein E in sporadic Alzheimer's disease: allelic variation and receptor interactions. *Neuron* 11:575–80
156. Robakis NK, Ramakrishna N, Wolfe G, Wisniewski HM. 1987. Molecular cloning and characterization of a cDNA encoding the cerebrovascular and the neuritic plaque amyloid peptides. *Proc. Natl. Acad. Sci. USA* 84:4190–94
157. Rockenstein EM, McConlogue L, Tan H, Power M, Masliah E, et al. 1995. Levels and alternative splicing of amyloid β protein precursor (APP) transcripts in brains of APP transgenic mice and humans with Alzheimer's disease. *J. Biol. Chem.* 270:28257–67
158. Rogaev EI, Sherrington R, Rogaeva EA, Levesque G, Ikeda M, et al. 1995. Familial Alzheimer's disease in kindreds with missense mutations in a gene on chromosome 1 related to the Alzheimer's disease type 3 gene. *Nature* 376:775–78
159. Rogers J, Cooper NR, Webster S, Schultz J, McGeer PL, et al. 1992. Complement activation by β-amyloid in Alzheimer disease. *Proc. Natl. Acad. Sci. USA* 89:10016–20
160. Rogers J, Luber-Narod J, Styren SC, Civin WH. 1988. Expression of immune system-associated antigens by cells of the human central nervous system: relationship to the pathology of Alzheimer's disease. *Neurobiol. Aging* 9:339–49
161. Roher A, Wolfe D, Palutke M, KuKurga D. 1986. Purification, ultrastructure, and chemical analysis of Alzheimer disease amyloid plaque core protein. *Proc. Natl. Acad. Sci. USA* 83:2662–66
162. Rothwell NJ, Hopkins SJ. 1995. Cytokines and the nervous system. II: Actions and mechanisms of action. *Trends Neurosci.* 18:130–36
163. Roullet P, Lassalle JM. 1995. Radial maze learning using exclusively distant visual cues reveals learners and nonlearners among inbred mouse strains. *Physiol. Behav.* 58:1189–95
164. Routtenberg A. 1997. Measuring memory in a mouse model of Alzheimer's disease. *Science* 277:839–40
165. Saido TC, Iwatsubo T, Mann DMA, Shimada H, Ihara Y, et al. 1995. Dominant and differential deposition of distinct β-amyloid peptide species, $A\beta_{N3(pE)}$, in senile plaques. *Neuron* 14:457–66
166. St George-Hyslop PH. 1998. Genetics of Alzheimer's disease. See Ref. 113a, 5:106–20
167. St George-Hyslop PH, Haines P, Rogaev E, Mortilla M, Vaula G, et al. 1992. Genetic evidence for a novel familial Alzheimer's disease locus on chromosome 14. *Nat. Genet.* 2:330–34
168. St George-Hyslop PH, Tanzi RE, Polinsky RJ, Haines JL, Nee L, et al. 1987. The genetic defect causing familial Alzheimer's disease maps on chromosome 21. *Science* 235:885–90
169. Saunders AM, Strittmatter WJ, Schmechel D, St George-Hyslop PH, Pericak-Vance MA, et al. 1993. Association of apolipoprotein E allele $\varepsilon4$ with late-onset familial and sporadic Alzheimer's disease. *Neurology* 43:1467–72
170. Schellenberg GD. 1995. Progress in Alzheimer's disease genetics. *Curr. Opin. Neurol.* 8:262–67
171. Scheuner D, Eckman C, Jensen M, Song X, Citron M, et al. 1996. Secreted amyloid β-protein similar to that in the senile plaques of Alzheimer's disease is increased *in vivo* by the presenilin 1 and 2 and *APP* mutations linked to familial Alzheimer's disease. *Nat. Med.* 2:864–70
172. Schmechel DE, Saunders AM, Strittmatter WJ, Crain BJ, Hulette CM, et al. 1993. Increased amyloid β-peptide deposition in cerebral cortex as a consequence of apolipoprotein E genotype in late-onset Alzheimer's disease. *Proc. Natl. Acad. Sci. USA* 90:9649–53
173. Schmidt ML, Lee VMY, Forman M, Chiu T-S, Trojanowski JQ. 1997. Monoclonal antibodies to a 100-kd protein reveal abundant $A\beta$-negative plaques throughout gray matter of Alzheimer's disease brains. *Am. J. Pathol.* 151:69–80
174. Schofield P, Mayeux R. 1998. Alzheimer's disease: clinical features, diagnosis and epidemiology. See Ref. 113a, 4:89–105
175. Shen J, Bronson RT, Chen DF, Xia W, Selkoe DJ, et al. 1997. Skeletal and CNS defects in *presenilin-1*-deficient mice. *Cell* 89:629–39
176. Sheng JG, Mrak RE, Griffin WST. 1997. Glial-neuronal interactions in Alzheimer disease: progressive association of IL-$1\alpha^+$ microglia and $S100\beta^+$ astrocytes with neurofibrillary tangle

stages. *J. Neuropathol. Exp. Neurol.* 56: 285–90

177. Sherrington R, Rogaev EI, Liang Y, Rogaeva EA, Levesque G, et al. 1995. Cloning of a gene bearing missense mutations in early-onset familial Alzheimer's disease. *Nature* 375:754–60
178. Sisodia SS. 1992. β-amyloid precursor protein cleavage by a membrane-bound protease. *Proc. Natl. Acad. Sci. USA* 89:6075–79
179. Sisodia SS, Koo EH, Beyreuther K, Unterbeck A, Price DL. 1990. Evidence that β-amyloid protein in Alzheimer's disease is not derived by normal processing. *Science* 248:492–95
180. Sisodia SS, Koo EH, Hoffman PN, Perry G, Price DL. 1993. Identification and transport of full-length amyloid precursor proteins in rat peripheral nervous system. *J. Neurosci.* 13:3136–42
181. Slunt HH, Thinakaran G, von Koch C, Lo ACY, Tanzi RE, et al. 1994. Expression of a ubiquitous, cross-reactive homologue of the mouse β-amyloid precursor protein (APP). *J. Biol. Chem.* 269:2637–44
182. Smith MA, Hirai K, Hsiao K, Pappolla MA, Harris PLR, et al. 1998. Amyloid-β deposition in Alzheimer transgenic mice is associated with oxidative stress. *J. Neurochem.* 70:2212–15
183. Smith MA, Rudnicka-Nawrot M, Richey PL, Praprotnik D, Mulvihill P, et al. 1995. Carbonyl-related posttranslational modification of neurofilament protein in the neurofibrillary pathology of Alzheimer's disease. *J. Neurochem.* 64:2660–66
184. Smith MA, Sayre LM, Monnier VM, Perry G. 1995. Radical AGEing in Alzheimer's disease. *Trends Neurosci.* 18:172–76
185. Snow AD, Mar H, Nochlin D, Kimata K, Kato M, et al. 1988. The presence of heparan sulfate proteoglycans in the neuritic plaques and congophilic angiopathy in Alzheimer's disease. *Am. J. Pathol.* 133:456–63
186. Strittmatter WJ, Saunders AM, Schmechel D, Pericak-Vance M, Enghild J, et al. 1993. Apolipoprotein E: high-avidity binding to β-amyloid and increased frequency of type 4 allele in late-onset familial Alzheimer disease. *Proc. Natl. Acad. Sci. USA* 90:1977–81
187. Sturchler-Pierrat C, Abramowski D, Duke M, Wiederhold K-H, Mistl C, et al. 1997. Two amyloid precursor protein transgenic mouse models with Alzheimer disease-like pathology. *Proc. Natl. Acad. Sci. USA* 94:13287–92
188. Suzuki N, Cheung TT, Cai X-D, Odaka A, Otvos L Jr, et al. 1994. An increased percentage of long amyloid β protein secreted by familial amyloid β protein precursor (βAPP_{717}) mutants. *Science* 264:1336–40
189. Sze C-I, Troncoso JC, Kawas CH, Mouton PR, Price DL, et al. 1997. Loss of the presynaptic vesicle protein synaptophysin in hippocampus correlates with cognitive decline in Alzheimer's disease. *J. Neuropathol. Exp. Neurol.* 56: 933–44
190. Tanzi RE, Gusella JF, Watkins PC, Bruns GAP, St George-Hyslop P, et al. 1987. Amyloid β protein gene: cDNA, mRNA distribution, and genetic linkage near the Alzheimer locus. *Science* 235:880–84
191. Tanzi RE, McClatchey AI, Lampert ED, Villa-Komaroff L, Gusella JF, et al. 1988. Protease inhibitor domain encoded by an amyloid protein precursor mRNA associated with Alzheimer's disease. *Nature* 331:528–30
192. Tanzi RE, St George-Hyslop PH, Haines JL, Polinsky RJ, Nee L, et al. 1987. The genetic defect in familial Alzheimer's disease is not tightly linked to the amyloid β-protein gene. *Nature* 329:156–57
193. Tanzi RE, Vaula G, Romano DM, Mortilla M, Huang TL, et al. 1992. Assessment of amyloid β-protein precursor gene mutations in a large set of familial and sporadic Alzheimer disease cases. *Am. J. Hum. Genet.* 51:273–82

193a. Terry RD, Katzman R, Bick KL, eds. 1994. *Alzheimer Disease*. New York: Raven

194. Thinakaran G, Borchelt DR, Lee MK, Slunt HH, Spitzer L, et al. 1996. Endoproteolysis of presenilin 1 and accumulation of processed derivatives *in vivo*. *Neuron* 17:181–90
195. Thinakaran G, Regard JB, Bouton CML, Harris CL, Price DL, et al. 1998. Stable association of presenilin derivatives and absence of presenilin interactions with APP. *Neurobiol. Dis.* 4:438–53
196. Trojanowski JQ, Growdon JH. 1998. A new consensus report on biomarkers for the early antemortem diagnosis of Alzheimer disease: current status, relevance to drug discovery, and recommendations for future research. *J. Neuropathol. Exp. Neurol.* 57:643–44
197. Troncoso JC, Sukhov RR, Kawas CH, Koliatsos VE. 1996. *In situ* labeling of dying cortical neurons in normal aging and in Alzheimer's disease: corre-

lations with senile plaques and disease progression. *J. Neuropathol. Exp. Neurol.* 55:1134–42

198. Tysoe C, Whittaker J, Xuereb J, Cairns NJ, Cruts M, et al. 1998. A presenilin-1 truncating mutation is present in two cases with autopsy-confirmed early-onset Alzheimer disease. *Am. J. Hum. Genet.* 62:70–76
199. Upchurch M, Wehner JM. 1989. Inheritance of spatial learning ability in inbred mice: a classical genetic analysis. *Behav. Neurosci.* 103:1251–58
200. Van Broeckhoven C, Backhovens H, Cruts M, De Winter G, Bruyland M, et al. 1992. Mapping of a gene predisposing to early-onset Alzheimer's disease to chromosome 14q24.3. *Nat. Genet.* 2:334–39
201. Van Broeckhoven C, Backhovens H, Cruts M, Martin JJ, Crook R, et al. 1994. APOE genotype does not modulate age of onset in families with chromosome 14 encoded Alzheimer's disease. *Neurosci. Lett.* 169:179–80
202. Van Broeckhoven C, Haan J, Bakker E, Hardy JA, Van Hul W, et al. 1990. Amyloid *β* protein precursor gene and hereditary cerebral hemorrhage with amyloidosis (Dutch). *Science* 248:1120–22
203. Vogel G. 1998. Tau protein mutations confirmed as neuron killers. *Science* 280:1524–25
204. von Koch CS, Zheng H, Chen H, Trumbauer M, Thinakaran G, et al. 1997. Generation of APLP2 KO mice and early postnatal lethality in APLP2/APP double KO mice. *Neurobiol. Aging* 18:661–69
205. Wallace DC, Stugard C, Murdock D, Schurr T, Brown MD. 1997. Ancient mtDNA sequences in the human nuclear genome: a potential source of errors in identifying pathogenic mutations. *Proc. Natl. Acad. Sci. USA* 94:14900–5
206. Wasco W, Bupp K, Magendantz M, Gusella JF, Tanzi RE, et al. 1992. Identification of a mouse brain cDNA that encodes a protein related to the Alzheimer disease-associated amyloid-beta-protein precursor. *Proc. Natl. Acad. Sci. USA* 89:10758–62
207. Wasco W, Gurubhagavatula S, Paradis MD, Romano DM, Sisodia SS, et al. 1993. Isolation and characterization of *APLP2* encoding a homologue of the Alzheimer's associated amyloid *β* protein precursor. *Nat. Genet.* 5:95–99
208. Wavrant-DeVrieze F, Perez-Tur J, Lambert JC, Frigard B, Pasquier F, et al. 1997. Association between the low density lipoprotein receptor-related protein (LRP) and Alzheimer's disease. *Neurosci. Lett.* 227:68–70
209. Webster S, Lue L-F, Brachova L, Tenner AJ, McGeer PL, et al. 1997. Molecular and cellular characterization of the membrane attack complex, C5b-9, in Alzheimer's disease. *Neurobiol. Aging* 18:415–21
210. Weidemann A, König G, Bunke D, Fischer P, Salbaum JM, et al. 1989. Identification, biogenesis, and localization of precursors of Alzheimer's disease A4 amyloid protein. *Cell* 57:115–26
211. Weisgraber KH, Pitas RE, Mahley RW. 1994. Lipoproteins, neurobiology, and Alzheimer's disease: structure and function of apolipoprotein E. *Curr. Opin. Struct. Biol.* 4:507–15
212. Weidemann A, Paliga K, Dirrwany U, Czech C, Erin G, et al. 1997. Formation of stable complexes between two Alzheimer's disease gene products: presenilin 2 and *β*-amyloid precursor protein. *Nat. Med.* 3:328–32
213. Whitehouse PJ, Price DL, Struble RG, Clark AW, Coyle JT, et al. 1982. Alzheimer's disease and senile dementia: loss of neurons in the basal forebrain. *Science* 215:1237–39
214. Wilhelmsen KC, Clark LN. 1998. Chromosome 17-linked dementias. See Ref. 113a, 9:170–80
215. Wisniewski T, Frangione B. 1992. Apolipoprotein E: a pathological chaperone protein in patients with cerebral and systemic amyloid. *Neurosci. Lett.* 135:235–38
216. Wong PC, Zheng H, Chen H, Becher MW, Sirinathsinghji DJS, et al. 1997. Presenilin 1 is required for *Notch1* and *Dll1* expression in the paraxial mesoderm. *Nature* 387:288–92
217. Wyss-Coray T, Masliah E, Mallory M, McConlogue L, Johnson-Wood K, et al. 1997. Amyloidogenic role of cytokine TGF-β1 in transgenic mice and in Alzheimer's disease. *Nature* 389:603–6
218. Xia M, Qin S, McNamara M, Mackay C, Hyman BT. 1997. Interleukin-8 receptor B immunoreactivity in brain and neuritic plaques of Alzheimer's disease. *Am. J. Pathol.* 150:1267–74
219. Xia W, Zhang J, Perez R, Koo EH, Selkoe DJ. 1997. Interaction between amyloid precursor protein and presenilins in mammalian cells: implications for the pathogenesis of Alzheimer disease. *Proc. Natl. Acad. Sci. USA* 94:8208–13
220. Yankner BA. 1996. Mechanisms of

neuronal degeneration in Alzheimer's disease. *Neuron* 16:921–32

221. Young AB, Penney JB Jr. 1994. Neurotransmitter receptors in Alzheimer disease. See Ref. 193a, pp. 293–303
222. Zheng H, Jiang M-H, Trumbauer ME, Sirinathsinghji DJS, Hopkins R, et al. 1995. β-Amyloid precursor protein-deficient mice show reactive gliosis and decreased locomotor activity. *Cell* 81:525–31
223. Zhou J, Liyanage U, Medina M, Ho C, Simmons AD, et al. 1997. Presenilin 1 interaction in the brain with a novel member of the armadillo family. *Neuroreport* 8:2085–90

1972, 507; *Bull. Chem. Soc. Japan*, **46**, 2105 (1973).

2) S. Naga, Y. Kidani, H. Koike : *Bull. Chem. Soc. Japan*, 投稿中.

3) Y. Kidani, S. Naga, H. Koike : *Chem. Pharm. Bull.* (Tokyo), 投稿中.

4) 吉岡正則, 田村善蔵 : 医学のあゆみ, **74**, 320 (1970).

5) 河合 忠, 河野均也, 加庭信二, 片岡喜久男, 国分豊明, 天野正道, 蓬原三郎 : 同上, **77**, 729 (1971).

6) J. Charalambous, M. J. Frazer, R. K. Lee, A. H. Qureshi, F. B. Taylor : *Org. Mass Spectrom.*, **5**, 1169 (1971).

☆

Mass spectrometry of 5-chloro-7-iodo-8-quinolinol metal chelates. Yoshinori KIDANI, Shinobu NAGA* and Hisashi KOIKE** (*Faculty of Pharmaceutical Sciences, Nagoya City University, 3-1, Tanabe-dori, Mizuho-ku, Nagoya-shi, Aichi; **School of Medical Technology and Nursing, Fujita Gakuen University, Kutsukake-cho, Toyoake-shi, Aichi)

As a part of mass spectrometric study of metal chelates, the authors attempted to apply mass spectrometry to the qualitative analysis of 5-chloro-7-iodo-8-quinolinol (chinoform) metal chelates (Fe, Co, Ni, Cu, Zn).

Mass spectra were measured with a Hitachi RMU-7 mass spectrometer according to the direct inlet system under the following conditions: ionizing voltage 70 eV, ion accelerating voltage 1800 V, total emission current 80 μA, ion source temperature 250°C, and sample evaporating temperature 180～250°C.

In the case of Fe(III) chelate, the peak being attributable to the molecular ion was observed, and the mass units corresponded to a 3 : 1 molar ratio chelate. The loss of 304 mass units from the molecular ion was observed and it indicated a cleavage of one molecule of the coordinated chinoform from the molecular ion to afford the fragment ion of a 2 : 1 ratio chelate. The loss of 304 mass units from the 2 : 1 chelate occurred successively to afford the fragment ion of a 1 : 1 ratio chelate. Simultaneously another fragmentation of the subsequent loss of the iodine atom from the 2 : 1 chelate was observed.

In the case of Co(II), Ni(II), Cu(II), and Zn(II) chelates, the molecular ion peaks corresponding to metal chelates of a 2 : 1 ratio, were observed in every spectrum. The loss of 304 mass units, corresponding to one molecule of coordinated chinoform from the molecular ion occurred to afford the fragment ion of a 1 : 1 ratio metal chelates. On the other hand, another fragmentation of the loss of the iodine atoms from the molecular ion was observed, simultaneously.

It has been disclosed qualitatively that mass spectrometry will be one of the useful and effective methods to know, 1) whether chinoform forms metal chelate or not, 2) what kind of metals are participating in the chelate formation, and 3) what is the binding ratio of the chinoform metal chelates in the living body.

In conclusion, the mass spectrometric method gives a useful information about the fate of chinoform in the living body of the SMON patients by detecting metal linkages directly in the biological specimens, such as feces, urine, body fluid, blood, and tongue fur.

(Received May 20, 1974)

アルシン-原子吸光法による鉄鋼中の微量ヒ素の迅速分析

辻野隆三, 山本秀彦, 上田貞夫, 須藤 徹, 沢崎陽次*

(1974 年 5 月 20 日受理)

鉄鋼中の微量ヒ素の迅速分析法について検討した．試料 1 g をはかりとり，王水で溶解したのち，1～2 *ml* になるまで加熱し，冷却後，検液中のヒ素の濃度が 0.02～0.06 μg/*ml* になるよう 1.2*N* 塩酸で希釈し，その 25 *ml* を耐圧反応そうに採取した．この試料溶液に 20% 塩化スズ(II) 溶液 0.5 *ml* および 20% ヨウ化カリウム溶液 1 *ml* を加えて振り混ぜ，10 分間放置後，反応そうをアルシン発生装置にセットし，バインダー配合亜鉛末で作った錠剤を 1 個加え，アルシンを発生させ，水素とアルシンとを混合したガスのゲージ圧が 0.5 kg になったとき，コックを切り替えてたまったガスをアルゴン-水素フレームに導入して原子吸光分光分析法でヒ素の測定を行なった．前処理をしたのちのヒ素の測定時間は 1 分以内で，鉄鋼の標準試料について，標準値の 90～100% の範囲で測定できた．

---

* 日本ジャーレル・アッシュ株式会社：京都府京都市伏見区下鳥羽浄春ケ前町 28

The material on this page was copied from the collection of the National Library of Medicine by a third party and may be protected by U.S. Copyright law.

NCBI PubMed National Library of Medicine NLM

Entrez PubMed Nucleotide Protein Genome Structure OMIM PMC Journals E

Search PubMed for Go Clear

Limits Preview/Index History Clipboard Details

Display Abstract Show: 20 Sort Send to Text

About Entrez

Text Version

Entrez PubMed
- Overview
- Help | FAQ
- Tutorial
- New/Noteworthy
- E-Utilities

PubMed Services
- Journals Database
- MeSH Database
- Single Citation Matcher
- Batch Citation Matcher
- Clinical Queries
- LinkOut
- Cubby

Related Resources
- Order Documents
- NLM Catalog
- NLM Gateway
- TOXNET
- Consumer Health
- Clinical Alerts
- ClinicalTrials.gov
- PubMed Central

☐ 1: Lab Invest. 1993 Jul;69(1):101-10.

Related Articles,

Chelation of intracellular zinc triggers apoptosis in mature thymocytes.

McCabe MJ Jr, Jiang SA, Orrenius S.

Department of Toxicology, Karolinska Institute, Stockholm, Sweden.

BACKGROUND: Thymocyte apoptosis has been shown to be regulated by intracellular levels of cations. Elevation of [Ca2+]i can induce cell death by apoptosis, whereas, Zn2+ prevents it. EXPERIMENTAL DESIGN: A membrane permeable metal ion chelator, N,N,N'N',-tetrakis (2-pyridylmeth ethylenediamine (TPEN), was used to examine the role of intracellular zinc thymocyte (rat and human) apoptosis. Characteristics of apoptosis that were assessed included: chromatin degradation into oligosomal-sized fragments nuclear condensation. The necessity for protein synthesis in TPEN-induced apoptosis was ruled out using the inhibitors, cycloheximide and emetine. M ion specificity for TPEN was established by competition with exogenous cations. FACS analysis was employed to determine the phenotype of the TPEN-sensitive thymocyte populations. RESULTS: TPEN induced DNA fragmentation within 4 hours of exposure before the onset of cell death (6 hours). Addition of equimolar exogenous Zn2+ or Cu2+, but not Mn2+ or Fe2+, at the initiation of culture prevented TPEN-induced apoptosis. A membrane impermeable chelator, diethylenetriaminepentaacetic acid, did n induce thymocyte apoptosis indicating that chelation of intracellular Zn2+ required to trigger DNA fragmentation. The identity of the critical intracell Zn(2+)-binding site(s) is currently unknown, but it appears that increased thymocyte [Ca2+]i may displace Zn2+ from these intracellular sites. TPEN treatment resulted in the depletion of thymocytes having a mature phenotyp with respect to CD3, CD4, and CD8. Moreover, lymph node cells were mo sensitive to TPEN than thymocytes. CONCLUSIONS: These experiments show that Zn2+ chelation has disparate effects on immature and mature T c and suggest that zinc availability controls the cell death or selection pathwa during thymopoiesis.

PMID: 8331893 [PubMed - indexed for MEDLINE]

NCBI PubMed National Library of Medicine NLM

Entrez PubMed Nucleotide Protein Genome Structure OMIM PMC Journals E

Search PubMed for Go Clear

Limits Preview/Index History Clipboard Details

Display Abstract Show: 20 Sort Send to Text

About Entrez

Text Version

Entrez PubMed
Overview
Help | FAQ
Tutorial
New/Noteworthy
E-Utilities

PubMed Services
Journals Database
MeSH Database
Single Citation Matcher
Batch Citation Matcher
Clinical Queries
LinkOut
Cubby

Related Resources
Order Documents
NLM Catalog
NLM Gateway
TOXNET
Consumer Health
Clinical Alerts
ClinicalTrials.gov
PubMed Central

☐ 1: Biochem J. 1993 Dec 1;296 (Pt 2):403-8. Related Articles,

Correlation of apoptosis with change in intracellular labile Zn(using zinquin [(2-methyl-8-p-toluenesulphonamido-6-quinolyloxy)acetic acid], a new specific fluorescent probe for Z (II).

Zalewski PD, Forbes IJ, Betts WH.

Department of Medicine, University of Adelaide, Australia.

Zinquin [(2-methyl-8-p-toluenesulphonamido-6-quinolyloxy)-acetic acid], membrane-permeant fluorophore specific for Zn(II), was used with spectrofluorimetry and video image analysis to reveal and quantify labile intracellular Zn. Zinquin labelled human chronic-lymphocytic-leukaemia lymphocytes, rat splenocytes and thymocytes with a weak diffuse fluoresce that was quenched when intracellular Zn was chelated with NNN'N'-tetraki pyridylmethyl)ethylenediamine (TPEN) and was greatly intensified by pretreatment of cells with the Zn ionophore pyrithione and exogenous Zn. There was substantial heterogeneity of labile Zn among ionophore-treated cells, and fluorescence was largely extranuclear. The average contents of la Zn in human leukaemic lymphocytes, rat splenocytes and rat thymocytes w approx. 20, 31 and 14 pmol/10(6) cells respectively. Morphological change and internucleosomal DNA fragmentation indicated substantial apoptosis i these cells when the level of intracellular labile Zn was decreased by treatm with TPEN. Conversely, increasing labile Zn by pretreatment with Zn plus pyrithione suppressed both spontaneous DNA fragmentation and that induc by the potent apoptosis-induced agents colchicine and dexamethasone. The results suggest that prevention of apoptosis is a function of labile Zn, and t reduction below a threshold concentration in this Zn pool induces apoptosis

PMID: 8257431 [PubMed - indexed for MEDLINE]

Display Abstract Show: 20 Sort Send to Text

Table II. Spiro[tetralin-1,3′-pyrrol. e] Derivatives 2a–n

compd	formula[a]	yield,[b] %	mp, °C	writhing test, mg/kg po	hot-plate test: ED_{50}, mg/kg po[g]
2a	$C_{13}H_{18}NCl$[c]	79	164–176	30, ++++	13.3 (10.5–15.7)
2b	$C_{14}H_{20}NCl$[c]	81	202–210	30, ++++	12.1 (8.4–14.3)
2c	$C_{17}H_{21}NO_5$[d]	85	182–189	30, ++	48.6 (30.3–57.6)
2d	$C_{18}H_{23}NO_5$[d]	92	132–136	100, +++	ND[f]
2e	$C_{14}H_{20}NOCl$[c]	90	174–192	100, +	ND[f]
2f	$C_{18}H_{23}NO_5$[d]	92	147–151	100, ++	ND[f]
2g	$C_{14}H_{20}NOCl$[c]	78	162–169	100, +	ND[f]
2h	$C_{18}H_{23}NO_5$[d]	85	129–135	30, ++	>50
2i	$C_{13}H_{18}NOBr$[e]	60	230–232	30, ++	>50
2j	$C_{14}H_{20}NOBr$[e]	88	255–259	100, +	ND[f]
2k	$C_{13}H_{18}NOBr$[e]	39	195–203	100, ++	ND[f]
2l	$C_{14}H_{20}NOBr$[e]	50	218–230	30, ++	>50
2m	$C_{13}H_{18}NOBr$[e]	67	258–261	100, ++	ND[f]
2n	$C_{14}H_{20}NOBr$[e]	52	182–193	30, ++	42.8 (35.6–49.4)
morphine hydrochloride				10, ++++	1.2 (0.9–1.5)
profadol				10, ++++	3.9 (2.5–5.9)

[a,b] See corresponding footnotes in Table I. [c] Isolated as the hydrochloride salt and recrystallized from ethanol–ether. [d] Isolated as the fumarate salt and recrystallized from ethanol. [e] Isolated as the hydrobromide salt and recrystallized from ethanol. [f] Not determined. [g] Confidence limits in parentheses.

Evaporation of the solvent afforded a yellow oil, which was distilled in vacuo to afford the appropriate spiro[tetralin-1,3′-pyrrolidine] as a colorless oil. Bases were converted immediately to their hydrochloride or fumarate salts.

Synthesis of *N*-Methylspiro[tetralin-1,3′-pyrrolidines]. The appropriate spiro[tetralin-1,3′-pyrrolidine] (1.1 g, 0.005 mol), HCO_2H (2.5 mL), and HCHO (37%, 1.0 mL) were heated together on a water bath for 7 h. After evaporation of the solution to dryness, the residual oil was dissolved in 5% HCl, washed with ether, basified with 10% NaOH, extracted with ether, and dried ($MgSO_4$). After evaporation of the solvent, the residual oil was distilled in vacuo to give the corresponding *N*-methyl derivative as a clear, colorless oil. The free base was converted to either the hydrochloride or fumarate salt (see Table II).

O-Demethylation of Compounds 2c–h. As a general procedure, the appropriate spiro[methoxytetralin-1,3′-pyrrolidine] (0.01 mol) was refluxed under nitrogen for 2 h at 125 °C in 48% aqueous hydrobromic acid (25 mL). The resulting yellow-brown solution was evaporated to dryness under nitrogen, and the residue was taken up in absolute ethanol. On addition of ether and refrigeration, buff crystals of the crude O-demethylated product were obtained. Recrystallization from ethanol–ether afforded a purer product (see Table II).

Pharmacology. Analgesia was determined by the acetic acid writhing test[15] in groups of six mice. Each group was dosed orally with either vehicle ("Dispersol") or compound under test and injected intraperitoneally 30 min later with dilute acetic acid (0.4 mL, 0.25%). The total number of writhes was recorded, and the protection afforded was expressed as a percentage of control values according to the following scale: ++++, 100% inhibition; +++, 75–99% inhibition; ++, 50–74% inhibition; +, 25–49% inhibition. Compounds showing 50% or more inhibition at 30 mg/kg in the above test were also tested for analgesia in mice by the hot-plate[16] method (see Table II).

Acknowledgment. We gratefully acknowledge the support of Imperial Chemical Industries in carrying out and releasing results of the biological testing and the Pharmaceutical Society of Great Britain for providing a research grant for one of us (R.S.).

Relationship of Octanol/Water Partition Coefficient and Molecular Weight to Rat Brain Capillary Permeability

Victor A. Levin*

Brain Tumor Research Center, Department of Neurological Surgery, School of Medicine, University of California, San Francisco, California 94143. *Received September 27, 1979*

The rat brain capillary permeability coefficient was determined for 27 compounds. The relationship of permeability to octanol/water partition coefficient and molecular weight was found to be predictable for drugs with molecular weights less than 400.

It is generally believed that the blood–brain barrier (BBB) is restrictive for small molecules at capillary endothelial cells and for large molecules at the interendothelial tight junctions. Although a great deal has been learned about the effects of BBB physiology on the passage of electrolytes and hydrophobic nonelectrolytes, a limited amount of information that correlates lipophilicity, molecular size, and the ability to cross the BBB has been published.[1-3]

We report the brain capillary permeability coefficient (P_c) determined in ether-anesthetized rats for 27 compounds for which the octanol/water partition coefficients are known.

Experimental Section

Isotopes. ^{14}C-labeled urea, creatinine, 5-fluorouracil, sodium ascorbate, and sucrose, ^{3}H-labeled water, glycerol, and galactitol, and ^{24}NaCl were purchased from New England Nuclear Corp. and/or Amersham-Searle, Inc. Radiopurity was satisfactory by manufacturer's specifications. ^{14}C-Labeled dianhydrogalactitol, dibromodulcitol, 1,3-bis(2-chloroethyl)-1-nitrosourea (BCNU), 1-(2-chloroethyl)-3-cyclohexyl-1-nitrosourea (CCNU), 1-(2-chloroethyl)-3-(2,6-dioxo-3-piperidyl)-1-nitrosourea (PCNU), *N*-(1-methylethyl)-4-[(2-methylhydrazino)methyl]benzamide monohydrochloride (procarbazine), Baker's antifol, adriamycin,

---

(1) W. H. Oldendorf, *Proc. Soc. Exp. Biol. Med.*, 147, 813 (1974).

(2) V. A. Levin, H. Landahl, and M. A. Freeman-Dove, *J. Pharmacokinet. Biopharm.*, 4, 499 (1976).

(3) S. I. Rapoport, K. Ohno, and K. D. Pettigrew, *Brain Res.*, in press.

0022-2623/80/1823-0682$01.00/0 © 1980 American Chemical Society

Table I. Rat Brain Capillary Permeability Coefficients (P_c)

compd no.	compd	N	M_r	log P	$P_c \times 10^{-6}$ cm/s
1	^3H_2O	13	18	−1.15	200
2	^{24}Na	9	58	−2.95	0.4
3	$[^{14}C]$urea	28	60	−2.80	0.82
4	$[^3H]$glycerol	10	92	−1.75	12
5	$[^{14}C]$creatinine	4	113	−1.77	0.28
6	5-fluoro$[^{14}C]$uracil	4	130	−0.95	1.7
7	$[^{14}C]$dianhydrogalactitol	6	150	−1.29	2.5
8	$[^{14}C]$metronidazole	11	171	−0.16	14
9	$[^{14}C]$ascorbate	5	176	−4.04	1.3
10	$[^3H]$galactitol	9	182	−3.10	0.39
11	$[^{14}C]$misonidazole	5	185	−0.37	10
12	$[^{14}C]$ftorafur	7	200	−0.48	6.4
13	$[^{14}C]$BCNU	2	214	1.54	154
14	$[^{14}C]$procarbazine	4	221	0.06	19
15	$[^{14}C]$CCNU	3	234	2.83	100
16	$[^{14}C]$pyrimethamine	4	249	2.69	120
17	$[^{14}C]$PCNU	5	263	0.37	11
18	DDMP	6	269	2.82	150
19	$[^{14}C]$DDEP	2	284	3.19	110
20	$[^{14}C]$dibromodulcitol	7	308	−0.29	1.9
21	$[^{14}C]$spirohydantoin mustard	7	315	2.47	29
22	$[^{14}C]$sucrose	3	342	−3.67	0.12
23	Baker's $[^{14}C]$antifol	2	398	−2.46	0.18
24	$[^{14}C]$adriamycin	4	543	−0.10	<0.014
25	$[^3H]$epipodophylotoxin	14	657	2.80	0.20
26	$[^3H]$vincristine	12	825	2.80	0.64
27	bleomycin	4	1400	−3.3	<0.014

misonidazole, ftorafur, and spirohydantoin mustard, and $[^3H]$-vincristine were supplied by Dr. Robert Engle (Chemical Resources Section, National Cancer Institute). Radiopurity and chemical purity were determined before use by thin-layer chromatography (TLC). Adriamycin and vincristine were repurified by TLC immediately before use (98% radiopurity). $[^{14}C]$Metronidazole was generously supplied by Dr. Rothwell Polk (Searle Laboratories). Radiopurity exceeded 98% by TLC. $[^3H]$Epipodophylotoxin (VM-26) was generously supplied by Dr. R. Dorrien Ven (Sandoz, Inc.). A radiopurity of 98% was confirmed by TLC. $[^{14}C]$Pyrimethamine and 2,4-diamino-5-(3′,4′-dichlorophenyl)-6-$[^{14}C]$methylpyrimidine ($[^{14}C]$DDMP) were generously supplied by Dr. Charles Nichol (Wellcome Research Laboratories).

Nonradioactive Compounds. Bleomycin was a gift of Dr. Stanley Crooke (Bristol Laboratories). Chemical quantification of bleomycin from plasma and tissue samples was performed by Dr. James Strong (Baylor College of Medicine, Houston).[4]

DDEP [2,4-diamino-5-(3′,4′-dichlorophenyl)-6-ethylpyrimidine] was supplied by Dr. Charles Nichol (Wellcome Research Laboratories). Chemical quantification of plasma and tissue levels of DDEP were performed by Ellen Levin.[5]

Octanol/Water Partition Coefficients. The value of spirohydantoin mustard was calculated using π constants.[6] Partition coefficients for $[^3H]$glycerol, $[^{14}C]$creatinine, and ^{57}Co-bleomycin were determined in our laboratories using the techniques of Hansch.[7] Other values have been published.[8]

Brain Capillary Permeability Measurements.[2,9] For capillary permeability measurements, male Fisher 344 rats weighing 160 to 220 g were anesthetized with ether; isotopes were injected intravenously and blood samples were taken from the femoral artery at different times up to 6 min (to calculate the plasma drug or tracer integral). Rats were sacrificed by decapitation, and the heads were immersed in liquid nitrogen for 45 s. The brain was removed and both cortical and subcortical tissue sections were taken; care was exercised not to include large cerebral vasculature. For radioactivity measurements, tissue and plasma samples were placed in tared scintillation vials, reweighed, and digested with a tissue solubilizer, after which a toluene base fluor was added. For chemical analysis, tissue was placed into tared vials, reweighed, and frozen at −60 °C until analyzed.

The formula used to compute the capillary permeability coefficient, P_c, is shown in eq 1,[2,9] where the tracer distribution,

$$P_c = (DS/t)0.28(ICD)(BV)^{-1/2} \tag{1}$$

DS, over time in seconds is as shown in eq 2. In eq 2, C = cpm/g

$$DS/t = 0.93[C - (C)(PW)](AUC)^{-1/2} \tag{2}$$

of tissue, AUC (the area under the plasma curve during the experimental period) = cpm·min/g of plasma, PW = fractional tissue plasma water volume (mL/g), ICD = the intercapillary distance (cm), and BV = the fractional brain blood volume (mL/g). Values for PW, ICD, and BV for rat brain were determined previously.[2]

Results and Discussion

If the mechanism of nonelectrolyte permeation through capillary endothelial cells is similar to permeation into bulk lipid phases,

$$P_c \propto KD \tag{3}$$

where K is the membrane/water or lipid/water partition coefficient and D is the diffusion coefficient.[10] Because the relationship of the diffusion coefficient to molecular weight, M_r, in bulk solvents for small molecules (M_r < 1000) is[11,12]

$$D(M_r)^{-1/2} \approx \text{constant} \tag{4}$$

it follows that

$$P_c \propto K(M_r)^{-1/2} \tag{5}$$

---

(4) A. Broughton and J. E. Strong, *Cancer Res.*, 35, 1418 (1976).

(5) E. M. Levin, R. B. Meyer, Jr., and V. A. Levin, *J. Chromatogr.*, 156, 181 (1978).

(6) G. W. Peng, V. E. Marquez, and J. S. Driscoll. *J. Med. Chem.*, 18, 846 (1975).

(7) A. Leo, C. Hansch, and D. Elkins, *Chem. Rev.*, 71, 525 (1971).

(8) C. Hansch and A. Leo, "Substituent Constants for Correlation Analysis in Chemistry and Biology", Wiley Interscience, New York, 1979.

(9) V. A. Levin, M. S. Edwards, and A. Byrd, *Int. J. Radiat. Oncol. Biol. Phys.*, 5, 1627 (1979).

(10) J. M. Diamond and E. M. Wright, *Annu. Rev. Physiol.*, 31, 581 (1969).

(11) W. D. Stein, "The Movement of Molecules Across Cell Membranes", Academic Press, New York, 1967.

(12) W. R. Lieb and W. D. Stein, *Curr. Top. Membr. Transp.*, 2, 1 (1971).

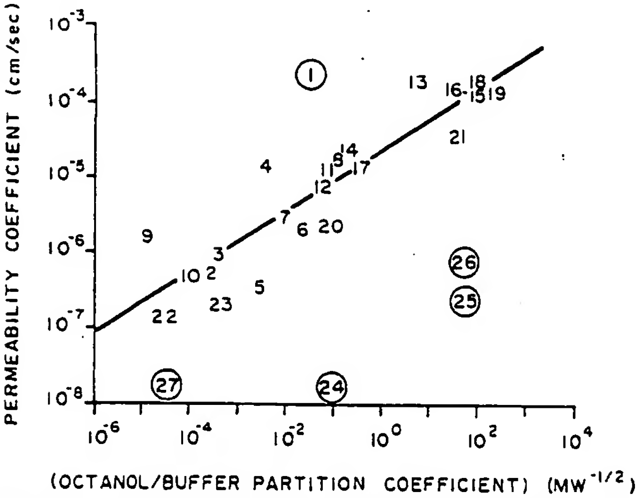

Figure 1. A plot of $P(M_r)^{-1/2}$ vs. P_c for the 27 compounds studied, fit by the method of least squares. The data are plotted as numbers that correspond to the list in Table I. Circled values were not used to compute the best fit line.

This conclusion has been reached by others,[10,11,12] although Collander concluded that eq 6 was a better fit for compounds with molecular weights between 70 and 480.[13]

$$P_c \propto (K_{\text{oil}})^{1.32}(M_r)^{-1.5} \qquad (6)$$

As a reasonable and first approximation, we evaluated the relationship of P_c to $P(M_r)^{-1/2}$, where P is the octanol/water partition coefficient. Table I lists the molecular weight, log P, and P_c used in this analysis. Figure 1 is a plot of P_c vs. $P(M_r)^{-1/2}$. The line was fit by the method of least squares to 22 of 27 data points. For molecular weights below 400, the line in Figure 1 was fit to eq 7 with

$$\log P_c = -4.605 + 0.4115 \log[P(M_r)^{-1/2}] \qquad (7)$$

an SE of estimate = 0.0431, SD of slope = 0.0423, $r = 0.91$, and $n = 22$. Of the five molecules not included, four (bleomycin, adriamycin, vincristine, and epipodophylotoxin) have molecular weights greater than 400, are extremely restricted in their ability to cross the BBB, and are considered to be excluded molecules.[2,9,14] Tritiated water was not included because other factors influence its membrane permeation.

The fact that epipodophyllotoxin and vincristine have permeability coefficients of 2.0×10^{-7} and 6.4×10^{-7} cm/s, respectively, yet are among drugs that do not cross the BBB[9,15] can be rationalized in two ways. First, the radioimpurities associated with these drugs may be smaller, and the more polar impurities may cross brain capillaries to a greater extent than the parent compounds. Second, because of high log P values (2.8), these drugs may penetrate and distribute into but not through brain capillary endothelia. In both cases, this would amount to a small net flux sufficient to produce the observed permeability. We support the second hypothesis because uptake of these labeled compounds over several hours did not indicate significant levels in rat brain.[14,15]

While it would be useful to compare a homologous series of compounds with different log P and molecular weights, it was not possible to do so. Only commercial radiolabeled molecules and labeled anticancer drugs supplied by the Chemical Resources Section, Division of Cancer Treatment, National Cancer Institute, were available to us. Nevertheless, the data are sufficient to derive useful insight into the physical criteria for passive BBB transport.

We draw two conclusions from this study. First, below a molecular weight of 400, increasing lipophilicity will improve P_c. For example, a molecule with $M_r = 400$ and $P = 1$ has a calculated P_c of 7.2×10^{-6} cm/s; for the same molecular weight and $P = 100$, however, P_c increases by nearly sevenfold to 4.8×10^{-5} cm/s. Second, although the absolute cutoff for "significant" BBB passage—regardless of lipophilicity—cannot be stated with certainty from the current study, it is clearly above 400 and below 657 daltons.

These studies have important implications for the design of psychotropic drugs, anticonvulsants, and brain tumor chemotherapeutic agents. The ability of an anticancer drug to cross the BBB is empirically associated with increased activity against CNS tumors when compared with like compounds that do not have this ability. BBB passage alone, however, is an insufficient criterion for antitumor activity. Plasma pharmacokinetics, rate and site of drug biotransformation, tumor capillary to cell transport and blood flow, and the mode of action of a drug are some of the factors that will modulate CNS antitumor activity.[16] Clearly, a logical step to developing better therapy and new therapeutic agents will be an understanding of physical transport factors, such as molecular size and lipophilicity, that influence brain capillary permeability.

Acknowledgment. Supported in part by American Cancer Society Grant CH-75 and Faculty Research Award FRA-155 (V.A.L.) and National Institutes of Health Center Grant CA-13525. We thank Anne Haley for technical assistance, Neil Buckley for editorial assistance, and Professor Herbert Landahl for many helpful discussions.

---

(13) R. Collander, *Physiol. Plant.*, 7, 420 (1954).

(14) S. M. El Dareer, V. M. White, F. P. Chan, L. B. Mellet, and D. L. Hill, *Cancer Treat. Rep.*, 61, 1269 (1977).

(15) Sandoz Pharmaceuticals. VM-26, Preclinical Brochure, 1967. Also cited in M. A. Goldsmith, "VM-26 (NSC-122819) Clinical Brochure", National Cancer Institute, National Institutes of Health, Bethedsa, Md., 1973.

(16) V. A. Levin, C. S. Patlak, and H. D. Landahl, *J. Pharmacokinet. Biopharm.*, in press (1980).

Synthesis, Physicochemical Properties, and Biological Evaluation of N-Substituted 2-Alkyl-3-hydroxy-4(1*H*)-pyridinones: Orally Active Iron Chelators with Clinical Potential

Paul S. Dobbin,[†] Robert C. Hider,[*,†] Adrian D. Hall,[‡] Paul D. Taylor,[§] Patience Sarpong,[†] John B. Porter,[⊥] Gaoyi Xiao,[∥] and Dick van der Helm[∥]

Department of Pharmacy, King's College London, Manresa Road, London, SW3 6LX, U.K., Department of Physics, The Royal Marsden Hospital, Downs Road, Sutton, Surrey, SM2 5PT, U.K., Department of Chemistry, University College London, Gower Street, London, WC1E 6BT, U.K., Department of Haematology, University College Hospital, London, WC1E 6HX, U.K., and Department of Chemistry, Oklahoma University, 620 Parrington Oval, Norman, Oklahoma 73019-0370

Received February 1, 1993

The synthesis of a range of novel bidentate ligands containing the chelating moiety 3-hydroxy-4(1*H*)-pyridinone is described. The pK_a values of the ligands and the stability constants of their iron(III) complexes have been determined. The crystal structures of one of the ligands and one of the iron(III) complexes are presented. The distribution coefficients of the ligands are reported and are related to the ability of the ligands to remove iron from hepatocytes. The influence of 3-hydroxy-4(1*H*)-pyridinones on oxidative damage to cells is described. In contrast to the iron chelator in current therapeutic use, desferrioxamine-B, many of the bidentate ligands described in this study are orally active in iron-overloaded mice.

There are a number of inherited disease states which are associated with the gradual accumulation of iron, β-thalassaemia major and thalassaemia intermedia being particularly well characterised.[1] Iron, due to its facile redox chemistry, is toxic when present in excess[2] and must be removed by chelation therapy. The naturally occurring siderophore desferrioxamine B was first demonstrated to increase excretion of iron in 1962,[3] and subsequent widespread use has demonstrated a definite prolonging of life in multiply transfused patients.[4] However, because the drug is inactive by mouth and has to be presented either subcutaneously or intravenously, compliance can be poor.[5]

During the worldwide search for an orally active specific iron chelator to replace desferrioxamine B, much effort has been channelled into the synthesis of catechol,[6] hydroxamate,[7] and carboxylate ligands.[8] This is a logical approach since the majority of natural siderophores (high affinity, low molecular weight, iron(III) multidentate ligands) are formed from one or more of these moieties.[9] Each of these chemical functions, however, has disadvantages when being considered for clinical use:[5] catechols are rapidly oxidized in the intestine, are generally poorly absorbed, and form charged iron(III) complexes;[10] hydroxamates are in principle susceptible to enzyme-catalyzed cleavage, and many possess poor oral bioavailability;[11] amino carboxylates are not sufficiently specific for iron(III)[5] and for oral presentation are best presented as ester pro-drugs.[12]

In view of these limitations, it was decided to investigate ligands, which although related in structure to both catechol and hydroxamate, might lack their relative instability under biological conditions. In particular, the ligands should be stable at strongly acid pH values and resistant to autoxidation and enzyme-catalyzed cleavage. The hydroxypyridinones 1–3 and the hydroxypyranones 4 (Figure 1) were considered as potential iron(III)-selective ligands, and preliminary investigation demonstrated their ability to chelate iron,[13] a finding confirmed by Scarrow *et al.*[14] The 3-hydroxy-4(1*H*)-pyridinones 1 and 3-hydroxy-2(1*H*)-pyridinones 2 have both been demonstrated to remove iron from iron-overloaded animals.[15,16] The 3-hydroxy-4(1*H*)-pyridinones 1 were found to be more effective than the other three molecular classes (2–4), and this is almost certainly directly related to their higher affinity for iron(III).[10,17]

In this paper we report the progress in the development of N-substituted 2-alkyl-3-hydroxy-4(1*H*)-pyridinones as orally active selective iron(III) chelators for clinical use. After description of synthetic pathways, we outline the investigation of physical and biochemical characteristics together with *in vitro* and *in vivo* iron removal studies. In conclusion, we compare the properties of an optimum hydroxypyridinone with those of desferrioxamine B.

Chemistry

All of the 1-substituted 2-alkyl-3-hydroxy-4(1*H*)-pyridinones in this study were synthesized utilizing the methodology of Harris and co-workers[18] (Scheme I). The commercially available 3-hydroxy-4(4*H*)-pyranones maltol and ethyl maltol[19] were benzylated in 90% aqueous methanol to give 5 and 6, respectively. Reaction of these adducts with primary amines was invariably performed by reflux in 50% aqueous ethanol with a catalytic amount of sodium hydroxide present. Where possible the benzylated pyridinones were isolated in a crystalline form as either the free base or the hydrochloride salt. Removal of the protecting benzyl group was achieved by catalytic hydrogenolysis to yield the bidentate chelators which were all isolated as the hydrochloride salts. The amide analogues 37 to 44 were obtained *via* reaction of the succinimidyl activated ester 18 with a variety of primary and secondary amines (Scheme II).

Determination of Solution Properties

3-Hydroxy-4(1*H*)-pyridinones 1 possess two pK_a values as indicated in Scheme III. These bidentate ligands also

---

[†] King's College London.
[‡] The Royal Marsden Hospital.
[§] University College London.
[⊥] University College Hospital.
[∥] Oklahoma University.

0022-2623/93/1836-2448$04.00/0 © 1993 American Chemical Society

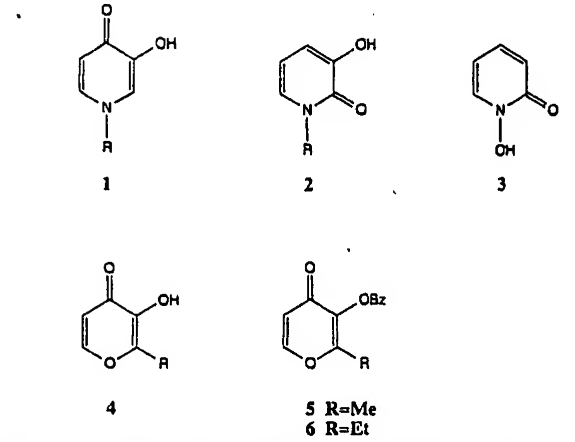

Figure 1. Structures of bidentate iron(III) ligands.

Scheme I

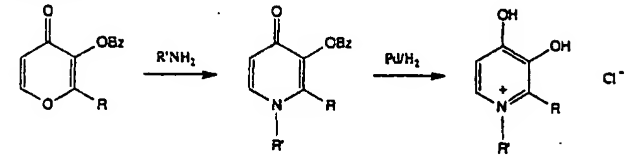

Scheme II

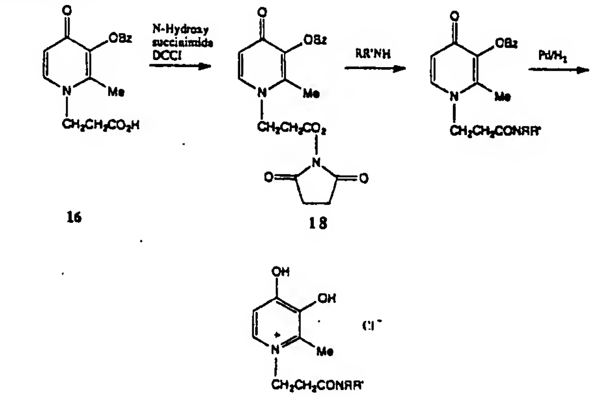

Scheme III

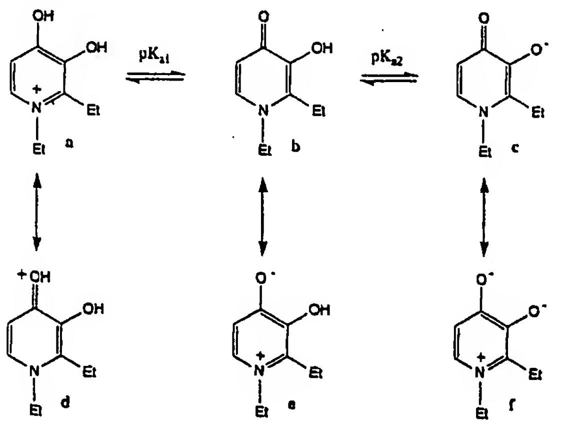

form a number of complexes with iron(III) so that aqueous solutions equilibrate to give mixtures in which the speciation depends on the metal ion, ligand, and hydrogen ion concentrations. A simple model of this system is shown in eq 1. This model has previously been shown to apply to 3-hydroxy-4(1*H*)-pyridinones.[17] Both the pK_a values and stability constants were obtained by global optimizations of parameters corresponding to titrations at several different ligand and iron(III) concentrations. The experimental conditions ensured that the most associated species predominated.

$$
\begin{aligned}
&Fe^{3+} + L^- \rightleftharpoons FeL^{2+} \quad K_1 \qquad (1)\\
&FeL^{2+} + L^- \rightleftharpoons FeL_2^{+} \quad K_2\\
&FeL_2^{+} + L^- \rightleftharpoons FeL_3 \quad K_3
\end{aligned}
$$

Distribution coefficients of the 3-hydroxy-4(1*H*)-pyridinones were determined in an aqueous/octanol system using a modified filter probe device.[20]

Biological Experiments

The rate of chelator-induced removal of iron from human serum transferrin and horse ferritin was monitored by spectrophotometric measurement. Chelator-induced efflux of iron across hepatocyte membranes was determined by quantification of ^{59}Fe. Iron-overloaded mice were used to establish the profile of ^{59}Fe excretion with time after administration of each chelator.

Results

Ligand pK_a Values. Some representative ligands have been studied by simultaneous spectrophotometric/potentiometric titrations. The optimized pK_a values obtained with the computer program NONLINGEN 15[21] are shown in Table I. The pK_{a1} values correspond to the protonation of the 4-oxo group and the pK_{a2} values to the dissociation of the 3-hydroxy group (Scheme III). The values were found to be relatively constant irrespective of the N-alkyl function.

Stability Constants of Iron(III) Complexes. For bidentate ligands the logarithm of the cumulative stability constants was determined. This value, log β_3, is obtained by summation of the logarithms of three stepwise equilibrium constants corresponding to eq 1. The optimized values are presented in Table II. Again, the values were found to be largely independent of the nature of the N-alkyl function.

Distribution Coefficients. Values of distribution coefficients between an aqueous phase buffered at pH 7.4 and octanol are presented in Tables IX and X. In general, the expected increase in distribution coefficient upon elongation of the alkyl chain was observed in the N-alkyl series (20–28 and 48–53), the N-alkylcarbamoyl series (37–41 and 42–44), and the hydroxyalkyl series (32–34). Surprisingly, the unsubstituted pyridinones 19 and 47 possess higher values than the corresponding *N*-methylpyridinones (20 and 48). The charged molecules (35, 36, 45, 46) possess low values. Some of the values presented in Tables IX and X are slightly different from those previously published.[16] The values presented in the previous study were produced by the "shake flask" method and are less accurate.

X-ray Crystallography. A stereoview of 1,2-diethyl-3-hydroxy-4(1*H*)-pyridinone hydrochloride (49·HCl) is shown in Figure 2. The bond distances of ligand 49 and its hydrochloride are listed in Table IV. The bond distances in 49 agree very well with those observed for its 2-methyl congener 1-ethyl-2-methyl-3-hydroxy-4-(1*H*)-pyridinone (21).[22,23] Like other 3-hydroxy-4(1*H*)-pyridinones[17,22-24] the heterocyclic ring of the neutral form is obviously in quinoid form b in Scheme III. On the other hand, the C(4)–O(2) bond is significantly longer (1.264 Å) than a pure ketone bond (1.210 Å). This provides the O(2) atom with a partial negative charge, resulting from resonance form e in Scheme III, which is important

Table I. Measurements Made at 22.5 °C, Ionic Strength 0.2

compd	R	R_1	pK_{a1}	pK_{a2}
57	H	H	3.34[a]	9.01[a]
19	Me	H	3.70	9.76
20	Me	Me	3.56	9.64
21	Me	Et	3.65	9.88
22	Me	nPr	3.62	9.92
24	Me	nBu	3.62	9.87

[a] Measurements by Scarrow *et al.*[14] at 25 °C, ionic strength 0.1.

Table II. Measurements Made at 22.5 °C, Ionic Strength 0.2

compd	R	R_1	$\log K_1$	$\log K_2$	$\log K_3$	$\log \beta_3$
57	H	H	14.2[a]	11.6[a]	9.3[a]	35.1
19	Me	H	15.4[b]	12.03	9.73	37.2
20	Me	Me	14.92	12.23	9.79	37.2
21	Me	Et	15.33	12.5[b]	9.90	37.7
22	Me	nPr	15.34	12.57	9.82	37.7
24	Me	nBu	15.34			

[a] Measurements by Scarrow *et al.*[14] at 25 °C, ionic strength 0.1. [b] Estimated values based on statistical and coulombic factors.

for chelation. This argument also explains why **49** forms relatively strong hydrogen bonding (O–H···O=C: 1.87 (3) Å) and crystallizes as centrosymmetric hydrogen bonded dimeric units, which is found in all other known 3-hydroxy-4-pyridinone crystal structures.[17,22–24]

In the crystal structure of **49**·HCl, the bond distances are comparable with those determined for 1,2-dimethyl-3-hydroxy-4(1*H*)-pyridinone hydrochloride (**20**).[17] Upon protonation of the carbonyl O(2) atom, there occurs a significant aromatic delocalization (form **a** in Scheme III) in which the C(4)–O(2) bond increases by 0.069 Å and the C(3)–C(4) and C(4)–(5) single bonds become shorter, while the C(2)–C(3) and C(5)–C(6) double bonds become longer. Meanwhile, the C(3)–O(1) bond shortens by 0.008 Å. The consistently shorter C(4)–O(2) bond against C(3)–O(1) bond, and longer C(3)–C(4) and C(4)–C(5) bonds against C(2)–C(3) and C(5)–C(6) bonds in the protonated ligands **49** and **20** suggest a contribution from resonance form **d** in Scheme III. There is a very strong hydrogen bond (1.68(3) Å) between the proton on the hydroxy O(1) atom and a water molecule.

An ORTEP plot of a single molecule for tris[1-(2′-methoxyethyl)-2-methyl-3-hydroxy-4-pyridinone]ferric trihydrate complex **58** (the tris complex of **29**) is depicted in Figure 3 with a numbering scheme, while its bond distances are listed in Table IV. When the bond distances in complex **58** are compared with its ligand,[25] there are several significant changes similar to those observed in the protonated ligand **49**. The C(3)–O(1) is reduced by 0.017 Å, while the C(4)–O(2) is greatly increased by 0.042 Å in complex **58** upon metal chelation. The delocalization in the C–O bonds results in obvious averaging of the single and double C–C bonds in the ring. Therefore, the resonance form similar to **f** in Scheme III is important. All the above geometric changes upon chelation have been found in complexes of tris(3-hydroxy-4(1*H*)-pyridinones) with metal(III) cations.[22,23,26–28]

Table III.

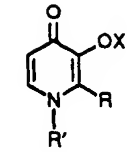

compd	R	R′	X
7	Me	H	Bz
8	Et	H	Bz
9	Me	Me	Bz
10	Me	Et	Bz
11	Me	CH_2CH_2OMe	Bz
12	Me	CH_2CH_2OH	Bz
13	Me	$CH_2CH_2CH_2OH$	Bz
14	Et	Me	Bz
15	Et	CH_2CH_2OH	Bz
16	Me	$CH_2CH_2CO_2H$	Bz
17	Me	$CH_2CH_2CH_2CO_2H$	Bz
19	Me	H	H
20	Me	Me	H
21	Me	Et	H
22	Me	nPr	H
23	Me	iPr	H
24	Me	nBu	H
25	Me	nPent	H
26	Me	nHex	H
27	Me	nOct	H
28	Me	nDec	H
29	Me	CH_2CH_2OMe	H
30	Me	$CH_2\text{-}CH_2\text{-}CH_2OEt$	H
31	Me	$CH(CH_3)CH_2OMe$	H
32	Me	CH_2CH_2OH	H
33	Me	$CH_2CH_2CH_2OH$	H
34	Me	$CH_2CH_2CH_2CH_2OH$	H
35	Me	$CH_2CH_2CO_2H$	H
36	Me	$CH_2CH_2CH_2CO_2H$	H
37	Me	$CH_2CH_2CONHMe$	H
38	Me	$CH_2CH_2CONHEt$	H
39	Me	$CH_2CH_2CONHnPr$	H
40	Me	$CH_2CH_2CONHisoPr$	H
41	Me	$CH_2CH_2CONHnBut$	H
42	Me	$CH_2CH_2CONMe_2$	H
43	Me	$CH_2CH_2CONMeEt$	H
44	Me	$CH_2CH_2CONEt_2$	H
45	Me	$CH_2CH_2NH_3^+Cl^-$	H
46	Me	$CH_2CH_2CH_2NH_3^+Cl^-$	H
47	Et	H	H
48	Et	Me	H
49	Et	Et	H
50	Et	nPr	H
51	Et	iPr	H
52	Et	nBu	H
53	Et	nHex	H
54	Et	CH_2CH_2OMe	H
55	Et	$CH_2CH_2CH_2OEt$	H
56	Et	CH_2CH_2OH	H
57	H	H	H

Ability of 3-Hydroxy-4(1*H*)-pyridinones To Remove Iron from Iron–Proteins. Transferrin. The addition of the colorless chelator solutions (100 μM) to Fe(III)–transferrin (50 μM) resulted in the removal of some iron from the protein as indicated by the change in absorbance in the visible wavelength region. The kinetics of removal were found to be biphasic, and after 2 h approximately 50% of the iron was removed. There was no significant difference in the behavior of any of the chelators investigated (Table V) irrespective of the nature of the N-substituent. Desferrioxamine B was essentially inactive in this assay.

Ferritin. Incubation of ferritin (containing iron cores with an equivalent concentration of 450 μM) with colorless chelator solutions (5 mM) resulted in the slow removal of iron, as monitored by the increase in absorbance at 450 nm of the filtrate after ultrafiltration of the incubate. The kinetics of iron removal were monophasic, and after 24 h approximately 25% of the iron core was mobilized (Table V). There was no significant difference in rate of removal of iron by the neutral ligands, although both the charged molecules **36** and **45** were found to be less efficient at iron removal. Desferrioxamine B was much less efficient than the neutral pyridinones. These results are in broad agreement with those previously reported.[29]

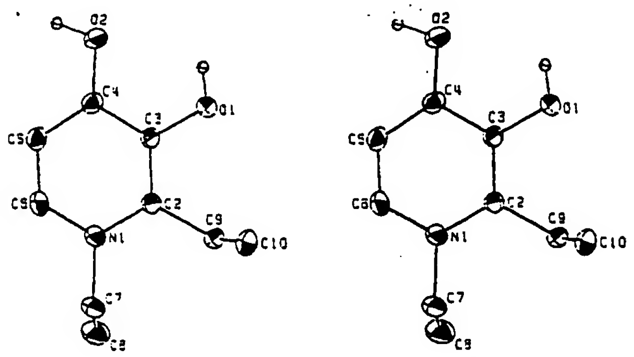

Figure 2. Stereoview of molecule 49·HCl showing numbering scheme. The H_2O and Cl^- are omitted for the purpose of numbering.

Table IV. Bond Distances (Å) for 49·HCl, 49, and 58 with esd's in Parentheses

	49	49·HCl	58
Fe–O(1)			2.001(2)
Fe–O(2)			2.047(3)
N(1)–C(2)	1.368(2)	1.379(2)	1.382(4)
N(1)–C(6)	1.354(2)	1.349(2)	1.353(7)
N(1)–C(7)	1.488(2)	1.480(2)	1.495(5)
C(2)–C(3)	1.388(2)	1.375(2)	1.399(5)
C(2)–C(9)	1.502(2)	1.509(2)	
C(2)–C(11)			1.489(7)
C(3)–C(4)	1.406(2)	1.433(2)	1.411(7)
C(3)–O(1)	1.346(2)	1.354(2)	1.337(5)
C(4)–C(5)	1.392(2)	1.421(2)	1.410(5)
C(4)–O(2)	1.333(2)	1.264(2)	1.306(4)
C(5)–C(6)	1.368(2)	1.361(2)	1.359(5)
C(7)–C(8)	1.513(2)	1.510(3)	1.498(7)
C(8)–O(9)			1.363(9)
O(9)–C(10)			1.575(4)
C(9)–C(10)	1.534(2)	1.525(5)	

Ability of 3-Hydroxy-4(1*H*)-pyridinones To Remove Iron from Hepatocytes. Rat hepatocytes were cultured overnight, preincubated with ^{59}Fe–transferrin, and then incubated with a range of chelators.[30] The rate of efflux of ^{59}Fe from the hepatocytes was monitored in the presence and absence of chelator, and the data are presented as the percentage of the ^{59}Fe efflux occurring in the absence of the chelator. Figure 4 shows the effect of increasing chelator concentration on ^{59}Fe release from hepatocytes, and Figure 5 shows the effect of the same chelators on LDH leakage from intact cells and on lipid peroxidation as estimated by measurement of cellular MDA at the end of 6 h of incubation. It can be seen that **29**, which is relatively lipophilic compared with **20**, is more effective at mobilizing intracellular iron at all concentrations studied (Figure 4) without producing significant cell damage. Indeed, there is a small decrease in LDH leakage at 100 μM with both **20** and **29** compared with control cells suggesting that low concentrations of these compounds may be beneficial to hepatocytes in culture. With increasing chelator concentrations, MDA content of the cells falls progressively with a more pronounced effect in the relatively hydrophilic **20** compared with the relatively lipophilic **29** (Figure 5).

There is a clear correlation between distribution coefficient *D* of a range of pyridinones and their efficiency of iron removal (Figure 6). Compounds with *D* values less than 0.5 are not particularly efficient at mobilizing iron, and there is an onset of a plateau effect at values greater than 1.5. Thus, a *D* value close to unity appears to be optimal for the pyridinone-facilitated removal of iron from hepatocytes. 1-(2′-Methoxyethyl)-2-methyl-3-hydroxy-4(1*H*)-pyridinone (**29**) is the single exception from this relationship, where with *D* = 0.39 it causes efficient mobilization of iron. With all pyridinones possessing *D* values < 2.0 there is no detectable cell damage as monitored by LDH release (see, for instance, Figure 5). The critical nature of both the affinity constant (log β_3) and *D* on the iron mobilization process is demonstrated in a comparative study of different iron ligand classes (Table VI). The closely related 2-pyridine aldoxime and 3-hydroxy-2(1*H*)-pyridinone (**2**), each of which are neutral at pH 7.4, fail to mobilize iron. This undoubtedly relates to their lower affinity constants for iron(III). 8-Hydroxyquinoline, which does possess a sufficiently high affinity constant, also possesses a high *D* value (80.0) and consequently is toxic to the cells as is demonstrated by the release of LDH (Table VI).

Mobilization of Iron from Iron-Overloaded Mice. Iron-overloaded mice[31] were treated either orally or intraperitoneally with buffered chelator solutions, and the chelator-induced excretion (urine and feces) of ^{59}Fe was monitored. Dose responses for the oral administration of the pyridinones **20**, **29**, and **49** are presented in Figure 7a. All three compounds are remarkably active, the most hydrophilic (**20**) being the least efficient scavenger. In contrast to desferrioxamine B, which is not orally active, the 3-hydroxy-4(1*H*)-pyridinones are effective when administered either intraperitoneally or orally (Figure 7b). Indeed, pyridinone **29** is far more active than desferrioxamine when presented intraperitoneally.

Discussion

Iron(III) Binding Properties. The affinity measurements in this study demonstrate the high affinity of 3-hydroxy-4(1*H*)-pyridinones for iron(III); the log β_3 value for 1,2-dimethyl-3-hydroxy-4(1*H*)-pyridinone (**20**), for instance, was determined in this study as 36.9, which compares favorably with the value 35.9 independently determined by Motekaitis and Martell.[32] (The small difference between these two values could partially result from the different temperatures used, namely 22.5 and 25 °C.) This value is higher than those associated with closely related dioxo-bidentate ligands (Table VII). Indeed, although the 4-pyridinones appear to be weaker ligands for iron(III) than catechol, catechol has a much greater affinity for protons, and consequently in the pH range 2–8 the 4-pyridinone will compete more effectively for iron(III) than catechol. This difference is highlighted by the different pM values of the two ligands, catechol, 15.1, and 4-pyridinone, 20.0.[33] Thus, the 3-hydroxy-4(1*H*)-pyridinone moiety appears to be the optimal dioxo-bidentate ligand for iron(III) at physiological pH values. The partial negative charge on the carbonyl oxygen atom in the deprotonated ligand ion (Scheme III, **f**), leads to more than one negative charge over the two oxygen atoms bonded to the iron atom. This is the reason for the large complexation constants of the 4-pyridinones when compared with the other closely related ligands (Table VII). The delocalization of charge on the 4-carbonyl function also gives rise to its acidic character (pK_{a1} = 3.6). The extensive delocalization of charge in this molecular class is unambiguously demonstrated by the X-ray studies (Table IV). Although there are three complex types, ML, ML_2 and ML_3 (eq 1), the 1:3 complex (Figure 3) predominates at neutral pH values due to the extreme avidity of the 4-pyridinone ligand for iron(III). This property is clearly demonstrated in the speciation plot for 1-ethyl-

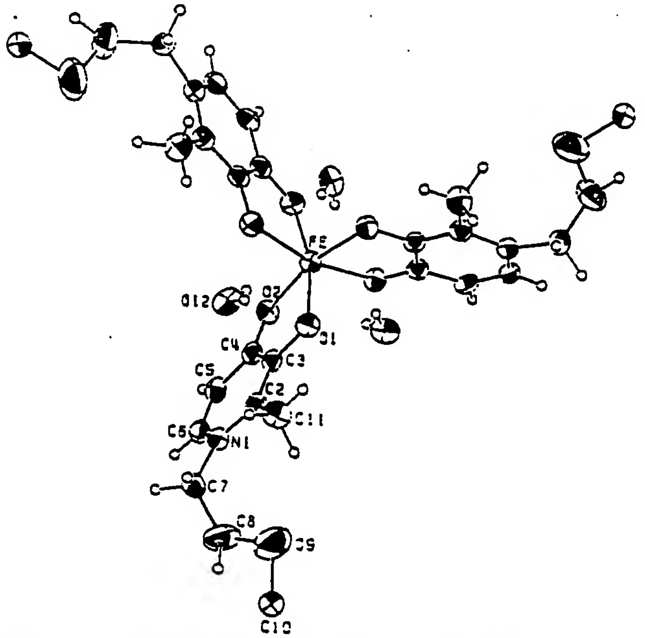

Figure 3. ORTEP plot of a single molecule of the iron(III) complex of pyridinone **29**.

Table V. Percentage of Removal of Iron from Transferrin and Ferritin

ligand	% iron removed[a]	
	transferrin	ferritin
20	54 ± 2	34 ± 2.5
22	52 ± 3	28 ± 1.1
23	51 ± 3	26 ± 1.2
24	52 ± 4	
29	55 ± 2	28 ± 2.0
30	49 ± 3	
32	47 ± 4	29 ± 0.8
36	53 ± 6	12 ± 1.1
45	56 ± 3	23 ± 4.1
desferrioxamine	5 ± 2	11 ± 2.2
control	0	0

[a] Mean of 3 ± SE.

2-methyl-3-hydroxy-4(1*H*)-pyridinone (**21**) (Figure 8). Thus, the major form of complexed iron under biological conditions is hexacoordinated (Figure 3), and as such is unlikely to generate oxygen radicals under aerobic conditions.[5]

A further important observation to emerge from these studies is that a range of different N-substitutions failed to influence dramatically the affinity for protons (Table I) or for iron(III) (Table II). This observation is indirectly confirmed by X-ray studies where the bond lengths of the coordinating oxygen atoms and the distances of those oxygen atoms to the iron atom remained relatively constant among a range of pyridinones with varying N-substituents (58 present results).[23,27] Thus, it has been possible to design a wide range of 4-pyridinones with different biodistribution properties while retaining a constant affinity for iron(III).

Competition Studies with Iron-Transport and Storage Proteins. Iron is transported in mammalian blood on the glycoprotein transferrin; thus, iron is transferred bound to this protein from the intestine and the liver to tissues that require a regular supply of iron, for instance, the bone marrow. The high affinity of transferrin for iron ensures that the concentration of other forms of iron in the plasma are vanishingly small, thereby exerting a powerful antibacterial and antifungal influence.[36] The possibility of exchange of iron between transferrin and

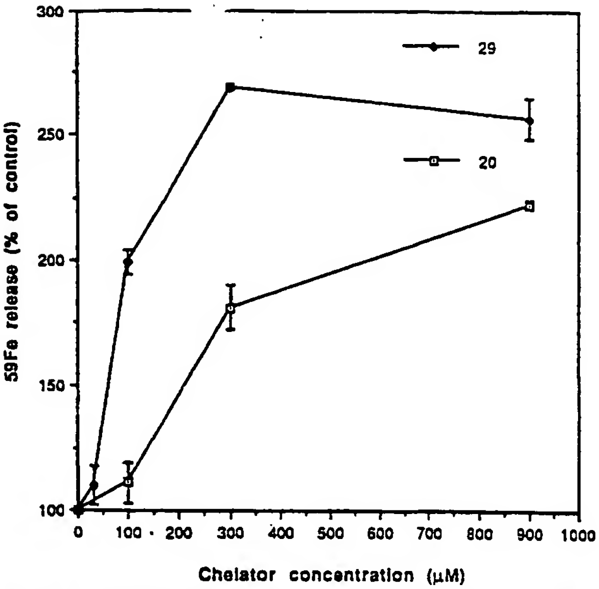

Figure 4. Hepatocyte ^{59}Fe release by hydroxypyridinone chelators (**20** and **29**). Hepatocytes derived from rat liver were placed on collagen plates and pulsed with [^{59}Fe]transferrin. Hepatocytes were subsequently exposed for 6 h to the chelators at the indicated concentrations. The mean of six independent determinations is shown with the standard error.

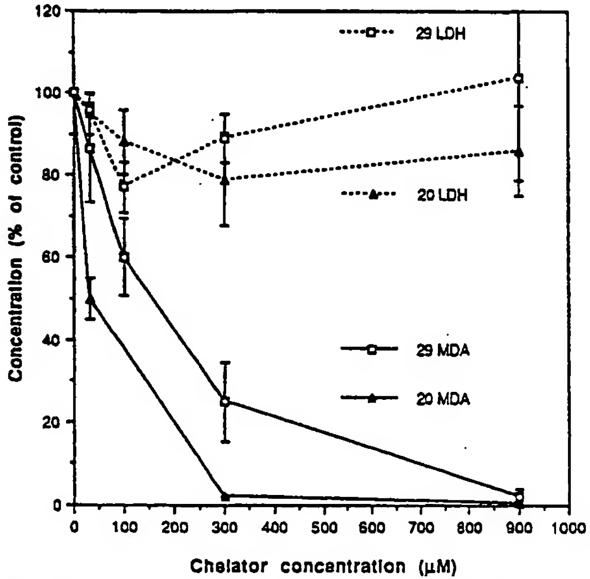

Figure 5. Influence of hydroxypyridinone chelators (**20** and **29**) on the release of lactate dehydrogenase (LDH) from hepatocytes and the production of malonyl dialdehyde by hepatocytes. Rat hepatocytes were incubated for 6 h on collagen plates. The mean of six independent determinations is shown with the standard error.

high affinity chelators is therefore a matter of considerable importance. To be clinically useful it is probably ideal that iron-scavenging molecules should not take iron from transferrin in view of the central role this molecule plays in iron metabolism. Most of the dioxo-bidentate ligands do not possess a sufficiently high affinity for iron(III) to compete with apotransferrin; however, the 3-hydroxy-4(1*H*)-pyridinone class, by virtue of their high p*M* value,[33] compete with transferrin at relatively high concentrations (10^{-3} M) (Table V). However, at lower concentrations of 10^{-4}–10^{-6} M, namely those likely to be experienced clinically, 4-pyridinoneiron(III) complexes donate iron to apotransferrin.[37]

The major intracellular storage form of iron is ferritin.

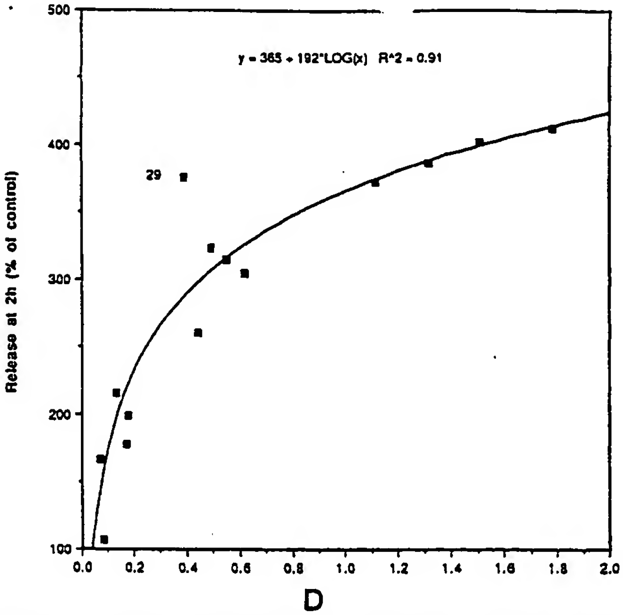

Figure 6. Relationship between distribution coefficients (D) and ability of hydroxypyridinones to remove iron from rat hepatocytes. Incubation conditions were as indicated in Figure 3.

Table VI. Percentage of Mobilization of Iron and Percentage of Release of Lactic Dehydrogenase (LDH) from Rat Hepatocytes

ligand	% mobilization of iron (2 h)	% LDH release	log β_3 (Fe III)
(22)	252 ± 14	105 ± 20	37
8-hydroxyquinoline	110 ± 8	260 ± 56	37
2-pyridine aldoxime	108 ± 6	108 ± 18	30
1-ethyl-3-hydroxy-2(1*H*)-pyridinone (2, (R = Et))	115 ± 9	102 ± 15	32

Ferritin consists of a protein shell surrounding an aqueous cavity in which water may be replaced by an "iron core" of the mineral ferrihydrite containing up to 4500 iron atoms.[38] In accumulating or removing iron from the core, access to the cavity is achieved *via* aqueous channels which penetrate the protein shell. Once stored in the core, the iron atoms are less liable to enter autoxidation reactions, which lead to the generation of potentially toxic oxygen radicals. Hexadentate ligands such as desferrioxamine B are too large to enter the pores of the ferritin molecule and consequently are relatively inefficient at removing iron from ferritin (Table V). In contrast, the 3-hydroxy-4(1*H*)-pyridinones are capable of removing iron from ferritin, albeit at a rather slow flux. Surprisingly, the bulk and hydrophobicity of the N-substituent has little effect on the efficiency of iron removal from ferritin, although negatively charged ligands are less effective (Table V). The rate-determining step for the removal of iron appears to be solubilization from the iron core.[29]

Iron Removal from Hepatocytes and Mice. The wide range of distribution coefficients obtained for the 3-hydroxy-4(1*H*)-pyridinones utilized in this study (0.001–750) has facilitated a systematic analysis of the relationship between membrane permeability and the efficiency of iron removal from intact cells and whole animals. The pK_a values of the 4-pyridinones are similar, falling in the ranges 3.3–3.7 and 9.0–9.9; thus, the predominant species in solution over the pH range 5–8 bears net zero charge (Scheme III, b and e).

Thus with molecular weights falling in the range 125–220, good membrane permeation is predicted for molecules with distribution coefficients >0.1. Indeed, ligands with distribution coefficients >0.5 were found to mobilize iron from hepatocytes extremely efficiently (Figure 6). 4-Pyridinones with distribution coefficients >5.0 were found to be toxic to cells.[16,39] Thus, although the N-substituent has little influence on the affinity of the 4-pyridinone for iron(III), it exerts a major effect on the ability of chelators

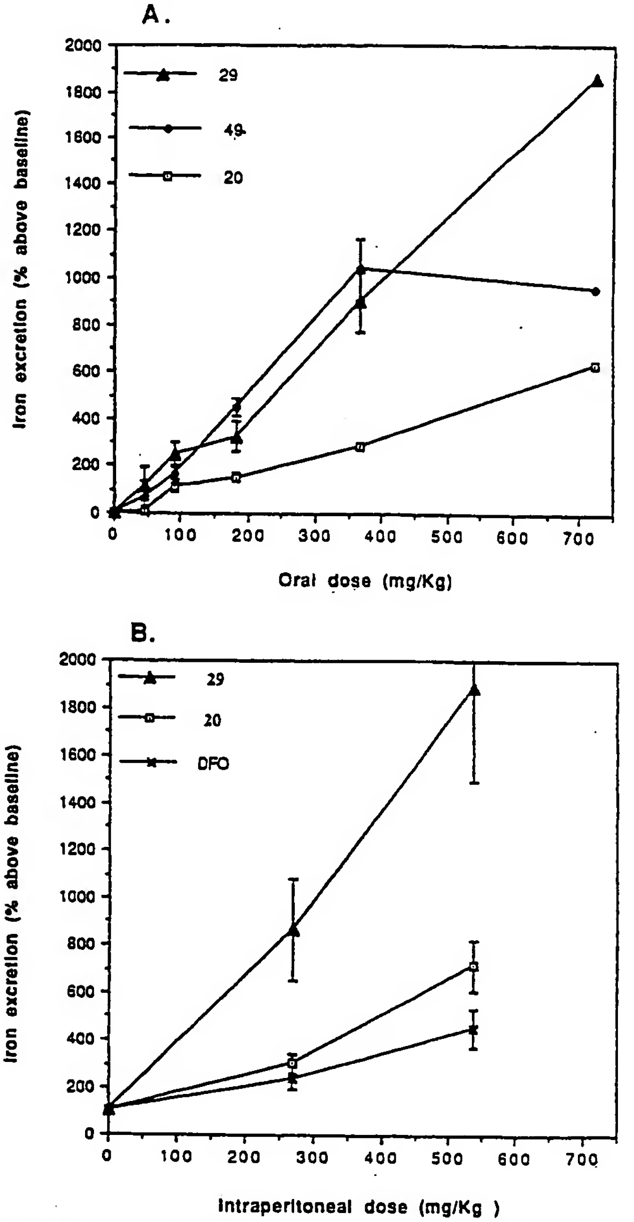

Figure 7. Removal of ^{59}Fe from iron-overloaded mice by chelators at various doses: (A) oral dosing, (B) intraperitoneal dosing. Mice were loaded with iron dextran, labeled with [^{59}Fe]lactoferrin, and allowed to stabilize for 3 weeks. After base-line excretion rates were recorded, chelators were administered. The amount of ^{59}Fe in the urine and feces over the next 24 h was measured with a γ-counter. The mean of four independent determinations is shown with the standard error.

Table VII. pK_a and log β_3 Values for Bidentate Ligands

	pK_{a2}	pK_{a1}	log β_3
catechol[a]	13.3	9.2	44.9
3-hydroxy-4(1*H*)-pyridinone (1)	9.6	3.6	36.9
3-hydroxy-2(1*H*)-pyridinone[b] (2)	8.8		32.3
1-hydroxy-2(1*H*)-pyridinone[c] (3)	5.8		26.9
3-hydroxy-4(4*H*)-pyranone[d] (4, R = Me)	8.7		28.4
acetohydroxamic acid[a]	9.4		28.3

[a] Reference 34. [b] Reference 15. [c] Reference 14. [d] Reference 35.

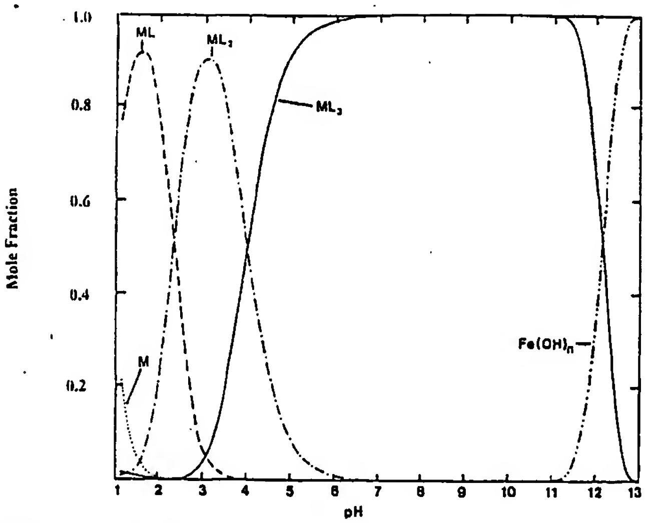

Figure 8. Speciation plot of 1-ethyl-2-methyl-3-hydroxy-4(1*H*)-pyridinone (21) and iron(III). Concentration of 21, 4×10^{-4} M, concentration of iron(III), 1×10^{-4} M. The following parameters were incorporated into the model for this system: log K_{11} ML = 15.3; log K_{12} ML_2 = 12.5; log K_{13} ML_3 = 9.9; pK_{a1} = 3.62; pK_{a2} = 9.88. ML_1 ML_2 and ML_3 are the 1:1, 1:2, and 1:3 iron/21 complexes, respectively.

to scavenge iron from intact cells and their associated toxicity. The reason for the anomalous behavior of 29 (Figure 6) is not clear; nevertheless, the potent activity observed in the hepatocyte system is mirrored in studies with iron-overloaded mice. In this work 29 was one of the most potent 4-pyridinones studied (Figure 7).

In contrast to desferrioxamine B, the 3-hydroxy-4(1*H*)-pyridinones are orally active. Compounds with distribution coefficients in the range 0.5–2.0 are more effective than those with lower values (<0.2).[40] More extensive biological studies are in progress with this promising family of molecules. Formal toxicity studies have been undertaken with 49 and this molecule, together with 20, is currently the subject of clinical trials.[41-43]

Experimental Section

General Procedures. Melting points are uncorrected. IR spectra were recorded on a Perkin-Elmer 298. Proton NMR spectra were determined with a Perkin-Elmer R32 (90 MHz). Mass spectra were taken using a Vacuum Generators 16F (35 eV). Elemental analyses were performed by Butterworth Laboratories Limited, Teddington, Middlesex. Full spectroscopic and analytical data are available as supplementary material.

2-Ethyl-3-(benzyloxy)-4(4*H*)-pyranone (6). To a solution of ethyl maltol (196 g, 1.4 mol) in methanol (1800 mL) was added sodium hydroxide (60 g, 1.5 mol) dissolved in water (200 mL) followed by benzyl chloride (190 g, 1.50 mol) and the mixture refluxed for 6 h. After removal of solvent by rotary evaporation the resultant oil was taken up in dichloromethane (750 mL) and washed with 5% aqueous sodium hydroxide (2 × 750 mL) followed by water (2 × 750 mL). The organic fraction was then dried over anhydrous sodium sulfate, filtered, and rotary evaporated to yield an orange oil which solidified on cooling, recrystallization from diethyl ether giving colorless needles (255 g, 79%): mp 33–34 °C. Anal. ($C_{14}H_{14}O_3$) C, H.

An analogous procedure using maltol gave 2-methyl-3-(benzyloxy)-4(4*H*)-pyranone (5) (83%): mp 53–55 °C (lit.[18a] oil). Anal. ($C_{13}H_{12}O_3$) C, H.

2-Ethyl-3-(benzyloxy)-4-hydroxypyridine (8). To a solution of 6 (28 g, 0.12 mol) in ethanol (200 mL) was added 35% aqueous ammonia (400 mL) and the mixture refluxed for 18 h. Removal of solvent by rotary evaporation gave an oil which solidified on addition of acetone and cooling, recrystallization from ethanol yielding colorless prisms (24 g, 89%): mp 168–169 °C. Anal. ($C_{14}H_{15}NO_2$) C, H, N.

An analogous procedure using 5 gave 2-methyl-3-(benzyloxy)-4-hydroxypyridine (7) (88%): mp 165–166 °C (lit.[18a] mp 162–163 °C). Anal. ($C_{13}H_{13}NO_2$) C, H, N.

2-Methyl-3,4-dihydroxypyridine Hydrochloride (19). A solution of 7 (20 g, 0.093 mol) in ethanol (270 mL)/water (30 mL) was adjusted to pH 1 with hydrochloric acid prior to hydrogenolysis for 4 h in the presence of 5% Pd/C catalyst (1 g). Filtration followed by rotary evaporation gave a white solid, recrystallization from ethanol/diethyl ether yielding a white powder (15.1 g, 95%): mp 172–173 °C. Anal. ($C_6H_8NO_2Cl\cdot{}^1/_2H_2O$) C, H, N.

An analogous procedure using 8 gave 2-ethyl-3,4-dihydroxypyridine hydrochloride 47 (90%): mp 166–167 °C. Anal. ($C_7H_{10}ClNO_2$) C, H, N.

1,2-Dimethyl-3-(benzyloxy)-4(1*H*)-pyridinone Hydrochloride (9). To a solution of 5 (25 g, 0.12 mol) in ethanol (200 mL)/water (200 mL) was added 40% aqueous methylamine (14 g, 0.18 mol) followed by 2 N sodium hydroxide solution (10 mL) and the mixture refluxed for 18 h. After adjustment to pH 1 with hydrochloric acid, the volume was reduced to 200 mL by rotary evaporation prior to addition of water (200 mL) and washing with diethyl ether (400 mL). Subsequent adjustment of the aqueous fraction to pH 7 with 10 N sodium hydroxide solution was followed by extraction into dichloromethane (3 × 400 mL), the organic layers then being dried over anhydrous sodium sulfate, filtered, and rotary evaporated to give an orange oil. This oil was dissolved in ethanol/hydrochloric acid and rotary evaporated, the resulting white solid being recrystallized from ethanol/diethyl ether to give a white powder (26 g, 85%): mp 207–208 °C. Anal. ($C_{14}H_{16}ClNO_2$) C, H, N.

Analogous reaction of 5 with ethylamine, 2-methoxyethylamine, ethanolamine, or 3-hydroxypropylamine and of 6 with methylamine or ethanolamine gave compounds 10–15 as shown in Table VIII.

1,2-Dimethyl-3-hydroxy-4(1*H*)-pyridinone Hydrochloride (20). A solution of 9 (20 g, 0.075 mol) in ethanol (270 mL)/water (30 mL) was subjected to hydrogenolysis for 4 h in the presence of 5% Pd/C catalyst (1 g). Filtration followed by rotary evaporation gave a white solid, recrystallization from ethanol/diethyl ether yielding a white powder (13 g, 89%): mp 189–190 °C. Anal. ($C_7H_{10}ClNO_2\cdot H_2O$) C, H, N.

Analogous reaction of 10–15 gave compounds 21, 29, 32, 33, 48, and 56, respectively, as shown in Table IX.

1-Propyl-2-methyl-3-hydroxy-4(1*H*)-pyridinone Hydrochloride (22). To a solution of 5 (25 g, 0.12 mol) in ethanol (200 mL)/water (200 mL) was added propylamine (10.6 g, 0.18 mol) followed by 2 N sodium hydroxide solution (10 mL) and the mixture refluxed for 18 h. After an extraction procedure identical to that used in the preparation of 9 an orange oil was obtained, which was subsequently dissolved in ethanol (270 mL)/water (30 mL) and adjusted to pH 1 with hydrochloric acid prior to hydrogenolysis for 4 h in the presence of 5% Pd/C catalyst (1 g). Filtration followed by rotary evaporation gave a white solid, recrystallization from ethanol/diethyl ether yielding a white powder (19 g, 81%): mp 206–207 °C. Anal. ($C_9H_{14}ClNO_2$) C, H, N.

Analogous syntheses starting with reaction of 5 or 6 with ethylamine, propylamine, isopropylamine, butylamine, pentylamine, hexylamine, octylamine, 2-methoxyethylamine, 3-ethoxypropylamine, (±)-2-amino-1-methoxypropane, 3-hydroxypropylamine, and 4-hydroxybutylamine gave compounds 21–27, 29–31, 33, 34, and 49–55 as shown in Table IX.

1-(2′-Carboxyethyl)-2-methyl-3-(benzyloxy)-4(1*H*)-pyridinone (16). To a solution of 5 (25 g, 0.12 mol) in ethanol (300 mL) was added β-alanine (12.5 g, 0.14 mol) dissolved in water (300 mL) followed by 10 N sodium hydroxide solution until pH 13 was attained. After reflux for 18 h, the resulting solution was reduced in volume to 200 mL by rotary evaporation prior to adjustment to pH 4 with hydrochloric acid and extraction into dichloromethane (3 × 250 mL). The organic fractions were then dried over anhydrous sodium sulfate, filtered, and rotary evaporated to give an orange oil which solidified on addition of acetone and cooling, recrystallization from ethanol/diethyl ether giving a yellow powder (24 g, 72%): mp 170–171 °C. Anal. ($C_{16}H_{17}NO_4$) C, H, N.

Table VIII. Syntheses of 1-Substitut Alkyl-3-(benzyloxy)-4(1*H*)-pyridinone Hydrochlor.

compd	R	R^1	mp, °C	% yield	formula	anal.
9	Me	Me	207–208	85	$C_{14}H_{16}NO_2Cl$	C,H,N
10	Me	Et	178–179	85	$C_{15}H_{18}NO_2Cl$	C,H,N
11	Me	$CH_2CH_2OCH_3$	150–151	81	$C_{16}H_{20}NO_3Cl\cdot H_2O$	C,H,N
12	Me	CH_2CH_2OH	205–206	73	$C_{15}H_{18}NO_3Cl$	C,H,N
13	Me	$CH_2CH_2CH_2OH$	160–161	77	$C_{16}H_{20}NO_3Cl$	C,H,N
14	Et	Me	176–177	80	$C_{15}H_{18}NO_2Cl$	C,H,N
15	Et	CH_2CH_2OH	169–170	82	$C_{16}H_{20}NO_3Cl$	C,H,N

Table IX. Synthesis of 1-Substituted 2-Alkyl-3-hydroxy-4(1*H*)-pyridinone Hydrochlorides and Their Distribution Coefficients between an Aqueous Phase Buffered at pH 7.4 and Octanol

R	R	R^1	mp, °C	% yield (from 5 or 6)	formula	anal.	distribn coeff
19	Me	H	172–173	84	$C_6H_8NO_2Cl\cdot{}^1/_2H_2O$	C,H,N	0.32 ± 0.01 (*n* = 10)
20	Me	Me	189–190	76	$C_7H_{10}NO_2Cl\cdot H_2O$	C,H,N	0.17 [illegible] 0.01 (*n* = 10)
21	Me	Et	205–206	74	$C_8H_{12}NO_2Cl$	C,H,N	0.49 ± 0.01 (*n* = 25)
22	Me	Pr	206–207	81	$C_9H_{14}NO_2Cl$	C,H,N	1.51 ± 0.01 (*n* = 25)
23	Me	iPr	225–226	72	$C_9H_{14}NO_2Cl$	C,H,N	1.12 ± 0.01 (*n* = 5)
24	Me	Bu	199–200	73	$C_{10}H_{16}NO_2Cl$	C,H,N	5.05 ± 0.02 (*n* = 11)
25	Me	pentyl	165–166	68	$C_{11}H_{18}NO_2Cl$	C,H,N	17.4 ± 0.2 (*n* = 24)
26	Me	hexyl	166–167	70	$C_{12}H_{20}NO_2Cl$	C,H,N	79 ± 5 (*n* = 6)
27	Me	octyl	134–135	59	$C_{14}H_{24}NO_2Cl$	C,H,N	750 ± 100 (*n* = 12)
28	Me	decyl	140–141	57	$C_{16}H_{28}NO_2Cl$	C,H,N	insoluble
29	Me	$CH_2CH_2OCH_3$	173–174	72	$C_9H_{14}NO_3Cl$	C,H,N	0.39 ± 0.01 (*n* = 5)
30	Me	$(CH_2)_3OCH_2CH_3$	145–146	76	$C_{11}H_{18}NO_3Cl$	C,H,N	1.32 ± 0.01 (*n* = 5)
31	Me	$CH(CH_3)CH_2OCH_3$	117–118	55	$C_{10}H_{16}NO_3Cl\cdot H_2O$	C,H,N	0.55 ± 0.09 (*n* = 5)
32	Me	CH_2CH_2OH	156–157	62	$C_8H_{12}NO_3Cl\cdot H_2O$	C,H,N	0.08 (*n* = 3)
33	Me	$CH_2CH_2CH_2OH$	120–121	67	$C_9H_{14}NO_3Cl$	C,H,N	0.132 ± 0.001 (*n* = 4)
34	Me	$(CH_2)_4OH$	144–145	60	$C_{10}H_{16}NO_3Cl$	C,H,N	0.181 ± 0.001 (*n* = 5)
35	Me	$CH_2CH_2CO_2H$	207–208	67	$C_9H_{12}NO_4Cl$	C,H,N	<0.001
36	Me	$(CH_2)_3CO_2H$	225–226	63	$C_{10}H_{14}NO_4Cl$	C,H,N	<0.001
45	Me	$CH_2CH_2NH_3Cl$	284–285	61	$C_8H_{14}N_2O_2Cl_2$	C,H,N	0.028 ± 0.001 (*n* = 4)
46	Me	$CH_2CH_2CH_2NH_3Cl$	260–261	68	$C_9H_{16}N_2O_2Cl_2\cdot H_2O$	C,H,N[a]	0.008 ± 0.003 (*n* = 5)
47	Et	H	166–167	80	$C_7H_{10}NO_2Cl$	C,H,N	1.11 ± 0.03 (*n* = 8)
48	Et	Me	219–220	73	$C_8H_{12}NO_2Cl$	C,H,N	0.624 ± 0.003 (*n* = 5)
49	Et	Et	188–189	75	$C_9H_{14}NO_2Cl$	C,H,N	1.78 ± 0.01 (*n* = 5)
50	Et	Pr	143–144	75	$C_{10}H_{16}NO_2Cl\cdot H_2O$	C,H,N	5.04 ± 0.02 (*n* = 5)
51	Et	iPr	206–207	53	$C_{10}H_{16}NO_2Cl$	C,H,N	5.4 ± 1.0 (*n* = 7)
52	Et	Bu	155–156	60	$C_{11}H_{18}NO_2Cl$	C,H,N	16.6 ± 0.8 (*n* = 10)
53	Et	hexyl	104–105	55	$C_{13}H_{22}NO_2Cl$	C,H,N	189 ± 5 (*n* = 5)
54	Et	$CH_2CH_2OCH_3$	132–133	58	$C_{10}H_{16}NO_3Cl$	C,H,N	1.1 ± 0.2 (*n* = 5)
55	Et	$(CH_2)_3OCH_2CH_3$	100–101	58	$C_{12}H_{20}NO_3Cl$	C,H,N	5.2 ± 0.2 (*n* = 5)
56	Et	CH_2CH_2OH	153–154	71	$C_9H_{14}NO_3Cl$	C,H,N	0.22 ± 0.01 (*n* = 5)

[a] N: calcd 10.26; found 9.76.

An analogous procedure using 4-aminobutyric acid gave 1-(3′-carboxypropyl)-2-methyl-3-(benzyloxy)-4(1*H*)-pyridinone (17) (70%): mp 169–170 °C. Anal. ($C_{17}H_{19}NO_4$) C, H, N.

1-(2′-Carboxyethyl)-2-methyl-3-hydroxy-4(1*H*)-pyridinone Hydrochloride (35). A solution of 16 (10 g, 0.035 mol) in ethanol (100 mL)/water (100 mL) was adjusted to pH 1 with hydrochloric acid prior to hydrogenolysis for 4 h in the presence of 5% Pd/C catalyst (0.5 g). Filtration followed by rotary evaporation gave a cream solid, recrystallization from ethanol/diethyl ether yielding a white powder (7.6 g, 93%): mp 207–208 °C. Anal. ($C_9H_{12}ClNO_4$) C, H, N.

An analogous procedure using 17 gave 1-(3′-carboxypropyl)-2-methyl-3-hydroxy-4(1*H*)-pyridinone (36) (90%): mp 225–226 °C. Anal. ($C_{10}H_{14}ClNO_4$) C, H, N.

1-[2′-[(Succinimidyloxy)carbonyl]ethyl]-2-methyl-3-(benzyloxy)-4(1*H*)-pyridinone (18). To a solution of 16 (10 g, 0.035 mol) in DMF (200 mL) was added *N*-hydroxysuccinimide (4 g, 0.035 mol) dissolved in DMF (50 mL) followed by *N,N′*-dicyclohexylcarbodiimide (7.2 g, 0.035 mol) dissolved in DMF (50 mL). After being stirred at room temperature for 18 h the resultant mixture was filtered and rotary evaporated to yield a white solid, recrystallization from dichloromethane/diethyl ether yielding a white powder (9.8 g, 73%): mp 144–146 °C. Anal. ($C_{20}H_{20}N_2O_6$) C, H, N.

1-[2′-(*N*-Methylcarbamoyl)ethyl]-2-methyl-3-hydroxy-4(1*H*)-pyridinone Hydrochloride (37). To a solution of 18 (5 g, 0.013 mol) in dichloromethane (100 mL) was added 40% aqueous methylamine (1 g, 0.013 mol) and the mixture stirred at room temperature for 4 h. After the solution was washed with water (3 × 100 mL) the organic layer was dried over anhydrous sodium sulfate, filtered, and rotary evaporated to give a yellow oil. This oil was subsequently dissolved in ethanol (90 mL)/water (10 mL) and adjusted to pH 1 with hydrochloric acid prior to room temperature hydrogenolysis for 4 h in the presence of 5% Pd/C catalyst (0.2 g). Filtration followed by rotary evaporation gave a white solid, recrystallization from ethanol/diethyl ether yielding a white powder (2.1 g, 62%): mp 182–183 °C. Anal. ($C_{10}H_{15}ClN_2O_3$) C, H, N.

Analogous procedures using a range of primary and secondary amines gave compounds 38 to 44 in Table X.

1-Decyl-2-methyl-3-hydroxy-4-(1*H*)-pyridinone Hydrochloride (28). To a solution of 5 (25 g, 0.12 mol) in ethanol (200 mL)/water (200 mL) was added decylamine (29 g, 0.18 mol) followed by 2 N sodium hydroxide solution (10 mL) and the mixture refluxed for 18 h. After adjustment to pH 1 with hydrochloric acid solvent was removed by rotary evaporation to give a red oil, which was reconstituted in ethanol (360 mL)/water (40 mL) and subjected to hydrogenolysis for 4 h in the presence of 5% Pd/C catalyst (1 g). Filtration followed by rotary evaporation gave an orange oil which was dissolved in water (500 mL) and washed with diethyl ether (2 × 500 mL) prior to adjustment to pH 7 with 10 N sodium hydroxide solution and extraction into dichloromethane (3 × 500 mL). The organic fractions were dried over anhydrous sodium sulfate, filtered, and rotary evaporated to give a yellow oil, which was reconstituted in ethanol/hydrochloric acid and rotary evaporated to yield a white solid. Recrystallization from ethanol/diethyl ether gave a white powder (20 g, 57%): mp 140–141 °C. Anal. ($C_{16}H_{28}ClNO_2$) C, H, N.

1-(2′-Aminoethyl)-2-methyl-3-hydroxy-4(1*H*)-pyridi-

Table X. Synthesis of 1-[2-(*N*-alkylcarbamoyl)ethyl]-2-methyl-3-hydroxy-4(1*H*)-pyridinone hydrochlorides and Their Distribution Coefficients between an Aqueous Phase Buffered at pH 7.4 and Octanol

compd	R	R[1]	mp, °C	% yield	formula	anal.	distribn coeff
37	Me	$(CH_2)_2CONHMe$	181–182	62	$C_{10}H_{15}N_2O_3Cl\cdot H_2O$	C,H,N	0.079 ± 0.003 ($n = 5$)
38	Me	$(CH_2)_2CONHEt$	156–157	63	$C_{11}H_{17}N_2O_3Cl\cdot H_2O$	C,[a]H,N	0.152 ± 0.003 ($n = 5$)
39	Me	$(CH_2)_2CONHPr$	156–157	77	$C_{12}H_{19}N_2O_3Cl\cdot {}^1/_2H_2O$	C,H,N	0.402 ± 0.003 ($n = 8$)
40	Me	$(CH_2)_2CONH^iPr$	103–104	70	$C_{12}H_{19}N_2O_3Cl\cdot 1^1/_2H_2O$	C,H,N	0.338 ± 0.004 ($n = 5$)
41	Me	$(CH_2)_2CONHBu$	77–78	79	$C_{13}H_{21}N_2O_3Cl\cdot 2H_2O$	C,[b]H,N	1.25 ± 0.06 ($n = 7$)
42	Me	$(CH_2)_2CON(Me)_2$	167–168	82	$C_{11}H_{17}N_2O_3Cl\cdot 2^1/_2H_2O$	C,H,N	0.069 ± 0.001 ($n = 5$)
43	Me	$(CH_2)_2CONMeEt$	171–172	80	$C_{12}H_{19}N_2O_3Cl$	C,H,N	0.206 ± 0.001 ($n = 5$)
44	Me	$(CH_2)_2CON(Et)_2$	140–141	86	$C_{13}H_{21}N_2O_3Cl$	C,[c]H,N	0.436 ± 0.002 ($n = 5$)

[a] C: calcd, 47.39; found 46.91. [b] C: calcd, 48.06; found 48.56. [c] C: calcd, 54.06; found 53.61.

none Dihydrochloride (45). To a solution of 5 (25 g, 0.12 mol) in ethanol (200 mL)/water (200 mL) was added ethylenediamine (7 g, 0.12 mol) followed by 2 N sodium hydroxide solution (10 mL) and the mixture refluxed for 18 h. After adjustment to pH 1 with hydrochloric acid, volume was reduced to 200 mL by rotary evaporation prior to addition of water (200 mL) and washing with diethyl ether (400 mL). Subsequent adjustment of the aqueous fraction to pH 12 with 10 N sodium hydroxide solution was followed by extraction into dichloromethane (3 × 400 mL), the organic layers then being dried over anhydrous sodium sulfate, filtered, and rotary evaporated to give an orange oil. This oil was reconstituted in ethanol (150 mL)/water (150 mL) and adjusted to pH 1 with hydrochloric acid prior to hydrogenolysis for 4 h in the presence of 5% Pd/C catalyst (1 g). Filtration followed by rotary evaporation gave a white solid, recrystallization from ethanol yielding a white powder (17 g, 61%): mp 284–285 °C. Anal. ($C_8H_{14}Cl_2N_2O_2$) C, H, N.

An analogous procedure using 1,3-diaminopropane gave 1-(3′-aminopropyl)-2-methyl-3-hydroxy-4-(1*H*)-pyridinone dihydrochloride (46) (68%): mp 260–261 °C. Anal. ($C_9H_{16}Cl_2NO_2\cdot H_2O$) C, H, N.

Simultaneous Potentiometric and Spectrophotometric Titrations. Absorbance and emf were measured after incremental titrant addition using an automated system. This comprises a Corning Delta 250 pH meter, a Perkin-Elmer Lambda 5 UV/vis spectrophotometer and an autoburette interfaced to a PC microcomputer.

Parameters describing the model for iron(III) coordination by the hydroxypyridinone were optimized by nonlinear regression to minimize the sum of squared residuals between the simulated and true data using the program NONLIGEN15 (21) (in Microsoft Quickbasic 4.0). The stability constants were optimized from the spectrophotometric titration of the metal–ligand system using the pK_a values, electrode slope, and electrode zero determined above. Ionic strength was maintained at 0.1 with potassium nitrate (BDH Aristar grade). All solutions were made up with 18 MΩ cm^{-1} water from a Millipore Milli-Q system. Temperature was maintained at 22.5 ± 0.1 °C. Metal ion solutions were prepared from Fisons Analar nitrate salts and standardized by EDTA titration according to established procedures.[44] Absorbance was monitored at a wavelength of 305 nm at which the uncomplexed ligand has a low absorbance compared with the complex.

Determination of Distribution Coefficients. Partition coefficients were determined using an automated system based on a modified filter probe device.[20] The system comprised an IBM compatible PC running the "TOPCAT" program,[45] which controlled both a Metrohm 665 Dosimat autoburette and a Pye-Unicam Lambda 5 UV/vis spectrophotometer, as well as performing all calculations of partition coefficients. All partition coefficient determinations were performed using AnalaR grade reagents under a nitrogen atmosphere in a sealed titration vessel at 25 °C. To ensure effective partition of the sample compound, continuous rapid stirring was employed, such that an emulsion of the two immiscible phases was formed. Use of a hydrophilic (Schleicher and Schueu 589/3) blauband filter paper on the filter probe ensured that none of the hydrophobic phase was measured, even with the small droplet sizes generated by the stirring. The ability to vary the volume of the two phases over a wide range (aqueous phase, 10–190 mL; nonaqueous phase, 0.1 μL–190 mL) enabled determination of partition coefficients in the range 10^{-5}–10^{5} to be determined, as evidenced by measurement of partition coefficients of a series of test compounds.[46] The two phases used in the determinations were MOPS buffer (50 mM, pH 7.4, prepared using Milli-Q water) and octan-1-ol, each of which was preequilibrated with the other phase before use. The solutions were gently purged with nitrogen. Upon commencement of the determination, absorbance measurements were automatically recorded at preselected time intervals, usually 1 s. When the absorbance readings had stabilized, as determined by the computer from equilibrium conditions selected by the operator (typically defined as an absorbance change of less than 0.002 absorbance units over a minimum of 100 individual readings), a suitable volume of octan-1-ol was added from the autoburette. Absorbance readings were subsequently recorded until the system had again reached equilibrium, at which point a further aliquot of octan-1-ol was added. This cycle was repeated for at least 10 additions of octan-1-ol. An estimate of the partition coefficient was obtained from each octan-1-ol addition, which enabled calculation of a mean partition coefficient value and standard deviation.

Table XI. Experimental Data and Final Refinement Results for 49, 49-HCl, and 58

	49	49-HCl	58
formula	$C_9H_{13}NO_2$	$C_9H_{13}NO_2\cdot HCl\cdot H_2O$	$C_{27}H_{36}FeN_3O_9\cdot 3H_2O$
formula wt	167.36	221.69	656.50
space group	$P2_1/n$	$P2_1/a$	$P\bar{3}$
a,Å	7.1025(6)	7.8933(7)	15.406(5)
b/Å	9.3441(9)	18.073(1)	
c/Å	13.495(1)	7.8424(4)	7.214(3)
β°	92.682(8)	98.588(4)	120.00
V/Å^3	894.7(4)	1106.2(7)	1482.6(9)
Z	4	4	2
D_c/g cm^3	1.25	1.34	1.48
radiatn	Cu K$\bar{\alpha}$	Cu K$\bar{\alpha}$	Mo K$\bar{\alpha}$
wavelength Å	1.541 78	1.541 78	0.710 73
T K	132(2)	132(2)	132(2)
$2\sigma max/\lambda$ = deg	150	150	53
total data	2119	2533	2029
obsd data	1480 ($I \geq 2(I)$)	1823 ($I \geq 2(I)$)	1332 ($I \geq 5(I)$)
R	0.046	0.039	0.068

X-ray Experimental. Compounds 49 and 49-Cl, and 58 were crystallized from ethanol/hexane, acetonitrile/cyclohexane, and dimethylformamide/heptane diffusion systems, respectively, at 4 °C. All data were taken on an Enraf-Nonius CAD4 diffractometer, using a $\omega - 2\omega$ scan technique. Lorentz-polarization corrections were applied. No absorption correction was made. Structures 49 and 49-HCl were solved by direct methods using SHELX86[47] and refined by full-matrix least-squares minimization of $\Sigma w\,(F_o - KF_c)^2$, where $w = 1/\sigma^2(F_o)$ using SHELX76.[48] In structure 58 the Fe atom was located on a special position on the 3-fold axis in space group $P\bar{3}$. The structure was refined with appropriate thermal parameter restraints for the Fe atom, using $w = 1/(\sigma^2(F_o) + 0.0005F_o^2)$. The terminal methyl group C(10) was found to be dynamically disordered even at 132 K. Three peaks were located bonded to the O(9) atom on the difference Fourier map and fixed through the refinement. The experimental data and final refinement results for 49, 49-HCl, and 58 are presented in Table XI. Full crystallographic details are available as supplementary material.

Biological Methods: Iron Removal from Proteins. Transferrin. Human transferrin (Sigma) was dissolved in MOPS buffer (0.05 M, pH 7.4, 25 °C) containing 25 mM $NaHCO_3$. Transferrin concentration was determined using an extinction coefficient of 2310 M^{-1} cm^{-1} per iron atom on the basis of a protein molecular mass of 81 000.[49] Solutions were monitored spectrophotometrically between 400–500 nm at 2-min intervals for the initial 10-min period and subsequently at 5-min intervals for periods up to 3 h.

Ferritin. Horse spleen ferritin (Boehringer) was incubated in HEPES (0.1 M, pH 7.2, 37 °C) with a range of chelators. One-mL samples were removed at given time intervals and immediately centrifuged through Amicon Centriflo ultrafiltration membrane cones to separate the hydroxypyridinone–Fe(III) complex from ferritin. The concentrations of Fe(III) complex were determined from ϵ_{max} values. Time courses of iron release was investigated for periods up to 36 h.

Iron Removal from Rat Hepatocytes. Primary rat hepatocyte monolayers were isolated, cultured, and pulsed with ^{59}Fe–transferrin.[16] Briefly, cells were plated at 1×10^6/dish and left for 4 h to adhere. Following washing, hepatocytes were pulsed for 17 h with human diferric ^{59}Fe–transferrin (100 μg/mL) before washing excess transferrin free with fresh medium. Cells were then incubated in triplicate with chelators at the concentrations shown, medium removed at 6 h, and the cells washed three times before being scraped from the plate with a rubber policeman and suspended in phosphate buffered saline. ^{59}Fe was measured in supernatant and expressed as a fraction of total cellular ^{59}Fe at time zero. Results are expressed as a percentage of ^{59}Fe release in control cells (medium without chelators added). Aliquots of supernatant were taken for measurement of LDH[16] and aliquots of cells for measurement of malonyl dialdehyde (MDA) and cellular DNA.[16] The MDA assay was adapted from previously described procedures using the thiobarbituric acid (TBA) assay method.[50] Standard curves were constructed using tetramethoxypropane (100–700 nM). One mL of standard or homogenized cells in phosphate-buffered saline were added to 1 mL of TBA solution (0.8%, pH 7.4) and incubated at 90 °C for 30 min. Cells were immediately cooled on ice and spun at 3000 rpm at 4 °C for 10 min. The red color was measured spectrophotometrically at 532 nm, corrected for cellular DNA content, and expressed as a percentage of the MDA present in control cells.

Iron Removal from Iron-Overloaded Mice. A modification of the mouse model developed by Huehns and co-workers was used.[51] The mice were overloaded with iron dextran given intraperitoneally at weekly intervals for 4 weeks. The iron stores were then radiolabeled with [^{59}Fe]lactoferrin. This treatment preferentially delivers iron to the liver.[52] Iron excretion was allowed to equilibrate for 3 weeks when a plateau was reached. At this stage the mice were used to measure the ^{59}Fe excretion induced by the test compounds given intraperitoneally. Both feces and urine were collected separately over defined time periods for a number of days, and the ^{59}Fe excretion was monitored. The excretion following the administration of each compound was expressed as a percentage of the counts excreted during the previous 24-h period.

Acknowledgment. This research was supported by the British Technology Group and NIH (Project Grants: GK42800 and GM21822).

Supplementary Material Available: Full elemental and spectral analyses of compounds 5–56 and tables of X-ray final atomic positional coordinates, atomic thermal parameters, bond distances, and bond angles of 49, 49-HCl, and 58 (19 pages). Ordering information is given on any current masthead page.

References

(1) Weatherall, D. J.; Clegg, J. B. *The Thalassaemia Syndromes*, 3rd ed.; Blackwell Scientific Publications: Oxford, 1981.

(2) Halliwell, B.; Gutteridge, J. M. C. Oxygen toxicity, oxygen radicals, transition metals and disease. *Biochem. J.* 1984, *219*, 1–4.

(3) Sephton-Smith, R. Iron excretion in thalassaemia major after administration of chelating agents. *Brit. Med. J.* 1962, *2*, 1577–1580.

(4) Modell, B.; Letsky, E. A.; Flynn, D. M.; Peto, R.; Weatherall, D. J. Survival and desferrioxamine in thalassaemia major. *Brit. Med. J.* 1982, *284*, 1081–1084.

(5) Porter, J. B.; Huehns, E. R.; Hider, R. C. The development of iron chelating drugs. In *Ballière's Clinical Haematology*; Hershko, C., Ed.; Bailliése Tindall: London, 1989; Vol. 2, pp 257–292.

(6) Rodgers, S. J.; Lee, Chi-Woo; Ng, C. Y.; Raymond, K. N. Ferric iron sequestering agents. 15. Synthesis, solution chemistry and electrochemistry of a new cationic analogue of enterobactin. *Inorg. Chem.* 1987, *26*, 1622–1625.

(7) Bergeron, R. J.; Wiegand, J.; McManis, J. S.; Perumal, P. T. Synthesis and biological evaluation of hydroxamate-based iron chelators. *J. Med. Chem.* 1991, *34*, 3182–3187.

(8) Martell, A. E.; Motekaitis, R. J.; Clarke, E. T.; Harrison, J. J. Synthesis of N,N′-di(2-hydroxybenzyl)ethylenediamine-N,N′-diacetic acid (HBED) derivatives. *Can. J. Chem.* 1986, *64*, 449–456.

(9) Hider, R. C. Siderophore mediated absorption of iron. *Struct. Bond.* 1984, *38*, 25–87.

(10) Hider, R. C.; Hall, A. D. Clinical useful chelators of tripositive elements. In *Progress in Medicinal Chemistry*; Ellis, G. P., West, G. B., eds.; Elsevier: New York, 1991; Vol. 28, pp 41–173.

(11) Summers, J. B.; Gunn, B. P.; Martin, J. G.; Mazdiyasni, H.; Stewart, A. O.; Young, P. R.; Goetze, A. M.; Bousko, J. B.; Dyer, R. D.; Brooks, D. W.; Carter, G. W. Orally active hydroxamic acid inhibitors of leukotriene biosynthesis. *J. Med. Chem.* 1988, *31*, 3–5.

(12) Hershko, C.; Link, G.; Pinson, A.; Avramovia-Grisaru, S.; Sarel, S.; Peter, H. H.; Hider, R. C.; Grady, R. W. New orally active iron chelators. *Ann. N. Y. Acad. Sci.* 1990, *612*, 351–360.

(13) (a) Hider, R. C.; Kontoghiorghes, G.; Silver, J.; Stockham, M. A. UK Patent 2117766, 1982. (b) Hider, R. C.; Kontoghiorghes, G.; Silver, J. UK Patent 2118176, 1983. (c) Hider, R. C.; Kontoghiorghes, G.; Silver, J. UK Patent 2136807, 1983. (d) Hider, R. C.; Kontoghiorghes, G.; Silver, J.; Stockham, M. A. UK Patent 2146989, 1984. (e) Hider, R. C.; Kontoghiorghes, G. K.; Silver, J.; Stockham, M. A. UK Patent 2146990, 1984. (f) Kontoghiorghes, G. K. Orally active α-ketohydroxypyridinone iron chelators: Studies in mice. *Mol. Pharmacol.* 1986, *30*, 670–673.

(14) Scarrow, R. C.; Riley, P. E.; Abu-Dari, K.; White, D. L.; Raymond, K. N. Ferric iron sequestering agents. 13. Synthesis structures and thermodynamics of complexation of Co(III) and Fe(III) tris complexes of several chelating hydroxypyridinones. *Inorg. Chem.* 1985, *24*, 952–967.

(15) Streater, M.; Taylor, P. D.; Hider, R. C.; Porter, J. B. Novel 3-hydroxy-2(1*H*)-pyridinones. Synthesis, iron(III)-chelating properties and biological activity. *J. Med. Chem.* 1990, *33*, 1749–1755.

(16) Porter, J. B.; Gyparaki, M.; Burke, L. C.; Huehns, E. R.; Sarpong, P.; Saez, V.; Hider, R. C. Iron metabolisation from hepatocyte monolayer cultures by chelators: the importance of membrane permeability and the iron binding constant. *Blood* 1988, *72*, 1497–1503.

(17) Hider, R. C.; Taylor, P. D.; Walkinshaw, M.; Wang, J. L.; van der Helm, D. Crystal structure of 3-hydroxy-1,2dimethylpyridin-4(1*H*)-one: An iron(III) chelation study. *J. Chem. Res., Synop.* 1990, 316–317.

(18) (a) Harris, R. L. N. Potential wool growth inhibitors. Improved synthesis of mimosine and related 4(1*H*)-pyridinones. *Aust. J. Chem.* 1976, *29*, 1329–1334. (b) Stünzi, H.; Perrin, D. D.; Teitei, T.; Harris, R. L. N. Stability constants of some metal complexes formed by mimosine and related compounds. *Aust. J. Chem.* 1979, *32*, 21–30. (c) Stünzi, H.; Harris, R. L. N.; Perrin, D. D.; Teitei, T. Stability constants for metal complexation by isomers of mimosine and related compounds. *Aust. J. Chem.* 1980, *33*, 2207–2220.

(19) Le Blanc, D. T.; Akers, H. A. Maltol and ethylmaltol. *Food Technol. (Chicago)* 1989, *43*, 78–84.

(20) Tomlinson, E. Filter probe extractor: A tool for the rapid determination of oil–water partition coefficients. *J. Pharm. Sci.* 1982, *71*, 602–604.

(21) Taylor, P. D.; Morrison, I. E. G.; Hider, R. C. Microcomputer application of non-linear regression analysis to metal-ligand equilibria. *Talanta* 1988, *35*, 507–512.

(22) Nelson, W. O.; Rettig, S. J.; Orvig, C. Aluminum and gallium complexes of 1-ethyl-3-hydroxy-2-methyl-4-pyridinone: A new exoclathrate matrix. *Inorg. Chem.* 1989, *28*, 3153–3157.

(23) Xiao, G.; van der Helm, D.; Hider, R. C.; Dobbin, P. S. Structure-stability relationships of 3-hydroxypyridin-4-one complexes. *J. Chem. Soc., Dalton Trans.* 1992, 3265–3271.

(24) Nelson, W. O.; Karpishin, T. B.; Rettig, S. J.; Orvig, C. Physical and structural studies of N-substituted-3-hydroxy-4(1*H*)-pyridinones. *Can. J. Chem.* 1988, *66*, 123–131.

(25) Xiao, G.; van der Helm, D.; Georlitz, F. H.; Hider, R. C.; Dobbin, P. S. The crystal structures of 1-(2′-methoxyethyl)-2-methyl-3-hydroxy-4-pyridinone, its hydrochloride and 1-ethyl-2-methyl-3-hydroxy-4-pyridinone hydrochloride hydrate. *Acta Crystallogr. C.*, in press.

(26) Nelson, W. O.; Karpishin, T. B.; Rettig, S. J.; Orvig, C. Aluminum and gallium compounds of 3-hydroxy-4-pyridinones. Synthesis characterisation and crystallography of biologically active complexes with unusual hydrogen bonding. *Inorg. Chem.* 1988, *27*, 1045–1051.

(27) Charalambous, J.; Dodd, A.; McP , M.; Matondo, S. O. C.; Pathirana, N. D.; Powell, H. R. Synthesis and x-ray crystal structure of tris(1,2-dimethyl-3-hydroxypyrid-4-onato)iron(III). *Polyhedron* 1988, *7*, 2235–2237.

(28) Simpson, L.; Rettig, S. J.; Trotter, J.; Orvig, C. 1-n-Propyl and 1-n-butyl-3-hydroxy-2-methyl-4-pyridinone complexes of group 13 (IIIA) metal ions. *Can. J. Chem.* 1991, *69*, 893–900.

(29) Brady, M. C.; Lilley, K. S.; Treffry, A.; Harrison, P. M.; Hider, R. C.; Taylor, P. D. Release of iron from ferritin molecules and their iron-cores by 3-hydroxypyridinone chelators *in vitro*. *J. Inorg. Biochem.* 1988, *35*, 9–22.

(30) Porter, J. B.; Gyparaki, M.; Huehns, E. R.; Hider, R. C. The relationship between lipophilicity of hydroxypyrid-4-one iron chelators and cellular iron metabolism using an hepatocyte culture model. *Biochem. Soc. Trans.* 1986, *14*, 1180.

(31) Porter, J. B.; Morgan, J.; Hoyes, K. P.; Burke, L. C.; Huehns, E. R.; Hider, R. C. Relative oral efficacy and acute toxicity of hydroxypyridin-4-one iron chelators in mice. *Blood* 1990, *76*, 2389–2396.

(32) Motekaitis, R. J.; Martell, A. E. Stabilities of the iron(III) chelators of 1,2-dimethyl-3-hydroxy-4-pyridinone and related ligands. *Inorg. Chim. Acta* 1991, *183*, 71–80.

(33) pM = log [Fe^{3+}] in the presence of [Fe^{3+}]$_{\text{total}}$ = 10^{-6} M and [ligand]$_{\text{total}}$ = 10^{-5} M at pH 7.4.

(34) Smith, R. M.; Martell, A. E. *Critical Stability Constants*; Plenum: New York, 1989; Vols. 1–6.

(35) Gerard, G.; Hugel, R. P. Iron(III) complexes of maltol including hydroxo-complexes, in an acidic medium. *J. Chem. Res., Synop.* 1980, 314.

(36) Bullen J. J.; Griffiths, E. *Iron and Infection*; Wiley: London, 1987.

(37) Stefanini, S.; Chiancone, E.; Cavallo, S.; Saez, V.; Hall, A. D.; Hider, R. C. The interaction of hydroxypyridinones with human serum transferrin and ovotransferrin. *J. Inorg. Biochem.* 1991, *44*, 27–37.

(38) Ford, G. C.; Harrison, P. M.; Rice, D. W.; Smith, J. M. A.; Treffry, A.; White, J. L.; Yariv, J. Ferritin: Design and formation of an iron-storage molecule. *Phil. Trans. Royal Soc. London B* 1984, *304*, 551–565.

(39) Gyparaki, M.; Hider, R. C.; Huehns, E. R.; Porter, J. B. Hydroxypyridinone iron chelators: *in vitro* and *in vivo* evaluation. *Thalassaemia Today* (Sirchia, G., Zanella, A., Eds.) Centro Transfusionale Ospedale Maggoire Polioclinico di Milano Editore, 1987, 521–526.

(40) Porter, J. B.; M. an, J.; Hoyes, K. P.; Burke, L. C.; Huehns, E. R.; Hider, R. C. Relative oral efficacy and acute toxicity of hydroxypyridin-4-one iron chelators in mice. *Blood* 1990, *76*, 2389–2396.

(41) Porter, J. B.; Weir, T. B.; Marshall, L.; Abeysinghe, R.; Round, J. M.; Brenton, D.; Huehns, E. R.; Epemolu, R. O.; Singh, S.; Dobbin, P. S.; Hider, R. C. Dose escalation and iron balance studies with the orally active hydroxypyridin-4-one iron chelator, CP94 in transfusionally iron overloaded humans. *Blood*, in press.

(42) Tondury, P.; Kontoghiorghes, G. J.; Ridolfi-Luthy, A.; Hirt, A.; Hoffbrand, A. V.; Lottenbach, A. M.; Sonderegger, T.; Wagner, H. P. L1 (1,2-dimethyl-3-hydroxypyrid-4-one) for oral iron chelation in patients with β-thalassaemia major. *Brit. J. Haematol.* 1990, *76*, 550–553.

(43) Brittenham, G. M. Development of iron-chelating agents for clinical use. *Blood* 1992, *80*, 569–575.

(44) Harris, W. R.; Carrano, C. J.; Cooper, S. R.; Sofen, S. R.; Avdeef, A. E.; McArdle, J. V.; Raymond, K. N. Co-coordination chemistry of microbial iron transport compounds. 19. Stability constants and electrochemical behaviour of ferric enterobactin and model complexes. *J. Am. Chem. Soc.* 1979, *101*, 6097–6104.

(45) Hall, A. D. TOPCAT Program for Determination of Distribution Coefficients, King's College, University of London, 1990.

(46) Sarpong, P. Ph.D. Thesis, University of London, 1992.

(47) Sheldrick, G. M. SHELX86. Programe for the Solution of Crystal Structures, University of Gottingen, Germany, 1986.

(48) Sheldrick, G. M. SHELX76. Program for the Solution of Crystal Structures, University of Cambridge, England, 1976.

(49) Aisen, P. In *Transferrin in Iron in Biochemistry and Medicine*; Jacobs, A., Worwood, M., Eds.; Academic Press: London, 1980; Vol. 2, 87–102.

(50) Stuart, M. J.; Scott, M.; Oski, F. A. A simple non-radioisotope technique for the determination of platelet life-span. *New Eng. J. Med.* 1975, *19*, 1310–1316.

(51) Gyparaki, M.; Porter, J. B.; Hirani, S.; Streater, M.; Hider, R. C.; Huehns, E. R. *In vivo* evaluation of hydroxypyridinone iron chelators in a mouse model. *Acta Haematol.* 1987, *78*, 217–221.

(52) Van Snick, J.; Mason, P. L.; Hermans, J. F. In *Proteins of Iron Storage and Transport in Biochemistry and Medicine*; North-Holland/Elsevier: Amsterdam, 1975; pp 433–438.

EXHIBIT I

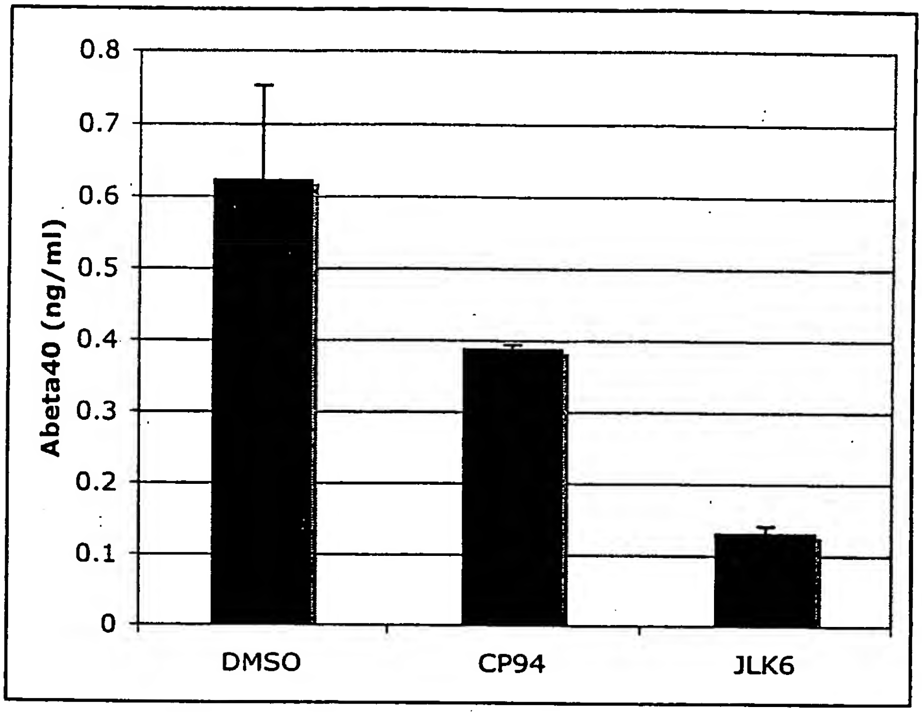

Figure 1

EXHIBIT J

PB	Structure
1076	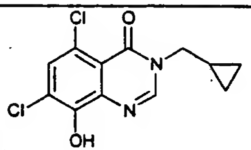
1084	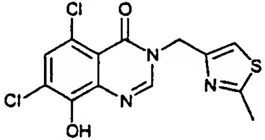
1085	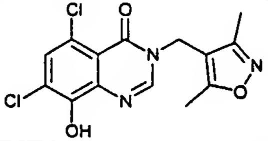
1089	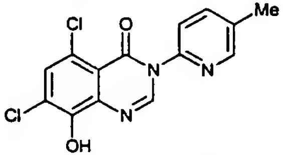
1090	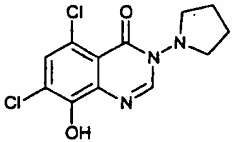
1091	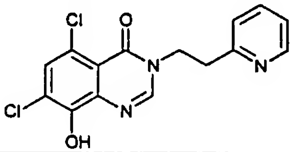

EXHIBIT K

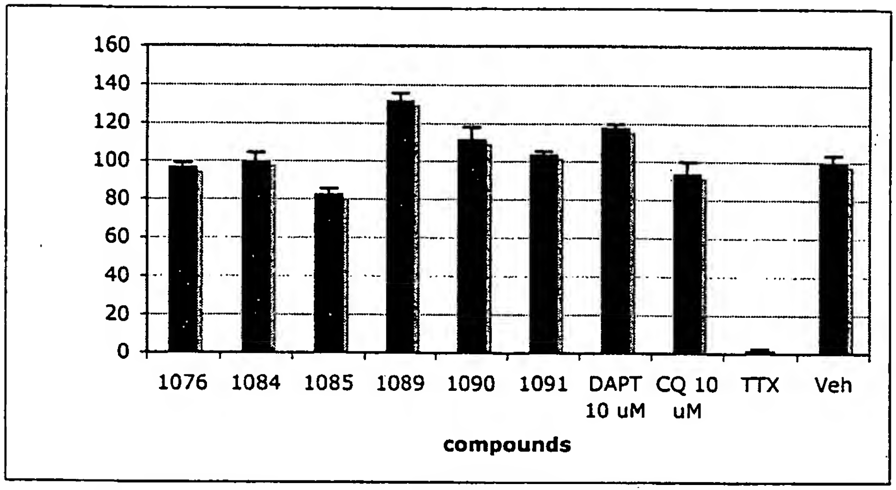

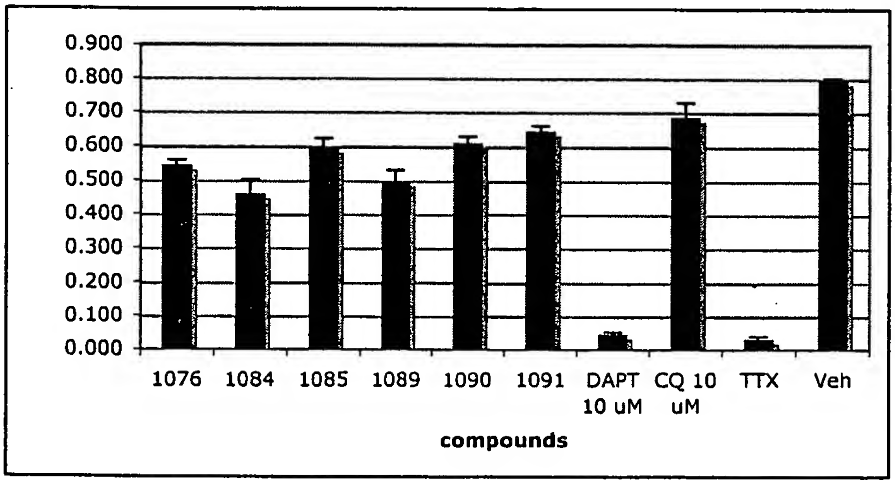

Figure 2

ORIGINAL CONTRIBUTION

Metal-Protein Attenuation With Iodochlorhydroxyquin (Clioquinol) Targeting Aβ Amyloid Deposition and Toxicity in Alzheimer Disease

A Pilot Phase 2 Clinical Trial

Craig W. Ritchie, MBChB, MRCPsych; Ashley I. Bush, MBBS, PhD, FRANZCP; Andrew Mackinnon, PhD; Steve Macfarlane, MBBS; Maree Mastwyk, BN; Lachlan MacGregor, MBBS; Lyn Kiers, MBBS, FRACP; Robert Cherny, PhD; Qiao-Xin Li, PhD; Amanda Tammer, PhD; Darryl Carrington, BSc; Christine Mavros, BSc; Irene Volitakis, BSc; Michel Xilinas, MD, DSc; David Ames, MD; Stephen Davis, MD, FRACP; Konrad Beyreuther, PhD; Rudolph E. Tanzi, PhD; Colin L. Masters, MD

Background: Alzheimer disease (AD) may be caused by the toxic accumulation of β-amyloid (Aβ).

Objective: To test this theory, we developed a clinical intervention using clioquinol, a metal-protein–attenuating compound (MPAC) that inhibits zinc and copper ions from binding to Aβ, thereby promoting Aβ dissolution and diminishing its toxic properties.

Methods: A pilot phase 2 clinical trial in patients with moderately severe Alzheimer disease.

Results: Thirty-six subjects were randomized. The effect of treatment was significant in the more severely affected group (baseline cognitive subscale score of the Alzheimer's Disease Assessment Scale, ≥25), due to a substantial worsening of scores in those taking placebo compared with minimal deterioration for the clioquinol group. Plasma $A\beta_{42}$ levels declined in the clioquinol group and increased in the placebo group. Plasma zinc levels rose in the clioquinol-treated group. The drug was well tolerated.

Conclusion: Subject to the usual caveats inherent in studies with small sample size, this pilot phase 2 study supports further investigation of this novel treatment strategy using a metal-protein–attenuating compound.

Arch Neurol. 2003;60:1685-1691

Author affiliations and statements of financial disclosure are listed at the end of the article.

ALZHEIMER DISEASE (AD) may result from the cortical accumulation of β-amyloid (Aβ). Several strategies to inhibit Aβ production and/or accumulation have been explored in experimental models of AD and are now being translated into double-blinded clinical trials.[1,2] We have developed a strategy of targeting Aβ through metal-protein–attenuating compounds (MPAC), which promote the solubilization (and clearance) of Aβ and inhibit redox-active copper ion (Cu^{2+})–Aβ interactions that generate neurotoxic hydrogen peroxide.[3,4] One such MPAC lead compound, iodochlorhydroxyquin (an anti-infective agent also known as clioquinol) induces a rapid decrease in brain Aβ deposition in a mouse model of AD.[5] Clioquinol also inhibits Aβ toxicity in neuronal cell cultures,[6] possibly acting through an additional mechanism of preventing Aβ-lipid interactions.[7]

CME course available at www.archneurol.com

For editorial comment see page 1678

Clioquinol was withdrawn for oral use in 1970 because of its association with subacute myelo-optic neuropathy, possibly caused by vitamin B_{12} deficiency.[5,8] We believed the drug should be reevaluated,[9] and therefore prepared a double-blind phase 2 clinical trial. We chose a dose escalation schedule to maximize the chance of detecting a cognitive or biochemical effect while minimizing the risk for adverse effects. The study was powered to detect only conspicuous effects on cognition. The starting dosage of 3.3 mg/kg per day was within the same order of magnitude of the effective dosage in the mouse model.

©2003 American Medical Association. All rights reserved.

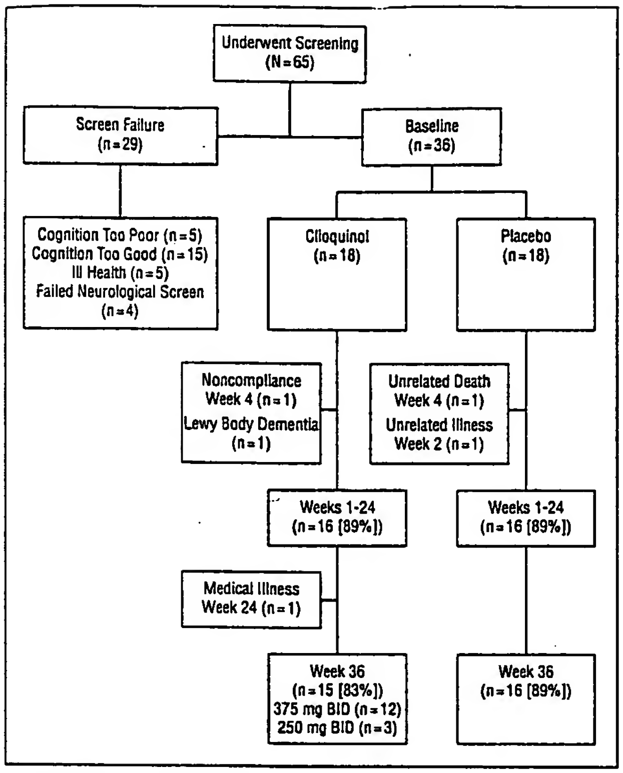
Underwent Screening (N=65)
Screen Failure (n=29)
Baseline (n=36)
Cognition Too Poor (n=5)
Cognition Too Good (n=15)
Ill Health (n=5)
Failed Neurological Screen (n=4)
Clioquinol (n=18)
Placebo (n=18)
Noncompliance Week 4 (n=1)
Lewy Body Dementia (n=1)
Unrelated Death Week 4 (n=1)
Unrelated Illness Week 2 (n=1)
Weeks 1-24 (n=16 [89%])
Weeks 1-24 (n=16 [89%])
Medical Illness Week 24 (n=1)
Week 36 (n=15 [83%]) 375 mg BID (n=12) 250 mg BID (n=3)
Week 36 (n=16 [89%])

Figure 1. Outline of the flowchart of subjects studied. BID indicates twice daily.

Herein we report the results demonstrating the efficacy of clioquinol treatment in producing effects on plasma $A\beta$ and zinc ion (Zn^{2+}) levels. In addition, the drug was well tolerated and inhibited cognitive decline in patients who, untreated, otherwise experienced deterioration.

METHODS

STUDY POPULATION

Criteria for participation in the study included informed consent (Consent to Special Procedures administered by the Victorian Civil and Administrative Tribunal, Melbourne, Victoria, and third-party consent); a diagnosis of probable AD by means of criteria of the National Institute of Neurological and Communicative Disorders and Stroke and the Alzheimer's Disease and Related Disorders Association; a cognitive subscale score on the Alzheimer's Disease Assessment Scale (ADAS-cog score) of 20 to 45; a Mini-Mental State Examination score of 10 to 24; and receipt of a 5- to 10-mg dose of donepezil for at least 6 months.

STUDY DESIGN

The study was a double-blind, placebo-controlled, parallel-group randomized design. Thirty-six patients and their caregivers were recruited. The duration of the study was 36 weeks. The oral dosage of clioquinol was 125 mg twice daily from weeks 0 to 12, 250 mg twice daily from weeks 13 to 24, and 375 mg twice daily from weeks 25 to 36.

STUDY PROCEDURES

Screening procedures consisted of a medical history, physical examination, psychometric tests, nerve conduction tests, and visual evoked responses. Blood was collected for apolipoprotein E allotyping and assays of metals and $A\beta$. All patients continued to receive donepezil and received intramuscular cyanocobalamin (vitamin B_{12}), 100 µg, every 4 weeks.

OUTCOME MEASURES

The primary efficacy variable was change from the baseline score on the ADAS-cog at weeks 4, 12, 24, and 36. Plasma $A\beta$, zinc, and copper levels were all measured every 4 weeks.

DOUBLE-ANTIBODY CAPTURE ENZYME-LINKED IMMUNOSORBENT ASSAY FOR $A\beta$ DETECTION

Plates were coated with monoclonal antibody (mAb) G210 (for $A\beta_{40}$) or mAb G211 (for $A\beta_{42}$) and washed, and biotinylated mAb WO2 was added. Bound antibody was detected with streptavidin-labeled Europium (PerkinElmer, Inc, Melbourne, Victoria).

THERAPEUTIC DRUG MONITORING

At weeks 12, 24, and 36, clioquinol blood levels were assayed by means of high-performance liquid chromatography at the Centre for Pharmaceutical Research, University of South Australia, Adelaide.

SAFETY MEASURES

Standard adverse event reporting was conducted. Visual evoked responses and results of nerve conduction studies and a full ophthalmic examination were obtained at screening, at week 16, and before the final trial visit.

DATA ANALYSIS

Data management was undertaken by independent contractors (Kendle International Inc, Oakleigh, Melbourne, Victoria). Evidence of efficacy was indicated by a significant difference in change from baseline between treatment arms. Analysis of variance was the principal method of evaluating statistical significance. Differences between groups on categorical measures were analysed using exact statistical methods. The baseline illness severity factor was created, as planned, by division of the sample into 2 groups at the median ADAS-cog score at baseline, yielding less severely and more severely affected groups (n=8 and n=8, respectively, in the clioquinol treatment arm; and n=7 and n=9, respectively, in the placebo arm).

RESULTS

SUBJECT RECRUITMENT AND DEMOGRAPHICS

Thirty-six subjects were recruited, and 32 had sufficient data for per protocol analysis (**Figure 1**). The groups did not differ across relevant demographic, biological, and clinical variables at baseline (**Table 1**), other than the treatment arm having a higher mean premorbid IQ than the placebo group as estimated using the National Adult Reading Test (111.4 vs 104.9; $t_{30}=2.27$; $P=.03$) and a lower level of thyrotropin (1.14 vs 2.00 mIU/L; $t_{30}=4.40$; $P<.001$). The National Adult Reading Test IQ and thyrotropin level were subsequently provisionally entered into analyses as covariates, but were found to be not significant in any analysis.

©2003 American Medical Association. All rights reserved.

Ideally, any drug targeting the Aβ pathway should have the following 2 principal effects: a disease-modifying effect as assessed by cognitive variables and a biological response assessed by measurement of Aβ levels in the blood, the cerebrospinal fluid, or the brain.

Changes in the ADAS-cog score at weeks 4, 12, 24, and 36 from baseline were subject to 2-way analysis of variance with factors of treatment arm and baseline illness severity. As planned in the protocol, the effect of severity of illness was examined by stratification of the sample into subjects less or more severely affected than the median score of the baseline ADAS-cog (<25 and ≥25). At baseline, there were no significant or near-significant differences between the main effect of the treatment arm ($F_{1,28}$=0.21; P=.65). Similarly, there were no significant differences between treatment arms at either level of severity. The main effect of the treatment arm was not significant at any week, although trends toward significance were noted at weeks 4 ($F_{1,28}$=3.55; P=.07) and 24 ($F_{1,28}$=3.31; P=.08) (**Figure 2**A). Simple effects tests within the level of severity showed the main effect to be separable into nonsignificant results for the less-severe stratum on all weeks and significant differences in the more-severe stratum at weeks 4 ($F_{1,28}$=7.73; P=.01) and 24 ($F_{1,28}$=6.63; P=.02) (Figure 2B). This trend was maintained at week 36 but narrowly escaped statistical significance ($F_{1,28}$=3.62; P=.07). The difference in mean change from baseline ADAS-cog score in the clioquinol arm compared with the placebo arm at weeks 24 and 36 was a difference of 7.37 (95% confidence interval, 1.51-13.24) and 6.36 (95% confidence interval, −0.50 to 13.23), respectively.

The Mini-Mental State Examination, a less sensitive measure of cognitive impairment, showed a similar pattern without reaching significance. By contrast, the noncognitive score on the ADAS and the Clinician Interview-Based Impression of Change did not show any clear differences or trends. Results of apolipoprotein E genotyping did not disclose any effect other than an overrepresentation of the ϵ4 allotype in both groups.

Table 1. Baseline Demographics and Key Clinical Variables

Variable	Total Sample (N = 32)	Clioquinol Group (n = 16)	Placebo Group (n = 16)	*P* Value
Age, y				
Mean (SD)	72.50 (8.37)	73.19 (8.61)	71.81 (8.35)	.65*
Range	56-87	58-87	56-87	
Sex, No. (%) male	17 (53.1)	8 (50.0)	9 (56.3)	>.99†
ApoE status, No. (%)				
ApoE4 heterozygote	15 (46.9)	7 (43.8)	8 (50.0)	>.99†
ApoE4 homozygote	3 (9.4)	2 (12.5)	1 (6.3)	
Estimated premorbid NART IQ				
Mean (SD)	108.1 (8.86)	111.4 (8.04)	104.9 (8.26)	.03*
Range	91-124	94-121	91-124	
ADAS-cog score				
Mean (SD)	26.31 (7.27)	25.56 (7.67)	27.06 (7.01)	.57*
Range	15-46	15-46	19-41	
Age at first diagnosis, y				
Mean (SD)	70.09 (7.98)	70.88 (8.50)	69.31 (7.61)	.59*
Range	54-83	57-83	54-83	
Duration of illness, y				
Mean (SD)	2.41 (1.19)	2.31 (1.08)	2.56 (1.32)	.66*
Range	1-5	1-4	1-5	

Abbreviations: ADAS-cog, cognitive score on the Alzheimer's Disease Assessment Scale; ApoE, apolipoprotein E; NART, National Adult Reading Test.

*Calculated by means of an independent-sample *t* test (*df*, 30).

†Calculated by means of an exact 2-tailed test.

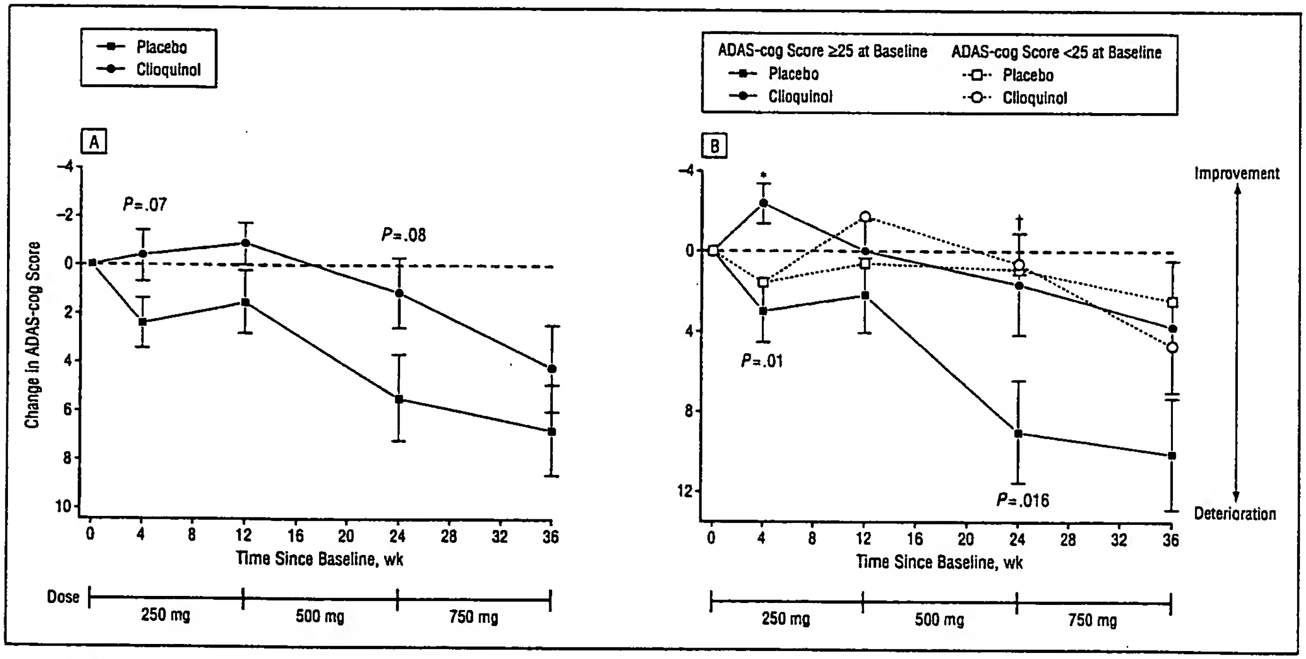

Figure 2. Mean±SE change from baseline in cognitive abilities (as assessed with the cognitive score of the Alzheimer's Disease Assessment Scale [ADAS-cog]) in the clioquinol vs placebo arms (A) and stratification by severity within the treatment arms (less severely affected, ADAS-cog score of <25; more severely affected, ADAS-cog score of ≥25) (B). Asterisk indicates P=.01; dagger, P=.02.

©2003 American Medical Association. All rights reserved.

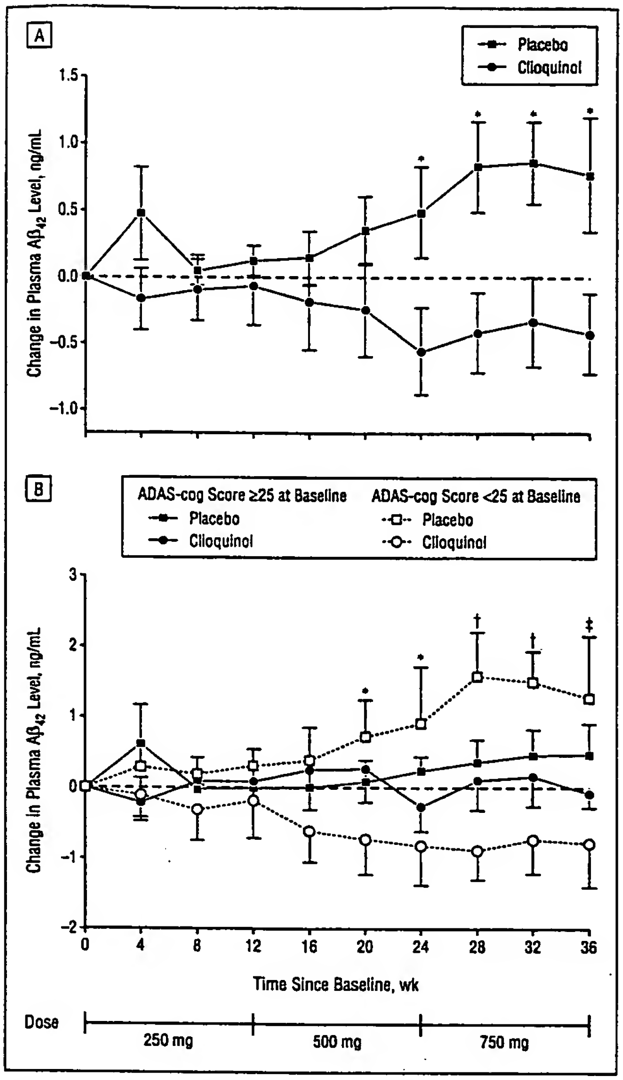

Figure 3. Mean±SE change from baseline in plasma β-amyloid$_{42}$ [Aβ$_{42}$] levels in the clioquinol vs placebo arms (A) and stratification by severity within the treatment arms (less severely affected, the cognitive score of the Alzheimer's Disease Assessment Scale [ADAS-cog score] of <25; more severely affected, ADAS-cog score of ≥25) (B). Asterisk indicates $P \leq .05$; dagger, $P \leq .001$; and double dagger, $P \leq .01$.

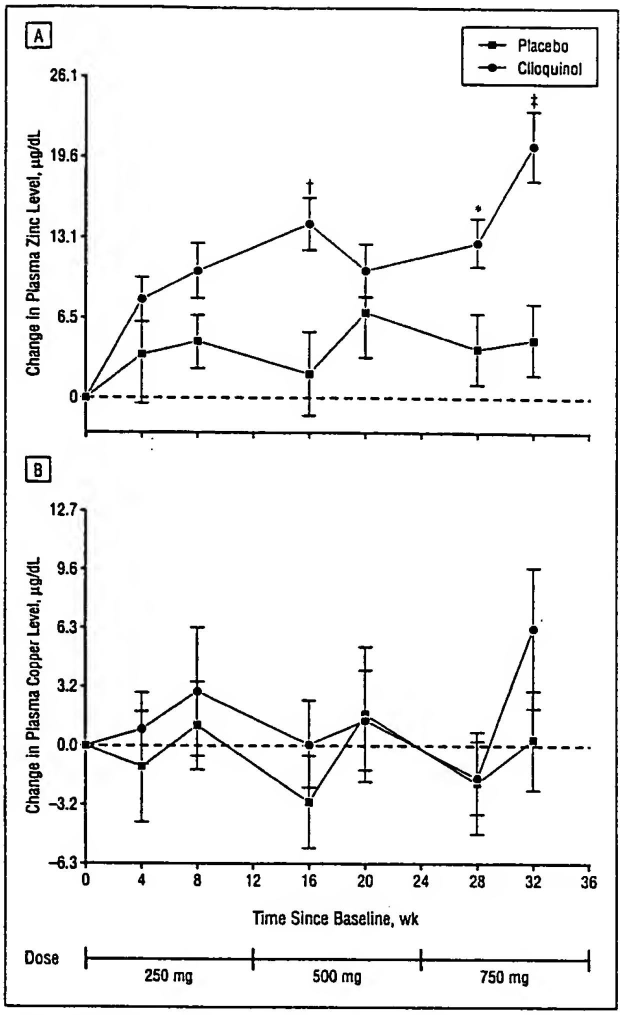

Figure 4. Mean±SE change from baseline in plasma zinc (A) and plasma copper (B) levels in the 2 arms of clioquinol vs placebo. Asterisk indicates $P \leq .05$; dagger, $P \leq .01$; and double dagger, $P \leq .001$. To convert copper levels to micromoles per liter, multiply by 0.157; zinc to micromoles per liter, multiply by 0.153.

There were no significant differences in baseline plasma Aβ$_{42}$ levels between treatment arms or severity strata. The plasma Aβ$_{42}$ level declined significantly from baseline in the clioquinol-treated group from week 20 onward; during the same time, the plasma Aβ$_{42}$ level in the placebo group increased (**Figure 3**A). Stratification by illness severity demonstrated that changes were evident only in the less severely affected group (Figure 3B). The wide variance in individual levels at baseline in plasma Aβ$_{40/42}$ led to reduced power of the study to detect any significant differences in mean changes between groups.

Analysis of plasma Aβ$_{40}$ levels showed overall similar trends, with significant differences between placebo and clioquinol groups observed at weeks 8, 32, and 36 in the less severely affected groups. For individuals, there was a highly significant ($P<.001$) correlation between Aβ$_{42}$ and Aβ$_{40}$ levels.

EFFECT ON PLASMA ZINC AND COPPER LEVELS

Administration of clioquinol was associated with a significant elevation of total plasma zinc level (**Figure 4**A) but with no effect on plasma copper level (Figure 4B). Samples collected with an indwelling catheter at weeks 12, 24, and 36 were found to be unreliable for technical reasons and were therefore omitted from this analysis. Mean absolute levels of zinc (61 µg/dL [9.4 µmol/L]) in all groups at baseline were below age-related normative values. Mean absolute levels of copper (83 µg/dL [13.1 µmol/L]) were within the age-related normative range. Correlation of plasma Aβ$_{42/40}$ levels with zinc and copper levels assayed on the same or on subsequent occasions showed no significant associations.

BLOOD LEVELS OF CLIOQUINOL

Mean±SD steady-state predose levels of clioquinol at total daily dosages of 250, 500, and 750 mg were 4.03±2.10, 6.74±3.70, and 7.60±2.15 µg/mL, respectively.

©2003 American Medical Association. All rights reserved.

Table 2. Attributable Adverse Events With a Risk of Greater Than 10% in Either Arm or Where Point Estimate Risk Ratio Is Greater Than 2.0 or Less Than 0.5*

	Clioquinol Treatment Group (n = 16)	Placebo Group (n = 16)	RR (95% CI)
Cardiovascular			
Postural hypotension	12	11	1.09 (0.67-1.79)
Postural tachycardia	12	8	1.33 (0.74-2.40)
Postural dizziness	7	3	2.33 (0.71-7.63)
Subjects with ≥1 postural symptom	13	14	0.93 (0.64-1.36)
Neurological			
Impaired nerve conduction	3	1	3.0 (0.34-26.2)
Impaired reflexes	1	2	0.5 (0.05-5.04)
Numb legs	2	0	
Subjects with ≥1 symptom	6	4	1.5 (0.51-4.43)
Gastrointestinal tract			
Diarrhea	1	4	0.25 (0.03-2.02)
Constipation	2	0	
Nausea	2	0	
Abdominal pain	2	1	2.0 (0.2-20.1)
Subjects with ≥1 symptom	5	4	1.25 (0.4-3.91)
Renal			
Microalbuminuria	5	5	1.00 (0.35-2.87)
Hematological			
Lymphopenia	0	3	
Liver function tests			
Raised γGT level	2	1	2.0 (0.2-20.1)
Raised bilirubin level	2	0	
Subjects with ≥1 abnormal result	4	1	4.0 (0.49-32.4)
Other			
Decreased vitamin B_{12} level	0	2	
Mean (SD) No. of discrete adverse events per subject	3.38 (2.14)	2.78 (1.48)	0.611 (−0.64 to 1.89)†

Abbreviations: CI, confidence interval; γGT, γ-glutamyltransferase; RR, relative risk.
*Unless otherwise indicated, data are expressed as number of subjects.
†Expressed as mean difference (95% CI) ($P = .33$).

SAFETY RESULTS AND ANALYSIS

Safety analysis was conducted on all data irrespective of the stage reached in the trial. There were a total of 123 attributable adverse events reported, 64 in the treatment group and 59 in the placebo group. Of the attributable adverse events with a risk of greater than 10% or where the point estimate risk ratio was greater than 2.0 or less than 0.5, the mean number of discrete events per subject was not significantly different between arms (**Table 2**). Serious adverse events developed in 5 subjects. Impaired visual acuity and color vision (in the absence of other neurological signs or symptoms) developed in a 66-year-old woman with hypertension, hyperlipidemia, and a history of glaucoma and visual migraine during weeks 31 to 36 of the trial, while she was receiving clioquinol, 375 mg twice daily. This event was considered to be possibly attributable to clioquinol, and her symptoms resolved on treatment cessation. The following 4 nonattributable serious adverse events were recorded: 1 death due to intracranial hemorrhage (placebo group) and 3 hospitalizations for hip pain (placebo group), syncope due to impaired cardiac function (clioquinol group), and confusion (placebo group).

COMMENT

The findings support a proof of concept in humans that a drug targeting metal-Aβ interactions can have a significant effect on Aβ metabolism and, through this, a beneficial modification on the progression of AD. The clinical benefit of clioquinol in this study population was only seen in the more severely affected subjects, probably due to the low power of the study and the nonlinear sensitivity of the ADAS-cog instrument to detect relatively slight cognitive differences in the less severely affected groups (**Figure 5**). The separation of 3 ADAS-cog points achieved after 24 weeks of treatment with the acetylcholinesterase inhibitor, donepezil, required a study population of more than 300 subjects.[10] The significant benefit seen in the more severely affected treatment group at 4 weeks is also of interest, as this may represent the short-term effect of clioquinol neutralizing the neurotoxicity of the soluble pool of Aβ.[11]

The data showing a significant lowering of plasma $A\beta_{42}$ levels are more compelling (Figure 3). The relationship between plasma Aβ level and ADAS-cog scores has not yet been determined, but is probably nonlinear

©2003 American Medical Association. All rights reserved.

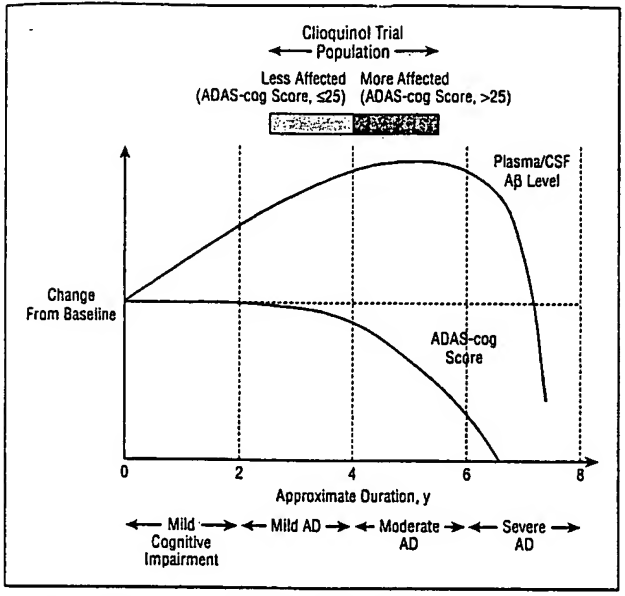

Figure 5. Relative changes in behavioral (the cognitive score of the Alzheimer's Disease Assessment Scale [ADAS-cog score]) and biochemical (plasma/cerebrospinal fluid [CSF] β-amyloid [Aβ]) levels during the course of Alzheimer disease (AD). This diagrammatic representation divides the natural history of AD into 4 major phases of equal duration and indicates how the nonlinear disparities between behavioral and biochemical indices might arise. In mild cognitive impairment and mild AD phases, the behavioral variables show little change, whereas it is suspected that levels of plasma/CSF Aβ may increase. In the middle (moderate) phases of illness, the behavioral measures decline rapidly, whereas the biochemical changes plateau. In the severe end stages of illness, the behavioral measures reach a floor, and the plasma/CSF Aβ levels are in sharp decline as the brain acts as an amyloid sink. The population in the present study is drawn from the less and more severely affected subgroups of the subjects with mild/moderate AD, among whom disparate trends in behavioral and biochemical measures were observed.

(Figure 5). Previous cross-sectional assays of blood Aβ levels have been complicated by large interindividual variations. However, plasma Aβ levels may still reflect brain Aβ load. One longitudinal study of preclinical AD disclosed higher plasma $A\beta_{42}$ levels.[12] A 12-week double-blind trial of lovastatin showed a 37% increase in the serum Aβ level for the placebo group, and a dose-related decrease of up to 24% for the drug-treated group.[13] The findings of the present longitudinal study are consistent with these observations, as they disclose a progressive increase in plasma $A\beta_{42}$ level in placebo-treated subjects, principally in the less severely affected group. Evidence of a biochemical relationship between plasma and brain Aβ pools in transgenic models for AD also help to interpret our current results.[14]

Although there were highly significant changes in the plasma of the less severely affected patients, the separation between treatment arms in the more severely affected patients did not reach statistical significance (Figure 3). An explanation for this may be linked to the exponential accumulation of brain Aβ level in advanced AD, associated with a marked fall in cerebrospinal fluid Aβ levels (Figure 5). We observed a trend over time toward lower mean levels in the more severely affected group (data not shown), which is consistent with the large body of data on cerebrospinal fluid Aβ levels that shows an elevation early in the disease, followed by a progressive fall as the disease evolves.[15]

An important result of clioquinol treatment of subjects with AD is the elevation in plasma zinc levels (Figure 4A). Experimental studies[7] of clioquinol on the mouse brain showed similar increases of zinc level of 13% and copper level of 19%. This finding also indicates that, in contrast to a typical metal chelator such as desferrioxamine, the MPAC drugs (of which clioquinol is but one example) are not gross tissue chelators. The affinity of clioquinol for copper and zinc ions is relatively modest (approximately nanomolar) and is likely to be facilitating their dissociation from the lowest-affinity metal binding sites on Aβ.

The measured basal levels of plasma clioquinol in the current study ranged from 13 to 25 µmol/L (4-8 µg/mL). After allowing for a large proportion of clioquinol being bound to protein, the available active compound in the brain should be 100 to 200 nmol/L. The concentration of total Aβ in the brain with AD varies considerably, but is estimated to range from the high nanomolar to the low micromolar range, of which less than 1% is available as a toxic soluble species.[11] Actual measurements of extracellular brain clioquinol levels will be required, together with plasma pharmacokinetics, before a more rational approach to dosing can be applied.

Safety issues are of concern in a study involving the chronic administration of a drug with a history of adverse events. We balanced the risks of treating a malignant disease such as AD against the relatively low risk for development of subacute myelo-optic neuropathy by careful monitoring and by ensuring complete normality of vitamin B_{12} and folate metabolism. Clioquinol-associated optic neuropathy was suspected in 1 subject with a prominent history of eye disease, but a direct causal link to clioquinol remains uncertain, given that disturbances of color vision and other ophthalmologic changes occur during the natural history of AD.[16] Twenty-seven subjects agreed to participate in an open-label extension study of clioquinol. Ten subjects have now been receiving this drug at a dosage of 500 to 750 mg/d for more than 18 months. No clioquinol-attributable adverse events have developed in any of these subjects.

CONCLUSIONS

The safety profile and biochemical efficacy of clioquinol in this population are sufficiently encouraging to allow for future trials to take this investigation of a novel therapeutic intervention (clioquinol itself or a pharmacologically improved backup) targeting Aβ amyloid to the next phase. This class of MPAC may also be considered for related conditions such as Parkinson disease,[17] in which α-synuclein and iron could interact in a manner analogous to Aβ and zinc and copper ions.

Accepted for publication August 7, 2003.

From the Departments of Pathology (Drs Ritchie, Bush, Macfarlane, Cherny, Li, Tammer, and Masters; Mss Mastwyk, Mavros, and Volitakis; and Mr Carrington), Medicine (Drs MacGregor, Kiers, and Davis), and Psychiatry (Dr Ames), The University of Melbourne, The Mental Health Research Institute of Victoria, Parkville, Victoria (Drs Ritchie, Bush, Mackinnon, Macfarlane, Cherny, Li, Tammer, and Masters; Mss Mastwyk, Mavros, and Volitakis; and Mr Carrington);

©2003 American Medical Association. All rights reserved.

the Department of Psychiatry and Behavioural Science, Royal Free Campus, University College London, London, England (Dr Ritchie); the Department of Psychological Medicine, Monash University, Clayton, Victoria (Dr Mackinnon); the Department of Neurology, Royal Melbourne Hospital, Parkville, Victoria (Drs MacGregor, Kiers, and Davis); the Institute of Clinical Neuroscience, Göteborg University, Göteborg, Sweden (Dr Xilinas); the Center for Molecular Biology, University of Heidelberg, Heidelberg, Germany (Dr Beyreuther); and the Genetics and Aging Research Unit, Massachusetts General Hospital, Boston (Drs Bush and Tanzi). *Dr Ritchie has been paid for his time and effort in analyzing the results from the trial sponsor, Prana Biotechnology. Drs Bush and Tanzi are paid consultants, are on the Scientific Advisory Committee, and are stockholders of Prana Biotechnology and had no input into the drafting or review of any portion of the manuscript other than those portions pertaining to study concept and design and consultation on biochemistry and no input into the analysis of the data from the other portions. Drs Macfarlane and MacGregor and Ms Mastwyk were employed by the Mental Health Research Institute through funds provided by Prana Biotechnology. Dr Cherny is a stockholder in Prana Biotechnology. Dr Xilinas has financial and intellectual interests in the development of clioquinol. Dr Beyreuther is on the Scientific Advisory Committee of Prana Biotechnology. Dr Masters is a director of Prana Biotechnology, chairperson of its Scientific Advisory Committee, and a stockholder.*

Author contributions: *Study concept and design* (Drs Ritchie, Bush, Mackinnon, Xilinas, Ames, Davis, Tanzi, and Masters and Ms Mastwyk); *acquisition of data* (Drs Macfarlane, MacGregor, Kiers, Li, Tammer, Ames, and Masters; Mss Mastwyk, Mavros, and Volitakis; and Mr Carrington); *analysis and interpretation of data* (Drs Ritchie, Mackinnon, Macfarlane, MacGregor, Kiers, Cherny, Xilinas, Ames, Beyreuther, and Masters); *drafting of the manuscript* (Drs Ritchie, Mackinnon, Tammer, and Masters and Ms Mastwyk); *critical revision of the manuscript for important intellectual content* (Drs Ritchie, Bush, Mackinnon, Macfarlane, MacGregor, Kiers, Cherny, Li, Xilinas, Ames, Davis, Beyreuther, Tanzi, and Masters; Mss Mastwyk, Mavros, and Volitakis; and Mr Carrington); *statistical expertise* (Drs Ritchie, Mackinnon, and Davis); *obtained funding* (Drs Bush and Masters); *administrative, technical, and material support* (Drs Ritchie, Bush, Macfarlane, MacGregor, Cherny, Li, Tammer, Ames, Beyreuther, and Masters; Mss Mastwyk, Mavros, and Volitakis; and Mr Carrington); *study supervision* (Drs Ritchie, Bush, Macfarlane, Kiers, Cherny, Li, Ames, and Masters); *consultation on biochemistry* (Drs Bush, Beyreuther, and Tanzi).

This study was supported in part by grants from the National Health and Medical Research Council of Australia (Canberra, Australian Capital Territory), Alzheimer Association (Chicago, Ill), Prana Biotechnology (Melbourne, Victoria), and the Baxter Trust (Sydney, New South Wales).

We thank the volunteer subjects and their caregivers who participated in this study; the Safety Committee (E. Chiu, FRANZCP, S. Collins, FRACP, M. Hopwood, FRACP, D. LoGiudice, FRACP, and J. Merory, FRACP); R. Shafiq-Antonacci for performing the Clinician Interview-Based Impression of Change; and K. Barnham, PhD, D. Darby, FRACP, P. Desmond, FRACP, K. Taubman, FRACP, and F. Fraser for technical advice.

Corresponding author and reprints: Colin L. Masters, MD, Department of Pathology, The University of Melbourne, Parkville, Victoria, Australia 3010 (e-mail: c.masters@unimelb.edu.au).

REFERENCES

1. Simons M, Schwärzler F, Lütjohann D, et al. Treatment with simvastatin in normocholesterolemic patients with Alzheimer's disease: a 26-week randomised, placebo-controlled, double-blind trial. *Ann Neurol.* 2002;52:346-350.
2. Hock C, Konietzko U, Streffer JR, et al. Antibodies against β-amyloid slow cognitive decline in Alzheimer's disease. *Neuron.* 2003;38:547-554.
3. Opazo C, Huang X, Cherny R, et al. Metalloenzyme-like activity of Alzheimer's disease β-amyloid: Cu-dependent catalytic conversion of dopamine, cholesterol and biological reducing agents to neurotoxic H2O2. *J Biol Chem.* 2002;277:40302-40308.
4. Cherny RA, Legg JT, McLean CA, et al. Aqueous dissolution of Alzheimer's disease Aβ amyloid deposits by biometal depletion. *J Biol Chem.* 1999;274:23223-23228.
5. Cherny RA, Atwood CS, Xilinas ME, et al. Treatment with a copper-zinc chelator markedly and rapidly inhibits β-amyloid accumulation in Alzheimer's disease transgenic mice. *Neuron.* 2001;30:665-676.
6. Barnham KJ, Ciccotosto GD, Tickler AK, et al. Neurotoxic, redox-competent Alzheimer's β-amyloid is released from lipid membrane by methionine oxidation. *J Biol Chem.* In press.
7. Abramov AY, Canevari L, Duchen MR. Changes in intracellular calcium and glutathione in astrocytes as the primary mechanism of amyloid neurotoxicity. *J Neurosci.* 2003;23:5088-5095.
8. Yassin MS, Ekblom J, Xilinas M, Gottfries CG, Oreland L. Changes in uptake of vitamin B12 and trace metals in brains of mice treated with clioquinol. *J Neurol Sci.* 2000;173:40-44.
9. Regland B, Lehmann W, Abedini I, et al. Treatment of Alzheimer's disease with clioquinol. *Dement Geriatr Cogn Disord.* 2001;12:408-414.
10. Rogers SL, Farlow MR, Doody RS, Mohs R, Friedhoff LT, Donepezil Study Group. A 24-week, double-blind, placebo-controlled trial of donepezil in patients with Alzheimer's disease. *Neurology.* 1998;50:136-145.
11. McLean C, Cherny R, Fraser F, et al. Soluble pool of Aβ amyloid as a determinant of severity of neurodegeneration in Alzheimer's disease. *Ann Neurol.* 1999;46:860-866.
12. Mayeux R, Tang MX, Jacobs DM, et al. Plasma amyloid β-peptide 1-42 and incipient Alzheimer's disease. *Ann Neurol.* 1999;46:412-416.
13. Buxbaum JD, Cullen EI, Freidhoff LT. Pharmacological concentrations of the HMG-CoA reductase inhibitor lovastatin decrease the formation of the Alzheimer β-amyloid peptide in vitro and in patients. *Front Biosci.* 2002;7:a50-a59.
14. DeMattos RB, Bales KR, Cummins DJ, Paul SM, Holtzman DM. Brain to plasma amyloid-β efflux: a measure of brain amyloid burden in a mouse model of Alzheimer's disease. *Science.* 2002;295:2264-2267.
15. Jensen M, Schroder J, Blomberg M, et al. Cerebrospinal fluid Aβ42 is increased early in sporadic Alzheimer's disease and declines with disease progression. *Ann Neurol.* 1999;45:504-511.
16. Katz B, Rimmer S. Ophthalmologic manifestations of Alzheimer's disease. *Surv Ophthalmol.* 1989;34:31-43.
17. Kaur D, Yantiri F, Rajagopalan S, et al. Genetic or pharmacological iron chelation prevents MPTP-induced neurotoxicity in vivo: a novel therapy for Parkinson's disease. *Neuron.* 2003;37:899-909.

©2003 American Medical Association. All rights reserved.

This Page is Inserted by IFW Indexing and Scanning Operations and is not part of the Official Record

BEST AVAILABLE IMAGES

Defective images within this document are accurate representations of the original documents submitted by the applicant.

Defects in the images include but are not limited to the items checked:

- ☐ BLACK BORDERS
- ☐ IMAGE CUT OFF AT TOP, BOTTOM OR SIDES
- ☐ FADED TEXT OR DRAWING
- ☐ BLURRED OR ILLEGIBLE TEXT OR DRAWING
- ☐ SKEWED/SLANTED IMAGES
- ☐ COLOR OR BLACK AND WHITE PHOTOGRAPHS
- ☐ GRAY SCALE DOCUMENTS
- ☐ LINES OR MARKS ON ORIGINAL DOCUMENT
- ☐ REFERENCE(S) OR EXHIBIT(S) SUBMITTED ARE POOR QUALITY
- ☐ OTHER: ______________________

IMAGES ARE BEST AVAILABLE COPY.
As rescanning these documents will not correct the image problems checked, please do not report these problems to the IFW Image Problem Mailbox.